

Fluctuation effects in disordered Peierls systems

Lorenz Bartosch

Institut für Theoretische Physik, Universität Frankfurt, Robert-Mayer-Strasse 8-10, 60054 Frankfurt am Main, Germany
bartosch@th.physik.uni-frankfurt.de

Received dd.mm.yyyy, accepted dd.mm.yyyy by ue

Abstract. We review the density of states and related quantities of quasi one-dimensional disordered Peierls systems in which fluctuation effects of a backscattering potential play a crucial role. The low-energy behavior of non-interacting fermions which are subject to a static random backscattering potential will be described by the fluctuating gap model (FGM). Recently, the FGM has also been used to explain the pseudogap phenomenon in high- T_c superconductors. After an elementary introduction to the FGM in the context of commensurate and incommensurate Peierls chains, we develop a non-perturbative method which allows for a simultaneous calculation of the density of states (DOS) and the inverse localization length. First, we recover all known results in the limits of zero and infinite correlation lengths of the random potential. Then, we attack the problem of finite correlation lengths. While a complex order parameter, which describes incommensurate Peierls chains, leads to a suppression of the DOS, i.e. a pseudogap, the DOS exhibits a singularity at the Fermi energy if the order parameter is real and therefore refers to a commensurate system. We confirm these results by calculating the DOS and the inverse localization length for finite correlation lengths and Gaussian statistics of the backscattering potential with unprecedented accuracy numerically. Finally, we consider the case of classical phase fluctuations which apply to low temperatures where amplitude fluctuations are frozen out. In this physically important regime, which is also characterized by finite correlation lengths, we present analytic results for the DOS, the inverse localization length, the specific heat, and the Pauli susceptibility.

Keywords: Peierls chains, fluctuating gap model, pseudogap

PACS: 71.23.-k, 02.50.Ey, 71.10.Pm

Contents

1	Introduction	2
2	Peierls systems and the fluctuating gap model	4
2.1	Fröhlich Hamiltonian and Peierls instability	4
2.2	Euclidean action	5
2.3	Generalized Ginzburg-Landau functional	8
2.4	Breakdown of the mean-field picture	9
2.5	The Hamiltonian of the fluctuating gap model	11
3	The Green function of the fluctuating gap model and related quantities	12
3.1	The retarded Green function	12

3.2	Dyson equation and perturbation theory	14
3.3	Non-Abelian Schwinger-ansatz	19
3.4	Gauge invariance	27
3.5	Lyapunov exponent and localization length	28
4	Exact results	29
4.1	The white noise limit	30
4.2	Infinite correlation lengths	41
5	Finite correlation lengths	43
5.1	Singularities in the density of states	43
5.2	Numerical algorithm	44
5.3	Phase fluctuations only	51
6	Conclusion	58

1 Introduction

As the temperature is lowered, some inorganic and organic conductors with a highly anisotropic crystal and electronic structure become unstable and undergo a Peierls transition, i.e. they develop a charge-density wave. This instability is due to their quasi one-dimensional nature which results in a (perfectly) nested Fermi surface. A qualitative understanding of the Peierls instability can already be gained by treating the phonon field of a quasi one-dimensional electron-phonon system in a mean-field picture [1–8]. However, because of reduced dimensionality, fluctuations of the phonon field which can be identified as the order parameter field $\Delta(x)$ are crucial and significant deviations are to be expected.

In a seminal paper, Lee, Rice and Anderson [9] introduced the one-dimensional so-called fluctuating gap model (FGM), in which fluctuations of the phonon field are modeled by a static disorder potential. Calculating the leading-order correction of the electronic self energy of an incommensurate chain which is described by a complex order parameter field with $\langle \Delta(x) \rangle = 0$ and $\langle \Delta(x) \Delta^*(x') \rangle = \Delta_s^2 e^{-|x-x'|/\xi}$, where ξ is the temperature-dependent correlation length, Lee, Rice, and Anderson obtained an approximate expression for the density of states (DOS), showing a suppression of the DOS near the Fermi energy, which is called a pseudogap.

A few years later, Sadovskii [10] apparently obtained an exact expression for the Green function of the FGM using Gaussian statistics for the higher correlation functions of the order parameter field which he could assume to be real or complex, referring to a band filling being commensurate or incommensurate with the underlying lattice. Recently, the experimental observation of a pseudo-gap state in the overdoped cuprates above the superconducting phase transition led to a reincarnation of the FGM and Sadovskii's exact solution in the field of high-temperature superconductivity [11–13]. However, the revived interest in Sadovskii's solution also brought to light a subtle error in this solution [14] which questions not only the solution itself, but also the work based on it.

Besides the limit $\xi \rightarrow \infty$ where Sadovskii's solution is indeed exact [14, 15], Sadovskii's solution can also be easily tested in the white-noise limit $\xi \rightarrow 0$, keeping $D \equiv \Delta_s^2 \xi$ constant, such that $\langle \Delta(x) \Delta^*(x') \rangle = 2D \delta(x - x')$. Solving a stationary Fokker-Planck equation, Ovchinnikov and Erikhman [16] obtained an exact expression for the DOS for real $\Delta(x)$. They showed that for small ω and $\langle \Delta(x) \rangle = 0$, the DOS diverges as $\langle \rho(\omega) \rangle \propto |\omega \ln^3 |\omega||^{-1}$. Singularities of this type at the band center of a random Hamiltonian have been discovered by Dyson [17] in the fifties and have recently also been found in one-dimensional spin-gap systems [18, 19]. It is important to note that in the FGM, the singularity is a consequence of phase resonance, and is *not* related to concrete probability properties of $\Delta(x)$ [20, 21]. In particular, the singularity is *not* an artifact of the exactly solvable limit $\xi \rightarrow 0$ considered in Ref. [16]. As argued in Ref. [22], it is therefore reasonable to expect that for any $\xi < \infty$ the average DOS of the FGM exhibits a singularity at $\omega = 0$. This general argument is in disagreement with Sadovskii's solution [10] which for large but finite ξ shows a pseudogap and no singularity. In this work we shall reexamine the DOS of the FGM which determines the whole thermodynamics of the FGM and resolve the above contradictions. This emerged from the PhD thesis of the author [23]. Some of the results presented here have been published in a series of recent research articles [22, 24, 25].

The organisation of this article is as follows: In Section 2, we give an elementary introduction to disordered Peierls systems whose Fermi wave vector can be commensurate or incommensurate with the underlying lattice structure. Starting from a Fröhlich Hamiltonian which describes a one-dimensional electron-phonon system, we will introduce the fluctuating gap model (FGM) as a low energy model in which the phonon system is essentially replaced by a fluctuating static backscattering potential which will serve as the order parameter field.

Section 3 focuses on the one-particle Green function of the FGM. After calculating the Green function in the leading-order Born approximation which reproduces the result obtained by Lee, Rice and Anderson, we will develop a formally exact non-perturbative expression of the Green function as a functional of the disorder potentials based on a non-Abelian generalization of the Schwinger-ansatz. To calculate the DOS and inverse localization length, the introduction of phase variables will turn out to be very convenient. While one phase variable is simply related to the integrated DOS and satisfies a non-linear equation of motion which is equivalent to a Riccati equation, the other phase variable is related to the inverse localization length and can be expressed in terms of the first phase variable. These equations of motions will serve as the starting point for detailed calculations of the DOS and inverse localization length for various probability distributions of the disorder potentials in the next sections.

In Section 4, we will review known exact results of the DOS and inverse localization length in the limit of infinite correlation lengths and in the white noise limit. Generalizing the phase formalism developed in Ref. [20] such that $\Delta(x)$ is allowed to be complex, we will derive a linear fourth-order Fokker-Planck equation previously only obtained within the framework of the method of supersymmetry [26]. The solution of this stationary Fokker-Planck equation encapsulates all known results for the DOS and inverse localization length of the FGM in the white noise limit including the above mentioned Dyson singularity in the Ovchinnikov and Erikhman limit. Results for the case of infinite correlation lengths will finally be obtained by averaging the

DOS and the inverse localization length calculated for a constant disorder potential over an appropriate probability distribution of the disorder potentials.

The case of finite correlation lengths of the order parameter field will be attacked in Section 5. Considering the equation of motion related to the integrated DOS, we will first argue that we expect for any finite ξ a Dyson singularity in the DOS. We will then set up an algorithm based on the equations of motion derived in Section 3 which will allow for a simultaneous numerical calculation of the DOS and inverse localization length for arbitrary disorder potentials with unprecedented accuracy. For complex $\Delta(x)$, Sadovskii's solution is not too far off from our numerical solution. In particular, for large correlation lengths $\Delta_s \xi \gg 1$, the DOS at the Fermi energy vanishes as $\rho(0) \propto (\Delta_s \xi)^{-0.64}$ instead of $\rho(0) \propto (\Delta_s \xi)^{-1/2}$, as predicted by Sadovskii. However, for real Δ , we will find a pseudogap in the DOS for $\Delta_s \xi \gg 1$ which for any finite ξ is overshadowed by a Dyson singularity of the form $\rho(\omega) = A |\omega \ln^{\alpha+1} |\omega||^{-1}$, where A and the exponent α depend on the correlation length ξ . As the correlation length ξ increases, α assumes the finite value $\alpha = 0.41$, but the weight of the Dyson singularity vanishes with increasing correlation length. At the end of Section 5, we shall also discuss the case of only phase fluctuations of the order parameter which applies to sufficiently low temperatures where the amplitude of the order parameter is confined to a narrow region around Δ_s such that Gaussian statistics do not apply any more. We will find exact analytic results for the DOS and inverse localization length and we will also calculate the low-temperature Pauli paramagnetic susceptibility and the electronic low-temperature specific heat.

2 Peierls systems and the fluctuating gap model

In this introductory section we will replace the dynamic phonon ensemble in Peierls systems by a static backscattering potential which we will identify as the order parameter. Due to reduced dimensionality, fluctuations of this order parameter field are very important and we will determine its statistics in the context of a brief discussion of a generalized Ginzburg-Landau functional. Finally, we introduce the fluctuating gap model (FGM) as a low-energy model which takes into account these fluctuations.

2.1 Fröhlich Hamiltonian and Peierls instability

The formation of periodic lattice distortions and charge-density waves in Peierls chains is due to the electron-phonon interaction in these quasi one-dimensional materials [1–3, 6–8]. Since particle-hole excitations with momentum¹ $2k_F$ are possible for very small excitation energies, the Lindhard density-density response function exhibits a singularity at $q = 2k_F$. Kohn showed that this singularity should be conveyed into a kink in the phonon spectrum [27]. While these Kohn anomalies are rather weak in isotropic materials, they can lead to a substantial alteration to the phonon dispersion in quasi one-dimensional materials with a topology of the Fermi surface which shows perfect nesting. At low enough temperatures, the renormalized phonon mode at $2k_F$ can scale all the way down to zero, i.e. become gapless. This process is called softening

¹In this work we choose units such that $\hbar = k_B = 1$.

of the phonon mode. Since $\omega_{\text{ren}}(2k_F) \rightarrow 0$, a static lattice distortion with wave vector $2k_F$ may now arise. Simultaneously, there is a formation of a charge density wave. As a consequence, the discrete translational invariance is broken. The same physics can also be described by considering the thermodynamics of a Peierls system. This approach will also allow to go beyond a mean-field picture and will therefore be followed here.

A Hamiltonian to describe a one-dimensional electron-phonon system was proposed in 1954 by Fröhlich [1]:

$$\mathcal{H} = \sum_{k,\sigma} \epsilon_k c_{k,\sigma}^\dagger c_{k,\sigma} + \sum_q \omega_q b_q^\dagger b_q + \sum_q \frac{g_q}{\sqrt{L}} \hat{\rho}_q^\dagger (b_q + b_{-q}^\dagger). \quad (1)$$

The system has length $L = Na$ where a is the lattice spacing, and periodic boundary conditions are assumed. c_k^\dagger and c_k are fermionic creation and annihilation operators with momentum k , spin σ , and energy ϵ_k . While $\epsilon_k = k^2/2m$ for free electrons, in the tight-binding approximation one has $\epsilon_k = -2t \cos ka$. The second term in the Fröhlich Hamiltonian (1) describes phonons with phonon dispersion ω_q . b_q^\dagger and b_q are bosonic creation and annihilation operators with momentum q which is confined to the first Brillouin zone. For a chain with only nearest-neighbor interactions we have (see for example Ref. [28]) $\omega_q = 2\omega_0 \sin |qa/2|$. Finally, the last term in Eq. (1) models the interaction of the phonon system with the fermions. The phonons are linearly coupled via the electron-phonon coupling constant g_q to the Fourier components of the electron density

$$\hat{\rho}_q^\dagger \equiv \sum_{k,\sigma} c_{k+q,\sigma}^\dagger c_{k,\sigma}. \quad (2)$$

The phonon operators b_q and b_q^\dagger are directly related to the operators of the normal coordinates u_q of the lattice system by

$$u_q = \left(\frac{1}{2M\omega_q} \right)^{1/2} (b_q + b_{-q}^\dagger). \quad (3)$$

Here, M is the ionic mass. The lattice displacement operators of the ions at $x_n = na$ are given by its Fourier transform,

$$u(x_n) = \sum_q e^{iqx_n} \left(\frac{1}{2NM\omega_q} \right)^{1/2} (b_q + b_{-q}^\dagger). \quad (4)$$

In a mean-field picture, the Peierls transition will lead to a non-vanishing expectation value $\langle u(x_n) \rangle$ which implies that the system exhibits a static lattice distortion [8, 23]. This static lattice distortion is accompanied by a single-particle gap, a charge density wave and unusual electronic transport properties [6–8, 29, 30].

2.2 Euclidean action

In an Euclidean functional integral approach, the Fröhlich Hamiltonian is conveyed into the action (see, for example, Negele and Orland [31])

$$S\{\psi^*, \psi; b^*, b\} = S_{\text{el}}\{\psi^*, \psi\} + S_{\text{ph}}\{b^*, b\} + S_{\text{int}}\{\psi^*, \psi; b^*, b\}, \quad (5)$$

where

$$S_{\text{el}}\{\psi^*, \psi\} = \beta \sum_{k, \tilde{\omega}_n, \sigma} \psi_{k, \tilde{\omega}_n, \sigma}^* [i\tilde{\omega}_n - \tilde{\epsilon}_k] \psi_{k, \tilde{\omega}_n, \sigma} , \quad (6)$$

$$S_{\text{ph}}\{b^*, b\} = -\beta \sum_{q, \omega_m} b_{q, \omega_m}^* [i\omega_m - \omega_q] b_{q, \omega_m} , \quad (7)$$

$$S_{\text{int}}\{\psi^*, \psi; b^*, b\} = \beta \sum_{q, \omega_m} \frac{g_q}{\sqrt{L}} \left(\sum_{k, \tilde{\omega}_n, \sigma} \psi_{k+q, \tilde{\omega}_n+\omega_m, \sigma}^* \psi_{k, \tilde{\omega}_n, \sigma} \right) \times [b_{q, \omega_m} + b_{-q, -\omega_m}^*] . \quad (8)$$

Here, $\beta \equiv 1/T$ is the inverse temperature and $\tilde{\epsilon}_k \equiv \epsilon_k - \mu$ is the energy dispersion measured with respect to the chemical potential μ . While the conjugated Grassmann variables $\psi_{k, \tilde{\omega}_n}$ and $\psi_{k, \tilde{\omega}_n}^*$ describe fermions with momentum k and fermionic Matsubara frequency $\tilde{\omega}_n \equiv (2n+1)\pi/\beta$, b_{q, ω_m} and b_{q, ω_m}^* are complex (bosonic) phonon fields with momentum q and bosonic Matsubara frequency $\omega_m \equiv 2\pi m/\beta$. In terms of the above action, the partition function reads

$$\mathcal{Z} = \int \mathcal{D}\{\psi^*, \psi\} \mathcal{D}\{b^*, b\} \exp[-S\{\psi^*, \psi; b^*, b\}] , \quad (9)$$

where $\mathcal{D}\{\psi^*, \psi\}$ and $\mathcal{D}\{b^*, b\}$ are appropriately normalized fermionic and bosonic integration measures [31]. Using the variable transformation $\phi_{q, \omega_m} \equiv \frac{g_q}{\sqrt{L}} (b_{q, \omega_m} + b_{-q, -\omega_m}^*)$, $\eta_{q, \omega_m} \equiv -i \frac{g_q}{\sqrt{L}} (b_{q, \omega_m} - b_{-q, -\omega_m}^*)$, such that $\phi_{q, \omega_m}^* = \phi_{-q, -\omega_m}$ and $\eta_{q, \omega_m}^* = \eta_{-q, -\omega_m}$, η may easily be integrated out resulting in

$$S\{\psi^*, \psi; \phi\} = S_{\text{el}}\{\psi^*, \psi\} + S_{\text{ph}}\{\phi\} + S_{\text{int}}\{\psi^*, \psi; \phi\} , \quad (10)$$

where $S_{\text{el}}\{\psi^*, \psi\}$ is unchanged and

$$S_{\text{ph}}\{\phi\} = \frac{1}{2} \beta L \sum_{q, \omega_m} \frac{1}{|g_q|^2} \phi_{q, \omega_m}^* \left[\frac{\omega_m^2 + \omega_q^2}{\omega_q} \right] \phi_{q, \omega_m} , \quad (11)$$

$$S_{\text{int}}\{\psi^*, \psi; \phi\} = \beta \sum_{q, \omega_m} \left(\sum_{k, \tilde{\omega}_n} \psi_{k+q, \tilde{\omega}_n+\omega_m}^* \psi_{k, \tilde{\omega}_n} \right) \phi_{q, \omega_m} . \quad (12)$$

So far, no approximation has been made. In the following, we will restrict ourselves to the low-energy physics of the weak-coupling limit, so that only fermions in the vicinity of the Fermi energy are involved. In this case the Fermi energy may be linearized around the two Fermi points, such that it assumes the form

$$\tilde{\epsilon}_k = v_F (|k| - k_F) . \quad (13)$$

To separate right- and left-moving Fermions, let us introduce the spinor field

$$\bar{\psi}_{k, \tilde{\omega}_n, \sigma} \equiv \begin{pmatrix} \psi_{+, k, \tilde{\omega}_n, \sigma} \\ \psi_{-, k, \tilde{\omega}_n, \sigma} \end{pmatrix} \equiv \begin{pmatrix} \psi_{k_F+k, \tilde{\omega}_n, \sigma} \\ \psi_{-k_F+k, \tilde{\omega}_n, \sigma} \end{pmatrix} \quad (14)$$

and its conjugated counterpart

$$\bar{\psi}_{k,\tilde{\omega}_n,\sigma}^\dagger \equiv (\psi_{+,k,\tilde{\omega}_n,\sigma}^*, \psi_{-,k,\tilde{\omega}_n,\sigma}^*) \equiv (\psi_{k_F+k,\tilde{\omega}_n,\sigma}^*, \psi_{-k_F+k,\tilde{\omega}_n,\sigma}^*) . \quad (15)$$

The electronic part of the action may easily be rewritten in terms of these spinor fields and the inverse non-interacting Matsubara Green function

$$\mathbf{G}_0^{-1}(k, \tilde{\omega}_n) \equiv \begin{pmatrix} i\tilde{\omega}_n - v_F k & 0 \\ 0 & i\tilde{\omega}_n + v_F k \end{pmatrix} . \quad (16)$$

Since the momentum transfer of the phonons is either small compared with the Fermi momentum or approximately $2k_F$, we decompose ϕ_{q,ω_m} according to

$$\mathbf{V}_{q,\omega_m} \equiv \begin{pmatrix} V_{q,\omega_m} & \Delta_{q,\omega_m} \\ \Delta_{-q,-\omega_m}^* & V_{q,\omega_m} \end{pmatrix} \equiv \begin{pmatrix} \phi_{q,\omega_m} & \phi_{q+2k_F,\omega_m} \\ \phi_{q-2k_F,\omega_m} & \phi_{q,\omega_m} \end{pmatrix} , \quad (17)$$

such that $|q| < k_F$. While $\phi_{q,\omega_m}^* = \phi_{-q,-\omega_m}$ directly translates into $V_{q,\omega_m}^* = V_{-q,-\omega_m}$, a similar relation for Δ_{q,ω_m} does only hold if $4k_F$ is a reciprocal lattice vector. $\Delta_{q,\omega_m}^* = \Delta_{-q,-\omega_m}$ is therefore only true for a half-filled band for which $\pi/a = 2k_F$. We will refer to this case as the *commensurate case*. The more general case for which $k_F a/\pi$ is an other fractional number is also called commensurate but will not be discussed here. In the *incommensurate case*, for which $k_F a/\pi$ is well separated from any simple fractional number, all Δ_{q,ω_m}^* and $\Delta_{-q',-\omega_{m'}}$ are independent. We will see in this work that commensurate and incommensurate Peierls systems can have very different physical properties.

Defining the matrices \mathbf{G}_0^{-1} and \mathbf{V} via

$$(\mathbf{G}_0^{-1})_{k,k',\tilde{\omega}_n,\tilde{\omega}_{n'}} \equiv \delta_{k,k'} \delta_{\tilde{\omega}_n,\tilde{\omega}_{n'}} \mathbf{G}_0^{-1}(k, \tilde{\omega}_n) , \quad (18)$$

$$(\mathbf{V})_{k,k',\tilde{\omega}_n,\tilde{\omega}_{n'}} \equiv \mathbf{V}_{k-k',\tilde{\omega}_n-\tilde{\omega}_{n'}} , \quad (19)$$

our action turns into

$$S\{\bar{\psi}^\dagger, \bar{\psi}; V, \Delta, \Delta^*\} = S_{\text{el-ph}}\{\bar{\psi}^\dagger, \bar{\psi}; V, \Delta, \Delta^*\} + S_{\text{ph}}\{V, \Delta, \Delta^*\} , \quad (20)$$

where

$$S_{\text{el-ph}}\{\bar{\psi}^\dagger, \bar{\psi}; V, \Delta, \Delta^*\} = \beta \sum_{k,k',\tilde{\omega}_n,\tilde{\omega}_{n'},\sigma} \bar{\psi}_{k,\tilde{\omega}_n,\sigma}^\dagger (\mathbf{G}_0^{-1} - \mathbf{V})_{k,k',\tilde{\omega}_n,\tilde{\omega}_{n'}} \bar{\psi}_{k',\tilde{\omega}_{n'},\sigma} , \quad (21)$$

$$\begin{aligned} S_{\text{ph}}\{V, \Delta, \Delta^*\} &= \frac{1}{2} \beta L \sum_{q,\omega_m} \frac{1}{|g_q|^2} \left[\frac{\omega_m^2 + \omega_q^2}{\omega_q} \right] V_{q,\omega_m}^* V_{q,\omega_m} \\ &+ \frac{1}{c} \beta L \sum_{q,\omega_m} \frac{1}{|g_{2k_F+q}|^2} \left[\frac{\omega_m^2 + \omega_{2k_F+q}^2}{\omega_{2k_F+q}} \right] \Delta_{q,\omega_m}^* \Delta_{q,\omega_m} , \quad (22) \end{aligned}$$

and

$$c \equiv \begin{cases} 2 , & \text{commensurate case (half-filled band)} , \\ 1 , & \text{incommensurate case} . \end{cases} \quad (23)$$

While in the incommensurate case $\pm 2k_F$ lie (up to a reciprocal lattice vector) inside the first Brillouin zone, $\pm 2k_F$ lie directly on the border of the first Brillouin zone in the commensurate case. In this case the factor of 1/2 in the last line in Eq. (22) avoids overcounting.

2.3 Generalized Ginzburg-Landau functional

Since the action $S\{\bar{\psi}^\dagger, \bar{\psi}; V, \Delta, \Delta^*\}$ is only Gaussian in both the Fermion and the phonon fields, either of them can easily be integrated out. To derive a time-independent (generalized) Ginzburg-Landau theory which will enable us to determine the statistics of the phonon field, we ignore quantum fluctuations, i.e. we ignore all terms involving finite bosonic frequencies. Because we will be only interested in static properties of the Peierls system, this should be a reasonable approximation for not too small temperatures. Integrating out the fermionic degrees of freedom, the action $S\{\bar{\psi}^\dagger, \bar{\psi}; V, \Delta, \Delta^*\}$ turns into the free energy functional $\beta F\{V, \Delta, \Delta^*\}$.

For the derivation of a generalized Ginzburg-Landau functional in which the free energy functional is expressed in terms of gradients of the order parameter field

$$\Delta(x) = \sum_q e^{iqx} \Delta_q, \quad (24)$$

we refer the reader to the PhD thesis of the author [23] or to Refs. [32–38] where the gradient-expansion is developed in the context of superconductivity. Up to terms of second order in the gradient, we find

$$F\{\Delta, \Delta^*\} = F^{(0)}\{\Delta, \Delta^*\} + F^{(2)}\{\Delta, \Delta^*\}, \quad (25)$$

$$F^{(0)}\{\Delta, \Delta^*\} = s\rho_0 \int_0^L dx \left(-\frac{2\pi}{\beta} \sum_{0 < \tilde{\omega}_n \lesssim \epsilon_0} \left[\sqrt{\tilde{\omega}_n^2 + |\Delta|^2} - \tilde{\omega}_n \right] + \frac{|\Delta|^2}{2\lambda} \right), \quad (26)$$

$$F^{(2)}\{\Delta, \Delta^*\} = s\rho_0 \int_0^L dx \frac{2\pi}{\beta} \sum_{\tilde{\omega}_n > 0} \left[\frac{1}{8} \frac{|\partial_x \Delta|^2}{(\tilde{\omega}_n^2 + |\Delta|^2)^{\frac{3}{2}}} - \frac{1}{32} \frac{[\partial_x |\Delta|^2]^2}{(\tilde{\omega}_n^2 + |\Delta|^2)^{\frac{5}{2}}} \right]. \quad (27)$$

For $F^{(0)}\{\Delta, \Delta^*\}$ to be finite and to avoid logarithmic divergences, the sum in Eq. (26) needs to be regularized by an ultraviolet cutoff ϵ_0 . Although the ultraviolet cutoff ϵ_0 was introduced here in the sum over Matsubara frequencies instead of as a cutoff in the momentum integral, expanding Eqs. (26) and (27) in the regime $\beta|\Delta| \ll 1$, we get the usual Ginzburg-Landau functional,

$$F\{\Delta, \Delta^*\} = \frac{s\rho_0}{2} \int_0^L dx \left[a(T) |\Delta(x)|^2 + b(T) |\Delta(x)|^4 + c(T) |\partial_x \Delta(x)|^2 \right], \quad (28)$$

where the coefficients $a(T)$, $b(T)$ and $c(T)$ are given by

$$a(T) = \ln \frac{T}{T_c^{\text{MF}}}, \quad T_c^{\text{MF}} = 1.134 \epsilon_0 \exp(-1/\lambda), \quad (29)$$

$$b(T) = \left(\frac{1}{4\pi T} \right)^2 7\zeta(3), \quad (30)$$

$$c(T) = \left(\frac{v_F}{4\pi T} \right)^2 7\zeta(3). \quad (31)$$

Here, $\zeta(3) \approx 1.2$ is the Riemann zeta-function of 3 and

$$\lambda \equiv \frac{cs}{2} \frac{\rho_0 |g_{2k_F}|^2}{\omega_{2k_F}} \quad (32)$$

is the dimensionless coupling constant. T_c^{MF} is the critical mean-field temperature for the Peierls distortion. If we include spin, $s = 2$, otherwise we have $s = 1$.

2.4 Breakdown of the mean-field picture

The experimentally observed Peierls transition, including the static lattice distortion, the charge-density wave and the occurrence of a single-particle gap can qualitatively already be understood in a mean-field picture. However, due to reduced dimensionality, fluctuations of the order parameter field are very important and dramatically change this scenario. The Mermin-Wagner theorem states that these fluctuations lead to the absence of long-range order, even at very low temperatures [39]. This precludes a spontaneously broken continuous symmetry. But how can one explain the experimentally observed charge-density wave which breaks a continuous translational symmetry in strongly anisotropic materials like blue bronze [8]? The answer is simply this: These materials are quasi one-dimensional, but *not* strictly one-dimensional. As we will see below, in a strictly one-dimensional material, the correlation length $\xi(T)$ increases with decreasing temperature, but for any finite temperature cannot approach infinity. At very low temperatures, however, even a very weak interchain-coupling can lead to the onset of three-dimensional order such that the system can undergo a Peierls transition. Of course, the transition temperature is not the mean-field transition temperature T_c^{MF} . Lee, Rice and Anderson [9] pointed out that one should expect $T_c^{\text{3D}} \approx \frac{1}{4}T_c^{\text{MF}}$. For a derivation of an adequate three-dimensional microscopic theory see McKenzie [40] and references given therein. Here, we will especially be interested in the temperature regime above the Peierls transition so that it suffices to consider only the strictly one-dimensional case.

2.4.1 Correlation functions of the order parameter field

We will now consider the fluctuations of the order parameter field $\Delta(x)$ and calculate the correlation functions of $\Delta(x)$ which describe the phonon statistics.

Gaussian approximation

At temperatures far above the mean-field critical temperature T_c^{MF} , the coefficient $a(T)$ becomes large enough such that anharmonic corrections to the free energy functional may be neglected. Truncating the free energy functional (28) at the second order, we find

$$\langle \Delta(x) \rangle = 0, \quad (33)$$

$$\langle \Delta(x) \Delta^*(x') \rangle = \Delta_s^2(T) e^{-|x-x'|/\xi(T)}, \quad (34)$$

where $\Delta_s^2(T) = \frac{T}{s\rho_0 \sqrt{a(T) c(T)}}$ and $\xi^{-1}(T) = \left(\frac{a(T)}{c(T)} \right)^{1/2}$. While $\langle \Delta(x) \Delta(x') \rangle$ vanishes for complex Δ , it is equal to $\langle \Delta(x) \Delta^*(x') \rangle$ for real Δ . In the considered Gaussian approximation, higher correlation functions are simply given by Wick's theorem. The Gaussian approximation is good at sufficiently high temperatures and is the usual approximation made when higher correlation functions are too complicated or not known.

Anharmonic corrections and the case of only phase fluctuations

As the temperature is lowered and approaches the mean-field critical temperature T_c^{MF} , fluctuation effects become important and the mean-field picture breaks down. However, as shown by Scalapino, Sears and Ferrel [41] using the transfer matrix technique, the first two moments of a one-dimensional Ginzburg-Landau theory are still approximately given by Eqs. (33) and (34). For temperatures well below T_c^{MF} , one finds for real $\Delta(x)$ an exponential increase of the correlation length with decreasing temperature, while for complex $\Delta(x)$ the correlation length increases as the inverse temperature. This last result can be understood as follows: For small temperatures $T \ll T_c^{\text{MF}}$, the generalized Ginzburg-Landau functional has the shape of a ‘‘Mexican hat’’ and is dominated by its minima. Amplitude fluctuations get gradually frozen out and, for complex $\Delta(x)$, the phase of the order parameter $\Delta(x) \approx \Delta_s e^{i\vartheta(x)}$ fluctuates at the bottom of the ‘‘Mexican hat’’. Ignoring, as before, quartic terms in the gradient expansion of the free energy, the free energy is given up to an irrelevant constant by

$$F^{(\text{phase})}\{V\} = F^{(\text{phase})}\{\partial_x \vartheta/2\} = \frac{1}{2} s \rho_s(T) \int_0^L dx V^2(x). \quad (35)$$

In analogy to the theory of superconductivity,

$$V(x) = \partial_x \vartheta(x)/2 \quad (36)$$

can be interpreted (up to a constant $1/m^*$) as the superfluid velocity and

$$\rho_s(T) = \rho_0 \frac{2\pi}{\beta} \sum_{\tilde{\omega}_n > 0} \frac{\Delta_s^2}{(\tilde{\omega}_n^2 + |\Delta_s|^2)^{\frac{3}{2}}} \quad (37)$$

can be interpreted as the superfluid density. Formally, the free energy is identical to the kinetic energy of a superflow. A two-dimensional analogue of Eq. (35) has been used by Emery and Kivelson [42, 43] in their theory describing superconductors with a small phase-stiffness. At $T = 0$, the sum in Eq. (37) turns into an integral which can be done analytically and gives $\rho_s(0) = \rho_0$, i.e. at $T = 0$, the superfluid density is equal to the density of states. Plots of $\rho_s(T)$ for $\Delta_s(T)$ given by the BCS gap equation [23, 44–46]

$$\frac{1}{\lambda} = \frac{2\pi}{\beta} \sum_{0 < \tilde{\omega}_n \lesssim \epsilon_0} \frac{1}{\sqrt{\tilde{\omega}_n^2 + \Delta_0^2(T)}}, \quad (38)$$

and for $\Delta_s = 1.76 T_c^{\text{MF}}$ are shown in Fig. 1.

Since $F^{(\text{phase})}\{V\}$ is only quadratic in $V(x)$, correlation functions of $\Delta(x)$ can easily be calculated. The first two moments are given by Eqs. (33) and (34), where

$$\xi(T) = \frac{s \rho_s(T)}{2T}. \quad (39)$$

For $T \lesssim T_c^{\text{MF}}/4$ we have $\rho_s(T) \approx \rho_s(0) = 1/\pi$, such that in this strictly one-dimensional theory we find $\xi(T) = s/2\pi T \propto 1/T$ which for fermions with spin $1/2$ agrees with Grüner’s [8] result $\xi(T) = 1/\pi T$.

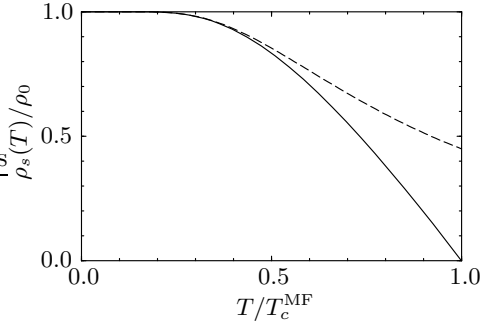


Fig. 1 Plot of the superfluid density as a function of temperature for $\Delta_s = 1.76T_c^{\text{MF}}$ (dashed line) and $\Delta_s(T)$ given by the BCS gap equation (38) (solid line).

2.5 The Hamiltonian of the fluctuating gap model

The fluctuating gap model (FGM) describes electrons subject to a static disorder potential which can be seen as an approximation of a phonon field. For a particular realization of the disorder, the electronic part of the action given in Eq. (21) corresponds to the Hamiltonian

$$\mathcal{H} = \sum_{k,k'} \begin{pmatrix} c_{+,k}^\dagger & c_{-,k}^\dagger \end{pmatrix} H_{k,k'} \begin{pmatrix} c_{+,k'} \\ c_{-,k'} \end{pmatrix}, \quad (40)$$

where

$$H_{k,k'} = \begin{pmatrix} v_F k \delta_{k,k'} + V_{k-k'} & \Delta_{k-k'} \\ \Delta_{-(k-k')}^* & -v_F k \delta_{k,k'} + V_{k-k'} \end{pmatrix}. \quad (41)$$

A Fourier transformation leads to

$$\mathcal{H} = \int_0^L dx \begin{pmatrix} \psi_+^\dagger(x) & \psi_-^\dagger(x) \end{pmatrix} \hat{H}(x, -i\partial_x) \begin{pmatrix} \psi_+(x) \\ \psi_-(x) \end{pmatrix}, \quad (42)$$

with

$$\hat{H}(x, -i\partial_x) = -iv_F \partial_x \sigma_3 + V(x) \sigma_0 + \Delta(x) \sigma_+ + \Delta^*(x) \sigma_-. \quad (43)$$

This is the Hamiltonian of the FGM. σ_i are the usual Pauli matrices, σ_0 is the 2×2 unit matrix, and $\sigma_\pm = \frac{1}{2}(\sigma_1 \pm i\sigma_2)$. Recall that we have linearized the energy dispersion such that the FGM can only describe the low-energy physics of Peierls chains in the weak-coupling regime. As a further approximation, we have considered the phonon field to be static. It will now be our aim to calculate disorder-averaged quantities for the model described by this Hamiltonian. As we will discuss in Section 5, instead of averaging over the disorder, it is also possible to consider a typical realization of the disorder potential.

2.5.1 The fluctuating gap model in other physical contexts

In this section, the fluctuating gap model (FGM) emerged as an effective low-energy model to describe quasi one-dimensional materials which undergo a Peierls transition. Our strictly one-dimensional theory applies to temperatures above the Peierls transition before three-dimensional fluctuations become important and eventually lead to

a phase transition. Formally, the Hamiltonian of the FGM is of the Dirac type and describes electrons in a disordered potential. In the language of relativistic quantum field theory, the backscattering potential can be interpreted as a random (and complex) mass. The FGM has also applications in other fields of physics. As shown in Refs. [18, 47], the Hamiltonian of disordered spin Peierls systems [8, 19, 48–50] can be mapped by a Jordan-Wigner transformation onto the Hamiltonian of the FGM. In a semiclassical approximation of superconductivity, it is also possible to replace the original three-dimensional problem by a directional average over effectively one-dimensional problems [51] which in the weak coupling limit are described by the FGM. This method has been used in Refs. [36–38] to derive the gradient expansion of a clean superconductor. A generalization of the FGM towards higher dimensions to describe the phase above the phase-transition in underdoped high- T_c superconductors by antiferromagnetic short-range order fluctuations was considered in Refs. [11–13].

3 The Green function of the fluctuating gap model and related quantities

In this section, we will introduce different concepts to calculate the Green function and related quantities of the fluctuating gap model. The density of states and the localization length will be of special interest. In particular, we will develop a non-perturbative method which allows to calculate these quantities simultaneously for arbitrary given disorder potentials.

3.1 The retarded Green function

In the following, we are going to consider the retarded Green function $\mathcal{G}^R(x, x'; \omega)$ of the fluctuating gap model. This retarded Green function is of special interest because it can be related to several quantities which are in principle experimentally accessible. The trace of the imaginary part of the Green function at coinciding space points determines the *local* density of states (DOS),

$$\rho(x, \omega) = -\pi^{-1} \text{ImTr}[\mathcal{G}^R(x, x; \omega)]. \quad (44)$$

Averaging $\rho(x, \omega)$ over all space points gives the DOS $\rho(\omega)$, which is the fundamental quantity that determines the whole thermodynamics of the FGM. It will turn out that the trace of the energy-integrated space averaged Green function at coinciding space points $\Gamma(\omega)$ will be easier to calculate than its non-integrated form. While its imaginary part is proportional to the integrated DOS $\mathcal{N}(\omega)$, the Thouless formula states that $\text{Re}\Gamma(\omega)$ is equal to the inverse localization length $\ell^{-1}(\omega)$. As in the following sections, we will usually only consider the DOS and the inverse localization length for positive frequencies ω . Due to particle-hole symmetry, the DOS and the localization length are symmetric with respect to the Fermi energy so that after setting the Fermi energy equal to zero we have $\rho(\omega) = \rho(-\omega)$ and $\ell^{-1}(\omega) = \ell^{-1}(-\omega)$. It therefore suffices to consider the case $\omega > 0$.

The retarded 2×2 matrix Green function $\mathcal{G}^R(x, x'; \omega)$ to the Schrödinger operator $\omega - \hat{H}$ satisfies the differential equation

$$[\omega + i0^+ - \hat{H}(x, -i\partial_x)] \mathcal{G}^R(x, x'; \omega) = \delta(x - x')\sigma_0. \quad (45)$$

The positive but infinitesimal imaginary part added to the frequency ω indicates that we have to impose the correct boundary conditions applying to a retarded Green function.

3.1.1 Free fermions

It is easy to calculate the Green function for free fermions. In this case, $V(x) = \Delta(x) = 0$, such that the system is translational invariant, and Eq. (45) simplifies to²

$$[\omega + i0^+ + i\sigma_3\partial_x] \mathcal{G}_0^R(x - x'; \omega) = \sigma_0\delta(x - x'). \quad (46)$$

Taking the Fourier transform of this equation from real space to momentum space gives

$$[\omega + i0^+ - k\sigma_3] \mathcal{G}_0^R(k; \omega) = \sigma_0. \quad (47)$$

$\mathcal{G}_0^R(k; \omega) \equiv \int dx e^{-ikx} \mathcal{G}_0^R(x; \omega)$ can now be found by a simple matrix inversion. If $\alpha = 1$ accounts for right- and $\alpha = -1$ for left-moving fermions, the matrix elements of $\mathcal{G}_0^R(k; \omega)$ are given by

$$(\mathcal{G}_0^R)_{\alpha\alpha'}(k; \omega) = \frac{\delta_{\alpha,\alpha'}}{\omega - \alpha k + i0^+}. \quad (48)$$

A simple Fourier transformation back to real space now gives the retarded propagator of free fermions in real space,

$$i(\mathcal{G}_0^R)_{\alpha\alpha'}(x; \omega) = \delta_{\alpha,\alpha'}\theta(\alpha x)e^{i\alpha\omega x}. \quad (49)$$

Here, $\theta(x)$ is the Heaviside step function

$$\theta(x) = \begin{cases} 0 & , \quad x < 0 \\ 1 & , \quad x > 0 \end{cases}. \quad (50)$$

For concreteness, let us also define $\theta(0) = \lim_{x \rightarrow 0} [\theta(x) + \theta(-x)]/2 = 1/2$. While the matrix elements at $x = 0$ are sensitive to the definition $\theta(0) = 1/2$ which amounts to defining $\mathcal{G}^R(x = 0; \omega) \equiv \frac{1}{2} \lim_{x \rightarrow 0^+} [\mathcal{G}^R(+x; \omega) + \mathcal{G}^R(-x; \omega)]$, the local DOS $\rho(x, \omega) = -\pi^{-1} \text{ImTr}[\mathcal{G}_0^R(0; \omega)]$ does not depend on this definition because it only involves the harmless quantity $\theta(x) + \theta(-x) \equiv 1$. Due to translational symmetry, the total DOS is equal to the space-independent local DOS,

$$\rho_0(\omega) = \pi^{-1}. \quad (51)$$

Note that the DOS of free fermions is independent of the frequency because we have linearized the energy dispersion.

A further Fourier transformation of Eq. (49) from frequency to time gives

$$i(\mathcal{G}_0^R)_{\alpha\alpha'}(x; t) = \delta_{\alpha,\alpha'}\theta(t)\delta(\alpha x - t). \quad (52)$$

This free retarded Green function in space and time allows for a simple interpretation: A fermion put into the system at $t' = 0$ as a right- or left-mover will at time $t > 0$ have traveled a distance $|x| = t = v_F t$ in the positive or negative direction, respectively. The fermion can not be observed in the system at times $t < 0$.

²Besides \hbar and k_B , we also set the Fermi velocity v_F equal to one.

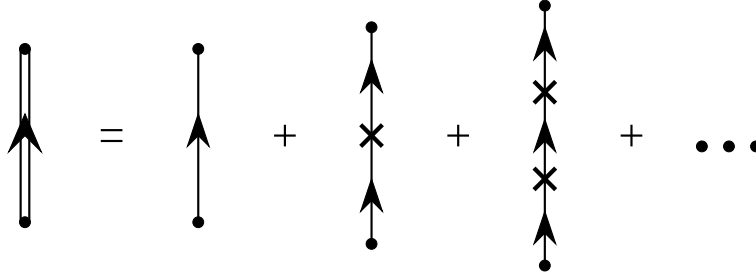


Fig. 2 Diagrammatic expansion of the matrix Green function. While the single line represents the Green function of free fermions, the double line is a graphical representation of the full Green function $\mathcal{G}^R(x, x'; \omega)$. The crosses denote the disorder potential $\mathbf{V}(x)$.

3.2 Dyson equation and perturbation theory

One way to handle the disorder is to consider the disorder potential as a perturbation and expand the Green function in powers of this potential. Defining $\mathbf{V}(x) \equiv V(x)\sigma_0 + \Delta(x)\sigma_+ + \Delta^*(x)\sigma_-$, Eq. (45) may be written as

$$[i\sigma_3\partial_x + \omega + i0^+] \mathcal{G}^R(x, x'; \omega) = \delta(x - x') \sigma_0 + \mathbf{V}(x) \mathcal{G}^R(x, x'; \omega). \quad (53)$$

Substituting x by x_1 , multiplying the resulting equation from the left with the free Green function $\mathcal{G}_0^R(x - x_1; \omega)$ and then integrating over x_1 gives the *Dyson equation*

$$\mathcal{G}^R(x, x'; \omega) = \mathcal{G}_0^R(x - x'; \omega) + \int dx \mathcal{G}_0^R(x - x_1; \omega) \mathbf{V}(x_1) \mathcal{G}^R(x_1, x'; \omega). \quad (54)$$

Iterating this Dyson equation, the exact Green function can be expressed in terms of the free Green function and the disorder potential:

$$\mathcal{G}^R(x, x'; \omega) = \sum_{n=0}^{\infty} \mathcal{G}_n^R(x, x'; \omega), \quad (55)$$

where $\mathcal{G}_0^R(x, x'; \omega) = \mathcal{G}_0^R(x - x'; \omega)$ is the free Green function calculated above, and for $n \geq 1$ the functions $\mathcal{G}_n^R(x, x'; \omega)$ are given by

$$\mathcal{G}_n^R(x, x'; \omega) = \int dx_1 \dots \int dx_n \mathcal{G}_0^R(x - x_n; \omega) \mathbf{V}(x_n) \mathcal{G}_0^R(x_n - x_{n-1}; \omega) \dots \mathbf{V}(x_1) \mathcal{G}_0^R(x_1 - x'; \omega). \quad (56)$$

Recall that the right-hand side of this equation involves the product of 2×2 -matrices. The perturbative expansion of the full Green function can be visualized by using Feynman diagrams (see Fig. 2).

The physical interpretation of the perturbation expansion is simple: The perturbative expansion takes into account all possibilities of a particle moving through the sample getting scattered at the various static impurities. While $\Delta(x)$ changes the direction in which the particle travels and therefore can be interpreted as a backscattering potential, $V(x)$ does not change the direction of the particle, so that it only leads to forward scattering.

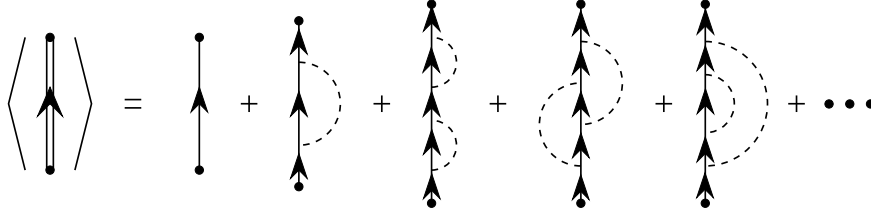


Fig. 3 Diagrammatic representation of the averaged matrix Green function. The single line represents the Green function of free fermions and in this case the (averaged) double line is a graphical representation of the full (averaged) Green function $\langle \mathcal{G}^R(x, x'; \omega) \rangle$. The dashed line denotes the disorder average $\langle \mathbf{V}(x)\mathbf{V}(x') \rangle$.

3.2.1 Boundary conditions of the retarded Green function

Below, we will consider a non-perturbative approach to calculate the Green function of the FGM. The above perturbative expansion can be used to obtain the correct boundary conditions of the full retarded Green function: Let us consider $(\mathcal{G}_n^R)_{\alpha\alpha'}(x, x'; \omega)$. According to Eq. (56), its expansion in a product of free Green functions and the static impurities starts with $(\mathcal{G}_0^R)_{\alpha\alpha}(x - x_n; \omega)$ and ends with $(\mathcal{G}_0^R)_{\alpha'\alpha'}(x_1 - x'; \omega)$. These terms are proportional to $\theta(\alpha(x - x_n))$ and $\theta(\alpha'(x_1 - x'))$, respectively, so that $(\mathcal{G}_n^R)_{\alpha\alpha'}(x, x'; \omega)$ has to vanish as $\alpha x \rightarrow -\infty$ or $\alpha' x' \rightarrow \infty$. Since this reasoning applies to all orders in perturbation theory, it also applies to the full Green function. If we demand the potentials to vanish outside the interval $[-\Lambda, L + \Lambda]$, the boundary condition can also be written as

$$(\mathcal{G}^R)_{\alpha\alpha'}(-\alpha\Lambda, x'; \omega) = 0, \quad (\mathcal{G}^R)_{\alpha\alpha'}(x, \alpha'(L + \Lambda); \omega) = 0. \quad (57)$$

3.2.2 Second order Born approximation

Let us now consider the disorder-averaged Green function. As discussed in Section 2, above the Peierls transition, the first two moments of the order parameter field $\Delta(x)$ are given by $\langle \Delta(x) \rangle = 0$ and $\langle \Delta(x)\Delta^*(x') \rangle = \Delta_s^2 e^{-|x-x'|/\xi}$. Following Lee, Rice and Anderson [9], we ignore the forward scattering disorder, i.e. set $V(x) \equiv 0$. For a perturbative approach we assume Gaussian statistics for the higher moments of the order parameter field such that these moments can be separated according to Wick's theorem. A diagrammatic representation of the averaged Green function is shown in Fig. 3. An infinite number of diagrams can be summed up by introducing *irreducible diagrams* which by definition cannot be separated into two disconnected diagrams by cutting a single propagator. The corresponding *amputated diagram* is obtained by eliminating all outer propagators. The sum of all amputated irreducible diagrams is known as the *self-energy* and is diagrammatically presented in Fig. 4. In terms of the self-energy, the averaged Green function reads in momentum space

$$\langle \mathcal{G}^R(k; \omega) \rangle = \left[(\mathcal{G}_0^R(k; \omega))^{-1} - \Sigma(k; \omega) \right]^{-1}. \quad (58)$$

The simplest approximation to take into account fluctuation effects of the order parameter is to consider only the first diagram in Fig. 4. This approximation is known

as the second order Born approximation and is essentially the approximation made by Lee, Rice and Anderson in their seminal paper [9] in which fluctuations of the order parameter of the FGM were taken into account for the first time. A special non-Gaussian probability distribution of $\Delta(x)$ involving only phase fluctuations for which the second order Born approximation turns out to be exact is presented in Ref. [52].

3.2.3 The self-energy

Since $\langle \mathbf{V}(x) \rangle = 0$, the self-energy in the second order Born approximation is given by

$$\Sigma_B(x - x'; \omega) = \langle \mathbf{V}(x) \mathcal{G}_0^R(x - x'; \omega) \mathbf{V}(x') \rangle. \quad (59)$$

Placing Eq. (49) into this equation, we get

$$\begin{aligned} (\Sigma_B)_{\alpha\alpha'}(x - x'; \omega) &= \delta_{\alpha,\alpha'} \Delta_s^2 e^{-|x-x'|/\xi} (\mathcal{G}_0^R)_{\bar{\alpha},\bar{\alpha}}(x - x'; \omega) . \\ &= -i\delta_{\alpha,\alpha'} \Delta_s^2 \theta(-\alpha(x - x')) e^{-i\alpha[\omega+i/\xi](x-x')} . \end{aligned} \quad (60)$$

As one should expect, the process of averaging restored translational invariance. Taking the Fourier transform of Eq. (60), we arrive at

$$(\Sigma_B)_{\alpha\alpha'}(k; \omega) = \int dx e^{-ikx} (\Sigma_B)_{\alpha\alpha'}(x; \omega) = \delta_{\alpha,\alpha'} \frac{\Delta_s^2}{\omega + \alpha k + i/\xi}. \quad (61)$$

Within the second order Born approximation, we therefore find for the one-particle Green function

$$(\mathcal{G}_B^R)_{\alpha,\alpha'}(k; \omega) = \frac{\delta_{\alpha,\alpha'}}{\omega - \alpha k - \frac{\Delta_s^2}{\omega + \alpha k + i/\xi}}. \quad (62)$$

This result was first obtained by Lee, Rice and Anderson [9].

3.2.4 The density of states and the inverse localization length

Integrating Eq. (62) over k and taking the trace, we obtain

$$\text{Tr} \mathcal{G}_B^R(x, x; \omega) = -i \frac{\omega + i/2\xi}{\sqrt{(\omega + i/2\xi)^2 - \Delta_s^2}}, \quad (63)$$

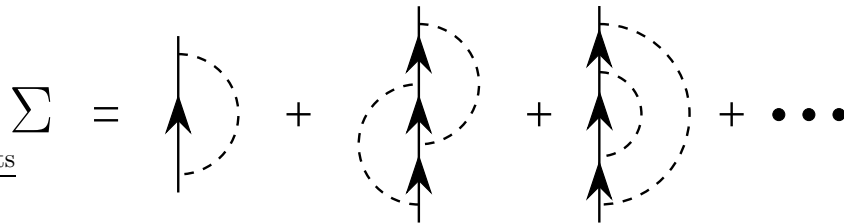


Fig. 4 Diagrammatic representation of the (irreducible) self-energy. As in the above Figure 3, the single line represents the Green function of free fermions and the dashed line denotes the disorder average $\langle \mathbf{V}(x) \mathbf{V}(x') \rangle$.

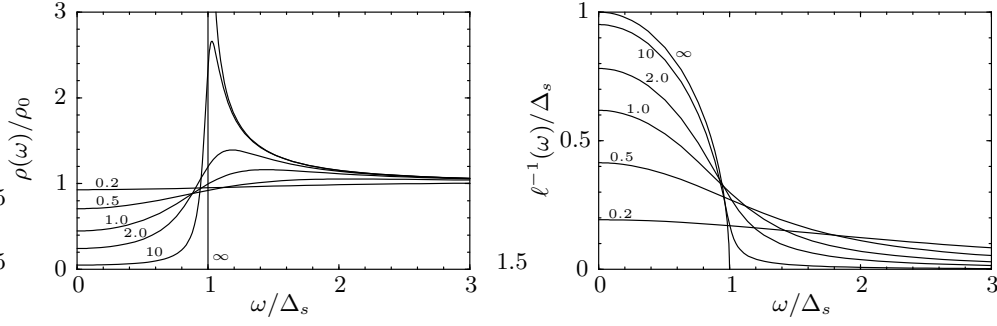


Fig. 5 Plot of the DOS $\rho_B(\omega)$ and the inverse localization length $l_B^{-1}(\omega)$ calculated for $\Delta_s\xi = 0.2, 0.5, 1.0, 2.0, 10.0$, and ∞ (mean-field result) in the second order Born approximation.

where \sqrt{z} is defined as the principal part of the square root with the cut chosen along the negative real axis. The imaginary part of Eq. (63) gives the (averaged) DOS,

$$\rho_B(\omega) = \rho_0 \operatorname{Re} \frac{\omega + i/2\xi}{\sqrt{(\omega + i/2\xi)^2 - \Delta_s^2}}. \quad (64)$$

As we will show in Subsection 3.5, the real part of the Green function is equal to the derivative of the inverse localization length $l_B^{-1}(\omega)$. Integrating this equation with respect to ω and setting the integration constant at infinity equal to zero, we obtain

$$l_B^{-1}(\omega) = \operatorname{Im} \sqrt{(\omega + i/2\xi)^2 - \Delta_s^2} - 1/2\xi. \quad (65)$$

A plot of both $\rho_B(\omega)$ and $l_B^{-1}(\omega)$ is shown for different values of the dimensionless parameter $\Delta_s\xi$ in Fig. 5. With increasing correlation length ξ , the DOS gets more and more suppressed for $\omega \lesssim \Delta_s$. However, instead of a real gap the fluctuations can only create a pseudogap. At $\omega = 0$, the DOS is given by

$$\rho_B(0) = \rho_0 \frac{1}{\sqrt{1 + (2\Delta_s\xi)^2}}, \quad (66)$$

such that for $\Delta_s\xi \gg 1$, the DOS vanishes as

$$\rho_B(0) \sim \frac{\rho_0}{2\Delta_s\xi} \propto \frac{1}{\Delta_s\xi}. \quad (67)$$

As the correlation length approaches infinity, the DOS assumes the mean-field result

$$\rho^{\text{MF}}(\omega) = \rho_0 \frac{|\omega|}{\sqrt{\omega^2 - \Delta_0^2}} \theta(\omega^2 - \Delta_0^2), \quad (68)$$

At zero frequency, the inverse localization length is given by

$$l_B^{-1}(0) = \Delta_s \left[\sqrt{1 + (1/2\Delta_s\xi)^2} - 1/2\Delta_s\xi \right]. \quad (69)$$

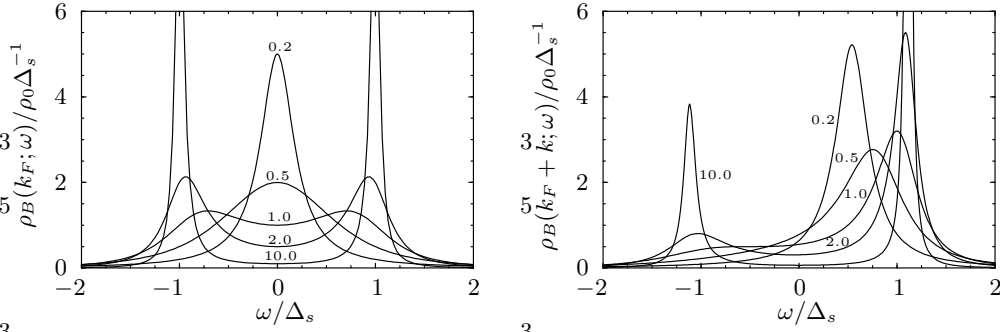


Fig. 6 Plot of the spectral function $\rho_B(k_F + k; \omega)$ with $\Delta k = 0.0$ (left-hand side) and 0.5 (right-hand side) calculated for $\Delta_s \xi = 0.2, 0.5, 1.0, 2.0, 10.0$ in the second order Born approximation.

3.2.5 The spectral function

Another interesting quantity related to the single-particle Green function is the spectral function

$$\rho(\alpha k_F + k; \omega) = -\frac{1}{\pi} \text{Im} (\mathcal{G}^R(k; \omega))_{\alpha, \alpha} . \quad (70)$$

Experimentally, the spectral function can be measured by angular resolved photoemission spectroscopy (ARPES). It follows from Eq. (62) that in the Born approximation, the spectral function is given by

$$\rho_B(\alpha k_F + k; \omega) = \rho_0 \frac{\Delta_s^2 \xi}{(\Delta_s^2 - (\omega^2 - k^2))^2 \xi^2 + (\omega - \alpha k)^2} . \quad (71)$$

Plots of the spectral function $\rho_B(\alpha k_F; \omega)$ and $\rho_B(\alpha k_F + k; \omega)$ with $k = 0.5 \Delta_s$ as functions of ω are shown for different values of $\Delta_s \xi$ in Figs 6. While for small correlation lengths, i.e. $\Delta_s \xi \ll 1$ the spectral function exhibits a maximum near $\omega = \alpha k$, for large correlation lengths we find two maxima near $\omega = \pm \sqrt{\Delta_s^2 + k^2}$, the closest one to αk having the larger weight.

Corrections to the second order Born approximation and Sadovskii's solution

An attempt to sum up all diagrams in the perturbative expansion of the averaged Green function was made by Sadovskii in the late seventies [10]. The first diagram in Fig. 4 which represents the contribution given by Eq. (61) can be calculated by attributing a factor of Δ_s^2 to the phonon line and a factor $(\mathcal{G}_0^R)_{\bar{\alpha}\bar{\alpha}}(k; \omega + i/\xi)$ to the fermion line. Sadovskii conjectured that all other non-vanishing diagrams could be calculated using a similar recipe. (In the general case, the imaginary part added to ω has to be multiplied by the number of phonon lines above a given fermion line.) This recipe enabled Sadovskii to give a continued fraction representation of the self-energy (or Green function). Sadovskii's solution was known as the only available exact solution of the pseudo-gap state (see Ref. [14]) and was therefore also used by other authors [11, 12, 53]. However, only recently, Tchernyshyov [14] discovered

an unfortunate error in Sadovskii's solution which also turned the work based on it into question. As pointed out by Tchernyshyov, Sadovskii's conjecture already breaks down for terms contributing to the next to leading order in the self-energy. While Sadovskii neglects the second term in Fig. 4, which is correct for the incommensurate case, the last term in this figure already gives a different contribution than conjectured by Sadovskii. Instead of trying to correctly sum up all diagrams in the perturbative expansion of the Green function we will now develop a method which will allow for a non-perturbative calculation of the Green function.

3.3 Non-Abelian Schwinger-ansatz

We base our non-perturbative approach to calculate the Green function of the FGM on a matrix generalization of the Schwinger-ansatz [54]. To make the differential operator $-i\partial_x$ proportional to the unit matrix, we first factor out a Pauli matrix σ_3 , so that the retarded Green function

$$\tilde{\mathcal{G}}^R(x, x'; \omega) = \sigma_3 \mathcal{G}^R(x, x'; \omega) \quad (72)$$

satisfies

$$[i\partial_x - M(x, \omega + i0^+)]\tilde{\mathcal{G}}^R(x, x'; \omega) = \delta(x - x')\sigma_0, \quad (73)$$

where

$$M(x, \omega) = [V(x) - \omega + \Delta(x)\sigma_+ + \Delta^*(x)\sigma_-]\sigma_3 \quad (74)$$

is a traceless matrix. We now try to solve Eq. (73) by making the ansatz

$$\tilde{\mathcal{G}}^R(x, x', \omega) = U(x, \omega) \tilde{\mathcal{G}}_0^R(x - x') U^{-1}(x', \omega), \quad (75)$$

where $U(x, \omega)$ is an invertible 2×2 matrix and $\tilde{\mathcal{G}}_0^R(x)$ is the Green function to the operator $i\partial_x + i0^+\sigma_3$, i.e.

$$\tilde{\mathcal{G}}_0^R(x) = -i \begin{pmatrix} \theta(x) & 0 \\ 0 & -\theta(-x) \end{pmatrix}. \quad (76)$$

The ansatz (75) resembles the transformation law for the comparator in non-Abelian Gauge theory (see, for example, the book on quantum field theory by Peskin and Schröder [55]), and since it is also similar to the scalar Schwinger-ansatz [54] which is sometimes used in functional bosonization of interacting fermions [56], we will refer to it as the non-Abelian Schwinger-ansatz [22, 24, 38]. But note that in contrast to earlier formulations of the non-Abelian Schwinger-ansatz [22, 38], we use the zero-frequency free retarded Green function, such that the whole ω dependence is included in $U(x, \omega)$.

In the following we are going to suppress the parameter ω . The ansatz (75) indeed solves Eq. (73) if $U(x)$ satisfies

$$[i\partial_x - M(x)]U(x) = 0. \quad (77)$$

To establish our formalism, let us first restrict the disorder potentials to the interval $(-\Lambda, L + \Lambda)$. While the potentials are assumed to be constant in the intervals $(-\Lambda, 0)$ and $(L, L + \Lambda)$, they are allowed to fluctuate in between. Later we can let $\Lambda \rightarrow \infty$ (or

we will set $\Lambda = 0$ and let $L \rightarrow \infty$). The boundary conditions for the retarded Green function given in Eq. (57) now renders into³

$$U_{12}(-\Lambda) = U_{21}(L + \Lambda) = 0. \quad (78)$$

Two different solutions of Eq. (77) are given by

$$U_+(x) = T \exp \left[-i \int_{-\Lambda}^x M(y) dy \right], \quad (79)$$

$$U_-(x) = T^{-1} \exp \left[i \int_x^{L+\Lambda} M(y) dy \right], \quad (80)$$

where $T \exp$ is the path-ordered and $T^{-1} \exp$ is the anti-path-ordered exponential function. Both, $U_+(x)$ and $U_-(x)$ can be expressed in terms of the S -matrix,

$$S(x, x') = T \exp \left[-i \int_{x'}^x M(y) dy \right]. \quad (81)$$

By definition, $U_+(x) = S(x, -\Lambda)$ and $U_-(x) = S^{-1}(L + \Lambda, x)$. Because $M^\dagger = \sigma_3 M \sigma_3$ and $\text{Tr} M = 0$, the S -matrices satisfy $S^\dagger = \sigma_3 S^{-1} \sigma_3$ and $\det S = 1$, which means that they belong to the non-compact group $SU(1, 1)$. It follows that the elements of S satisfy $S_{22} = S_{11}^*$, $S_{21} = S_{12}^*$, and $|S_{11}|^2 - |S_{12}|^2 = 1$. While each $U_\alpha(x)$ only obeys one of the two conditions (78), the combination

$$U(x) \equiv \frac{1}{\sqrt{u}} \begin{pmatrix} U_{-11}(x) & U_{+12}(x) \\ U_{-21}(x) & U_{+22}(x) \end{pmatrix} \quad (82)$$

satisfies both boundary conditions. Here, $u = S_{22}(L + \Lambda, -\Lambda) = U_{-11}(-\Lambda) = U_{+22}(L + \Lambda)$, so that $\det U(x) = 1$. Defining⁴

$$\mathbf{u}_\alpha \equiv (U_{\alpha 11}, -U_{\alpha 21})^T, \quad \mathbf{v}_\alpha \equiv (-U_{\alpha 12}, U_{\alpha 22})^T, \quad (83)$$

(such that $\mathbf{v}_\alpha = \sigma_1 \mathbf{u}_\alpha^*$), we obtain from Eqs. (72), (75) and (82)

$$i\mathcal{G}^R(x, x'; \omega) = \theta(x - x') \frac{\mathbf{u}_-(x) \mathbf{u}_+^\dagger(x')}{u} + \theta(x' - x) \frac{\mathbf{v}_+(x) \mathbf{v}_-^\dagger(x')}{u}. \quad (84)$$

\mathbf{u}_+^\dagger and \mathbf{v}_-^\dagger are the adjungated row vectors to the column vectors \mathbf{u}_+ and \mathbf{v}_- , so that $\mathbf{u}_- \mathbf{u}_+^\dagger$ and $\mathbf{v}_+ \mathbf{v}_-^\dagger$ are 2×2 -matrices. Note that Eq. (84) involves only U_{+12} , U_{+22} , U_{-12}^* and U_{-22}^* , but not its complex conjugates. In principle, Eq. (84) allows to determine the full Green function of the FGM by evaluating time-ordered exponential functions. Equivalent but more complicated forms of this equation were first derived

³In this work we will identify matrix elements as U_{ij} with $U_{\alpha\alpha'}$, where $i, j = 1, 2$ corresponds to $\alpha, \alpha' = +, -$, e.g. $U_{12} \equiv U_{+-}$.

⁴Note, that this definition deviates from the definition used in Ref. [24]. Here, the vectors \mathbf{u}_α and \mathbf{v}_α are given by the first and second column of the matrix U_α multiplied from the left by $\pm\sigma_3$.

by Abrikosov and Ryzhkin [57]. Of special interest will be the trace of the Green function at coinciding space points,

$$\text{Tr}[i\mathcal{G}^R(x, x; \omega)] = \frac{U_{+22}(x)U_{-22}^*(x) + U_{+12}(x)U_{-12}^*(x)}{U_{+22}(x)U_{-22}^*(x) - U_{+12}(x)U_{-12}^*(x)}. \quad (85)$$

It immediately follows from Eq. (44) that the local DOS is given by

$$\rho(x, \omega) = \frac{1}{\pi} \text{Re} \left(\frac{U_{+22}(x)U_{-22}^*(x) + U_{+12}(x)U_{-12}^*(x)}{U_{+22}(x)U_{-22}^*(x) - U_{+12}(x)U_{-12}^*(x)} \right). \quad (86)$$

3.3.1 Riccati equation

Since Eq. (86) only depends on the ratios⁵

$$\Phi_\alpha(x) \equiv U_{\alpha 12}(x)/U_{\alpha 22}(x), \quad (87)$$

we may also write the DOS as

$$\rho(x, \omega) = \frac{1}{\pi} \text{Re} \left(\frac{1 + \Phi_+(x)\Phi_-^*(x)}{1 - \Phi_+(x)\Phi_-^*(x)} \right). \quad (88)$$

More generally, it follows from Eq. (84) that the whole matrix Green function at coinciding space points can be written in terms of $\Phi_+(x)$ and $\Phi_-^*(x)$:

$$\begin{aligned} i\mathcal{G}^R(x, x; \omega) &\equiv \frac{i}{2} [\mathcal{G}^R(x + 0^+, x; \omega) + \mathcal{G}^R(x, x + 0^+; \omega)] \\ &= \frac{1}{1 - \Phi_+(x)\Phi_-^*(x)} \begin{pmatrix} \frac{1}{2}(1 + \Phi_+(x)\Phi_-^*(x)) & -\Phi_+(x) \\ -\Phi_-^*(x) & \frac{1}{2}(1 + \Phi_+(x)\Phi_-^*(x)) \end{pmatrix}. \end{aligned} \quad (89)$$

Using Eq. (77), we find that the $\Phi_\alpha(x)$ are both solutions of the same Riccati equation,

$$-i\partial_x \Phi_\alpha(x) = 2\tilde{\omega}(x)\Phi_\alpha(x) + \Delta(x) + \Delta^*(x)\Phi_\alpha^2(x). \quad (90)$$

Here, we have introduced $\tilde{\omega}(x) = \omega - V(x)$. Similar Riccati equations have recently been obtained by Schopohl [58] from the Eilenberger equations of superconductivity. To specify the initial conditions, let us assume that outside the interval $[0, L]$ the potentials $V(x)$ and $\Delta(x)$ are real constants, V_{BC} and $\Delta_{\text{BC}} \geq 0$. This amounts to taking the limit $\Lambda \rightarrow \infty$, but keeping L constant. The initial values $\Phi_+(0) = \lim_{\Lambda \rightarrow \infty} S_{12}(0, -\Lambda)/S_{22}(0, -\Lambda)$ and $\Phi_-(L) = \lim_{\Lambda \rightarrow \infty} (S^{-1})_{12}(L + \Lambda, L)/(S^{-1})_{22}(L + \Lambda, L)$ can be obtained by evaluating the S -matrix for constant potentials.

3.3.2 The S -matrix for constant potentials

For constant potentials V_n and Δ_n , the time-ordering operator T may be omitted in Eq. (81), and the S -matrix is given by

$$\begin{aligned} S_n(x - x') &= \cosh[\sqrt{|\Delta_n|^2 - \tilde{\omega}_n^2}(x - x')] \sigma_0 \\ &\quad + i \sinh[\sqrt{|\Delta_n|^2 - \tilde{\omega}_n^2}(x - x')] \frac{\tilde{\omega}_n \sigma_3 + \Delta_n \sigma_+ - \Delta_n^* \sigma_-}{\sqrt{|\Delta_n|^2 - \tilde{\omega}_n^2}}. \end{aligned} \quad (91)$$

⁵Note also that the definition of $\Phi_\alpha(x)$ does not involve the extra factor $\pm i$ used in Ref. [24].

For $|\Delta_n|^2 < \tilde{\omega}_n^2$, the argument of the square root is negative, so that in this case we write the S -matrix as

$$S_n(x-x') = \cos[\sqrt{\tilde{\omega}_n^2 - |\Delta_n|^2}(x-x')] \sigma_0 + i \sin[\sqrt{\tilde{\omega}_n^2 - |\Delta_n|^2}(x-x')] \frac{\tilde{\omega}_n \sigma_3 + \Delta_n \sigma_+ - \Delta_n^* \sigma_-}{\sqrt{\tilde{\omega}_n^2 - |\Delta_n|^2}}. \quad (92)$$

For notational simplicity, let us introduce $\Delta_n^{\text{red}} \equiv \sqrt{|\Delta_n|^2 - \tilde{\omega}_n^2}$. To calculate $\Phi_+(0)$ and $\Phi_-(L)$, we take the limit $x \rightarrow \pm\infty$ of the ratio $S_{n12}(x)/S_{n22}(x)$ and obtain

$$\lim_{x \rightarrow \pm\infty} \frac{S_{n12}(x)}{S_{n22}(x)} = \frac{\pm i \Delta_n^{\text{red}} - \tilde{\omega}_n}{\Delta_n^*}. \quad (93)$$

If we keep in mind that the frequency ω involves a small imaginary part, we see that this result is not restricted to the case $|\Delta_n|^2 > \tilde{\omega}_n^2$: For $|\Delta_n|^2 \leq \tilde{\omega}_n^2$ the square root has to be taken such that the right-hand side of Eq. (93) vanishes as $\Delta_n \rightarrow 0$. This follows directly from the definition of the S -matrix.

3.3.3 Initial conditions

It follows from Eq. (93) that the Riccati equation (90) should be integrated with the initial conditions

$$\begin{aligned} \Phi_+(0) &= \Phi_-^*(L) \\ &= \begin{cases} \frac{i\sqrt{\Delta_{\text{BC}}^2 - (\omega - V_{\text{BC}})^2} - (\omega - V_{\text{BC}})}{\Delta_{\text{BC}}} & , \Delta_{\text{BC}}^2 > (\omega - V_{\text{BC}})^2, \\ \frac{\text{sgn}(\omega - V_{\text{BC}})\sqrt{(\omega - V_{\text{BC}})^2 - \Delta_{\text{BC}}^2} - (\omega - V_{\text{BC}})}{\Delta_{\text{BC}}} & , \Delta_{\text{BC}}^2 \leq (\omega - V_{\text{BC}})^2, \end{cases} \end{aligned} \quad (94)$$

where $\text{sgn}(x)$ is equal to 1 for positive x and equal to -1 for negative x . While for $\Delta_{\text{BC}} = 0$ the initial conditions are given by $\Phi_+(0) = \Phi_-^*(L) = 0$, for $\Delta_{\text{BC}} \rightarrow \infty$ one gets $\Phi_+(0) = \Phi_-^*(L) = i$. Note that for arbitrary potentials V_{BC} and Δ_{BC} , the initial values are simply given by the stable stationary solution of the Riccati equation (90) with $V(x) = V_{\text{BC}}$ and $\Delta(x) = \Delta_{\text{BC}}$.

3.3.4 The case of a discrete spectrum

Defining the (complex) phase $\varphi_\alpha(x)$ via

$$\Phi_\alpha(x) = e^{i\varphi_\alpha(x)}, \quad (95)$$

and decomposing $\Delta(x)$ into its amplitude $|\Delta(x)|$ and its phase $\vartheta(x)$,

$$\Delta(x) = |\Delta(x)| e^{i\vartheta(x)}, \quad (96)$$

the Riccati equation (90) turns into

$$\boxed{\partial_x \varphi_\alpha(x) = 2\tilde{\omega}(x) + 2|\Delta(x)| \cos[\varphi_\alpha(x) - \vartheta(x)]}. \quad (97)$$

Note that this equation of motion is of the Langevin type [59, 60]

$$\partial_x v(x) = -a + b_1 V(x) + b_2^*(v) \Delta(x) + b_2(v) \Delta^*(x). \quad (98)$$

Let us consider the case $(\omega - V_{\text{BC}})^2 < \Delta_{\text{BC}}^2$: It directly follows from Eq. (94) that $|\Phi_+(0)| = |\Phi_-(L)| = 1$, such that the initial values $\varphi_+(0)$ and $\varphi_-(L)$ are real. Hence, the solutions of Eq. (97) remain real, which implies $|\Phi_\alpha(x)| = 1$ for all x . As can be seen from Eq. (94), $\varphi_+(0)$ and $\varphi_-(L)$ can be chosen to fulfill $\varphi_+(0) = -\varphi_-(L) \in [0, \pi]$, so that the initial values $\varphi_+(0)$ and $\varphi_-(L)$ are uniquely determined by

$$\cot \varphi_+(0) = -\cot \varphi_-(L) = -\frac{\omega - V_{\text{BC}}}{\sqrt{\Delta_{\text{BC}}^2 - (\omega - V_{\text{BC}})^2}}. \quad (99)$$

For the phases $\varphi_\alpha(x)$ to be continuous, they have to be unreduced phases which are not limited to take values between 0 and 2π . In terms of the $\varphi_\alpha(x)$, the local DOS can be written as

$$\begin{aligned} \rho(x, \omega) &= -\frac{1}{\pi} \text{Im} \cot \left[\frac{\varphi_+(x) - \varphi_-(x)}{2} + i0 \right] \\ &= 2 \sum_{m=-\infty}^{\infty} \delta(\varphi_+(x) - \varphi_-(x) - 2\pi m). \end{aligned} \quad (100)$$

It is easy to show that for $x \geq 0$ the phase $\varphi_+(x, \omega)$ is a monotonic increasing function of ω . For the initial value at $x = 0$, this follows from Eq. (99):

$$\partial_\omega \varphi_+(0) = -\partial_\omega \varphi_-(L) = \frac{1}{\sqrt{\Delta_{\text{BC}}^2 - (\omega - V_{\text{BC}})^2}} > 0. \quad (101)$$

It can be seen directly from Eq. (97) that $\partial_\omega \varphi_+(x) > 0$ is true for every $x \geq 0$. More formally, differentiating the equation of motion (97) with respect to ω gives

$$\partial_x \partial_\omega \varphi_\alpha(x, \omega) = 2 - 2|\Delta(x)| \sin[\varphi_\alpha(x) - \vartheta(x)] \partial_\omega \varphi_\alpha(x, \omega). \quad (102)$$

Solving this first-order differential equation for $\partial_\omega \varphi_\alpha(x, \omega)$, we obtain

$$\begin{aligned} \partial_\omega \varphi_\alpha(x, \omega) &= \partial_\omega \varphi_\alpha(x_0, \omega) \\ &+ 2 \int_{x_0}^x \exp \left[-2 \int_{x'}^x |\Delta(x'')| \sin[\varphi_\alpha(x'') - \vartheta(x'')] dx'' \right] dx'. \end{aligned} \quad (103)$$

Since both terms on the right-hand side of Eq. (103) are positive for $\alpha = +$ and $x_0 = 0$, we have $\partial_\omega \varphi_+(x, \omega) > 0$ for $x \geq 0$. Analogously we find $\partial_\omega \varphi_-(x, \omega) < 0$ for $x \leq L$. For arbitrary ω , $\varphi_+(x, \omega)$ integrated with the initial condition $\varphi_+(0, \omega)$ given in Eq. (99) will usually not be equal to $\varphi_-(L, \omega)$ up to a multiple of 2π at $x = L$. For certain discrete frequencies ω_m , however, this is the case. Since $\varphi_+(x, \omega)$ is a monotonic function of ω , we can uniquely define ω_m by the condition

$$\varphi_+(L, \omega_m) = \varphi_-(L, \omega_m) + 2\pi m. \quad (104)$$

Note that ω_m is only well-defined if it turns out that $(\omega_m - V_{\text{BC}})^2 < \Delta_{\text{BC}}^2$. Since the right-hand side of Eq. (97) is a 2π -periodic function of $\varphi_\alpha(x)$, we see that $\varphi_+(x, \omega_m)$ and $\varphi_-(x, \omega_m)$ are equal up to the constant $2\pi m$ for every $x \in [0, L]$,

$$\varphi_+(x, \omega_m) - \varphi_-(x, \omega_m) = 2\pi m. \quad (105)$$

Of course, the ω_m are the discrete eigenvalues of the system. This follows immediately from the fact that the local DOS $\rho(x, \omega)$ is equal to zero if not $\omega = \omega_m$ for one m . Therefore, the total DOS is given by

$$\rho(\omega) = \frac{1}{L} \sum_m \delta(\omega - \omega_m). \quad (106)$$

Using the well-known formula $\delta(f(\omega)) = \sum_m \frac{1}{|f'(\omega_m)|} \delta(\omega - \omega_m)$, where ω_m are the zeros of $f(\omega)$, we can write Eq. (100) as

$$\rho(x, \omega) = \sum_m \frac{2\delta(\omega - \omega_m)}{|\partial_\omega \varphi_+(x, \omega) - \partial_\omega \varphi_-(x, \omega)|}. \quad (107)$$

Expressing $\partial_\omega \varphi_\alpha(x, \omega)$ by the right-hand side of Eq. (103) with $\alpha = +$ and $x_0 = 0$ or $\alpha = -$ and $x_0 = L$, respectively, we arrive for $\Delta_{BC} = \infty$ at

$$\rho(x, \omega) = \sum_m \frac{\delta(\omega - \omega_m)}{\int_0^L dx' \exp(-2 \int_{x'}^x dx'' |\Delta(x'')| \sin[\varphi_\alpha(x'', \omega_m) - \vartheta(x'')])}. \quad (108)$$

Once the eigenvalues ω_m have been determined, this equation in principle allows to calculate the local DOS for arbitrary potentials $V(x)$ and $\Delta(x)$.

3.3.5 Integrated averaged Green function $\Gamma(\omega)$

In the last subsection, we have seen that the integrated DOS can be obtained by solving a simple initial value problem for the phase $\varphi(x)$, which is a functional of the disorder. To implement the correct boundary conditions for a system of length L , we have first assumed that outside the interval $(0, L)$ the potentials are constant over a range Λ , but then drop to zero. Finally, we have let Λ go to infinity. However, if we are only interested in the limit $L \rightarrow \infty$, i.e. the bulk properties, we can set $\Lambda = 0$ at the beginning of our calculations. The physical meaning of this is that bulk properties should be independent of the boundary conditions.

By setting the potential equal to zero outside the interval $(0, L)$, we will not only be able to recover the equation of motion (97) satisfied by the phase $\varphi(x)$ which determines the integrated DOS, we will also be able to derive an additional equation which allows to calculate the inverse localization length.

It follows from Eq. (85) that the trace of the space-averaged diagonal element of the retarded Green function is given by

$$\begin{aligned} \langle \text{Tr}[\mathcal{G}^R(x, x; \omega)] \rangle_x &\equiv \frac{1}{L} \int_0^L dx \text{Tr}[\mathcal{G}^R(x, x; \omega)] \\ &= \frac{1}{L S_{22}(L, 0)} \left[-i \int_0^L dx (S_{22}(L, x) S_{22}(x, 0) - S_{21}(L, x) S_{12}(x, 0)) \right]. \end{aligned} \quad (109)$$

The term in angular brackets can easily be identified to be equal to $\partial_\omega S_{22}(L, 0)$. We can therefore rewrite Eq. (109) as

$$\langle \text{Tr}[\mathcal{G}^R(x, x; \omega)] \rangle_x = \frac{\partial_\omega S_{22}(L, 0)}{L S_{22}(L, 0)} = \frac{1}{L} \partial_\omega \ln [S_{22}(L, 0)]. \quad (110)$$

To describe the bulk properties, one should now take the limit $L \rightarrow \infty$. If we introduce $\Gamma(\omega)$ as the trace of the energy-integrated space-averaged Green function at coinciding space points,

$$\Gamma(\omega) \equiv \lim_{L \rightarrow \infty} \frac{1}{L} \ln [S_{22}(L, 0; \omega)] , \quad (111)$$

we have

$$\langle \text{Tr}[\mathcal{G}^R(x, x; \omega)] \rangle = \partial_\omega \Gamma(\omega) . \quad (112)$$

While the integrated DOS is given by $\mathcal{N}(\omega) = -\pi^{-1} \text{Im} \Gamma(\omega)$, we will see in the next subsection that $\text{Re} \Gamma(\omega)$ is equal to the inverse localization length $\ell^{-1}(\omega)$. The decomposition of $\Gamma(\omega)$ into its real and imaginary part can therefore be written as

$$\Gamma(\omega) = \ell^{-1}(\omega) - i\pi \mathcal{N}(\omega) . \quad (113)$$

Both $\mathcal{N}(\omega)$ and $\ell^{-1}(\omega)$ can simultaneously be calculated by determining the logarithm of the S -matrix element S_{22} . It is convenient to express the S -matrix elements in terms of their phases. Let us define $\varphi_{\alpha\alpha'}(x)$ via

$$S_{\alpha\alpha'}(x, 0) \equiv e^{-i\varphi_{\alpha\alpha'}(x)} . \quad (114)$$

$\Gamma(\omega)$ is then given by

$$i\Gamma(\omega) = \lim_{L \rightarrow \infty} \frac{\varphi_{22}(L)}{L} . \quad (115)$$

Introducing $\bar{\alpha} \equiv -\alpha$, the properties of the S -matrix $S_{\alpha\alpha'} = S_{\bar{\alpha}\bar{\alpha}}^*$ render into $\varphi_{\alpha\alpha'} = -\varphi_{\bar{\alpha}\bar{\alpha}}^*$. The S -matrix can be expressed in terms of φ_{12} , φ_{22} and its complex conjugates.⁶ It follows from $i\partial_x S(x, 0) = M(x)S(x, 0)$ that the $\varphi_{\alpha\alpha'}$ satisfy

$$\partial_x \varphi_{\alpha\alpha'}(x) = M_{\alpha\alpha}(x) + M_{\alpha\bar{\alpha}}(x) \exp [i(\varphi_{\alpha\alpha'}(x) - \varphi_{\bar{\alpha}\alpha'}(x))] . \quad (116)$$

Recalling that $M(x) = -\tilde{\omega}(x)\sigma_3 - \Delta(x)\sigma_+ + \Delta^*(x)\sigma_-$, the two equations for φ_{12} and φ_{22} read

$$\partial_x \varphi_{22}(x) = \tilde{\omega}(x) + \Delta^*(x) \exp [i(\varphi_{22}(x) - \varphi_{12}(x))] , \quad (117)$$

$$\partial_x \varphi_{12}(x) = -\tilde{\omega}(x) - \Delta(x) \exp [-i(\varphi_{22}(x) - \varphi_{12}(x))] . \quad (118)$$

If we now introduce

$$\varphi(x) \equiv \varphi_{22}(x) - \varphi_{12}(x) , \quad (119)$$

$$\zeta(x) \equiv -i(\varphi_{22}(x) + \varphi_{12}(x)) , \quad (120)$$

we arrive at the following system of equations of motion:

$$\partial_x \varphi(x) = 2\tilde{\omega}(x) + 2|\Delta(x)| \cos [\varphi(x) - \vartheta(x)] , \quad (121)$$

$$\partial_x \zeta(x) = 2|\Delta(x)| \sin [\varphi(x) - \vartheta(x)] . \quad (122)$$

⁶Recall that instead of $\alpha, \alpha' = +, -$ we also use $i, j = 1, 2$ (see footnote 3 on page 20)

Note that Eq. (121), which determines $\varphi(x)$, is exactly the same Langevin equation that we derived before from the Riccati equation [see Eq. (97)] and is independent from Eq. (122). After having found a solution to Eq. (121), $\zeta(x)$ can in principle be obtained by integrating Eq. (122). In terms of $\varphi(x)$ and $\zeta(x)$, $\Gamma(\omega)$ is now given by

$$i\Gamma(\omega) = \lim_{L \rightarrow \infty} [\varphi(L) + i\zeta(L)] / 2L . \quad (123)$$

The initial condition $S(0, 0) = \sigma_0$ could be mapped on the initial conditions for $\varphi(0)$ and $\zeta(0)$ which are, strictly speaking, singular but integrable. In the limit $L \rightarrow \infty$, the initial conditions finally drop out, but to describe bulk properties for finite L , it is better to choose $\varphi(0) = \zeta(0) = 0$, such that $\varphi(x)$ and $\zeta(x)$ are real for all x and there is no contribution to $\Gamma(\omega)$ which as L becomes large only dies out as $1/L$. The integrated DOS and the inverse localization length can now be expressed as

$$\mathcal{N}(\omega) = \rho_0 \lim_{L \rightarrow \infty} \varphi(L) / 2L , \quad (124)$$

$$\ell^{-1}(\omega) = \lim_{L \rightarrow \infty} \zeta(L) / 2L . \quad (125)$$

These two equations in combination with the equations of motion (121) and (122) allow for simultaneous exact numerical computations of the (integrated) DOS and the inverse localization length for arbitrary given disorder potentials. Since the (integrated) DOS and the inverse localization length are self-averaging quantities [20], it is sufficient to consider just one typical realization of the disorder potential. We will do this for various interesting cases in Section 5.

In analytical calculations one does not usually work with a certain realization of the disorder. Instead, one tries to calculate *averaged* quantities by using the given statistical properties of the disorder potentials. Taking the average of Eq. (123) with respect to the distribution of the random potentials $V(x)$ and $\Delta(x)$, we obtain

$$i\langle \Gamma(\omega) \rangle = \lim_{L \rightarrow \infty} [\langle \varphi(L) \rangle + i\langle \zeta(L) \rangle] / 2L . \quad (126)$$

Integrating the equations of motion (121) and (122) with respect to x from 0 to L , $\langle \Gamma(\omega) \rangle$ can be rewritten as

$$i\langle \Gamma(\omega) \rangle = \lim_{L \rightarrow \infty} \frac{1}{L} \int_0^L dx \langle \tilde{\omega}(x) + \Delta^*(x) \exp[i\varphi(x)] \rangle . \quad (127)$$

The average in Eq. (127) has to be taken with respect to the probability distribution involving the disorder at x and via $\varphi(x)$ also at all space points between 0 and x , which can also be considered as an average with respect to the joint probability distribution of the random potentials at x and the *unreduced* phase $\varphi(x)$. However, since $\exp[i\varphi(x)]$ is a 2π -periodic function in $\varphi(x)$, it is also sufficient to use the joint probability distribution of the random potentials and the *reduced* phase $\varphi(x) \in [0, 2\pi)$. For large x , the joint probability distribution becomes stationary, and since $\langle V(x) \rangle = 0$, Eq. (127) reduces to

$$i\langle \Gamma(\omega) \rangle = \omega + \langle \Delta^*(x) \exp[i\varphi(x)] \rangle . \quad (128)$$

We will use Eq. (128) in Section 4 to calculate both $\mathcal{N}(\omega)$ and $\ell^{-1}(\omega)$ for the FGM in the white noise limit.

3.4 Gauge invariance

It turns out that fluctuations of the forward scattering disorder have similar effects on the DOS and localization length as have phase fluctuations of the gap parameter. To illuminate the hidden symmetry, let us again consider the equation satisfied by the retarded Green function $\mathcal{G}^R(x, x'; \omega)$,

$$\begin{pmatrix} \omega - V(x) + i\partial_x & -\Delta(x) \\ -\Delta^*(x) & \omega - V(x) - i\partial_x \end{pmatrix} \mathcal{G}^R(x, x'; \omega) = \delta(x - x')\sigma_0. \quad (129)$$

A crucial point of this equation is that its form is left invariant under the gauge transformation [61]

$$\mathcal{G}^R(x, x'; \omega) \rightarrow \exp[-(i/2)\chi(x)\sigma_3] \mathcal{G}^R(x, x'; \omega) \exp[(i/2)\chi(x')\sigma_3], \quad (130)$$

$$V(x) \rightarrow V(x) + \frac{1}{2}\partial_x\chi(x), \quad (131)$$

$$\Delta(x) \rightarrow \Delta(x) \exp[-i\chi(x)]. \quad (132)$$

Here, $\chi(x)$ is a local phase rotation which is allowed to vary arbitrarily from point to point. Since the trace of a product of matrices is invariant under cyclic permutations of the matrices, $\text{Tr} \mathcal{G}^R(x, x; \omega)$ and therefore the local DOS and the inverse localization length are also invariants under the above gauge transformation.⁷

Instead of directly looking at the trace of the Green function at coinciding space points, we can also consider the equations of motion (121) and (122). Their form is gauge invariant under the combined transformation

$$\varphi(x) \rightarrow \varphi(x) - \chi(x), \quad (133)$$

$$\zeta(x) \rightarrow \zeta(x), \quad (134)$$

$$V(x) \rightarrow V(x) + \frac{1}{2}\partial_x\chi(x), \quad (135)$$

$$\vartheta(x) \rightarrow \vartheta(x) - \chi(x). \quad (136)$$

It follows from Eqs. (124) and (125) that both the integrated DOS $\mathcal{N}(\omega)$ and the inverse localization length $\ell^{-1}(\omega)$ are invariant under the considered gauge transformations. Only in the unusual case of a finite limit $\lim_{L \rightarrow \infty} \chi(L)/L$ we get an irrelevant shift in the additive constant of $\mathcal{N}(\omega)$. The choices for which either $V(x)$ or $\vartheta(x)$ vanishes are especially convenient.

1. *Effectively vanishing phase fluctuations:* If $\vartheta(x)$ is differentiable, we can define $\chi(x) \equiv \vartheta(x)$, such that there are no phase fluctuations of $\Delta(x)$ left and $\Delta(x)$ can be taken to be real and positiv. We will use the resulting transformations $V(x) \rightarrow V(x) + \partial_x\vartheta(x)/2$ and $\Delta(x) \rightarrow |\Delta(x)|$ at the end of Section 5 to find an exact solution for the FGM involving only phase fluctuations.

⁷Strictly speaking, it follows only that $\partial_\omega \ell^{-1}(\omega)$ is left invariant. The integration constants at $\omega = \infty$ are, however, the same, so that $\ell^{-1}(\omega)$ is invariant under the gauge transformation.

2. *Effectively vanishing forward scattering potential:* Choosing the phase $\chi(x)$ such that $\partial_x \chi(x)/2 = -V(x)$, the forward scattering potential $V(x)$ can be eliminated by renormalizing the phase fluctuations $\vartheta(x)$ of the backscattering potential $\Delta(x)$.

3.5 Lyapunov exponent and localization length

In this subsection, we will explicitly show that the Thouless formula holds for the FGM and that $\text{Re} \Gamma(\omega)$ can indeed be identified with the inverse localization length $\ell^{-1}(\omega)$.

One of the striking properties of disordered systems treated in the independent electron approximation is the fact that the disorder can lead to a macroscopic large number of localized states. These states are eigenfunction of the Schrödinger equation falling off exponentially with distance from one point in space which is characteristic for the particular solution. In one dimension, an arbitrary weak disorder suffices to localize all eigenstates (excluding perhaps states at isolated energy values) [62]. As a consequence, the diffusion coefficient and the dc conductivity vanish. Therefore, there is no metal-insulator transition in one dimension.

3.5.1 Thouless formula

Since the energy dispersion of the FGM is linear, the Schrödinger equation of the FGM, $\hat{H}\psi(x) = \omega\psi(x)$, is a linear first order differential equation. Fixing the two-component wave function $\psi(x) \equiv (\psi_1(x), \psi_2(x))^T$ at one space point x_0 therefore constitutes the wave function at all space points x . As we will see explicitly below, for large distances $|x - x_0|$ the envelope of the wave function will grow exponentially with probability one, i.e. $\|\psi(x)\| \sim \|\psi_0\| \exp(+\gamma|x - x_0|)$, where $\|\psi(x)\|^2 \equiv |\psi_1(x)|^2 + |\psi_2(x)|^2$. Of course, $\psi(x)$ cannot be an eigenfunction of the Hamiltonian \hat{H} satisfying the right boundary conditions. The proportionality factor γ in the exponential function is called the Lyapunov exponent. The (mean) localization length is usually defined as the inverse Lyapunov exponent [20],

$$\ell^{-1}(\omega) \equiv \gamma(\omega) \equiv \lim_{L \rightarrow \infty} \frac{1}{L} \ln \left(\frac{\|\psi(L)\|}{\|\psi_0\|} \right). \quad (137)$$

Note that since we take the limit $L \rightarrow \infty$, the initial value $\|\psi_0\|$ drops out.

Let us now rewrite the Schrödinger equation such that the differential operator ∂_x is proportional to the unit matrix. As in the non-Abelian Schwinger-ansatz we factor out a σ_3 -matrix so that the wave function $\tilde{\psi}(x) \equiv \sigma_3 \psi(x)$ satisfies

$$[i\partial_x - M(x)] \tilde{\psi}(x) = 0. \quad (138)$$

Here, $M(x)$ is the matrix defined in Eq. (74). The solution to the Schrödinger equation (138) is therefore given by

$$\tilde{\psi}(x) = S(x, x_0) \tilde{\psi}_0. \quad (139)$$

It follows with $\|\tilde{\psi}(x)\| = \|\psi(x)\|$ that the Lyapunov exponent can be expressed in terms of the S -matrix,

$$\gamma(\omega) = \lim_{L \rightarrow \infty} \frac{1}{L} \ln \left\| S(L, 0) \tilde{\psi}_0 \right\|. \quad (140)$$

Due to $|S_{11}|^2 = |S_{12}|^2 + 1$, $S_{22} = S_{11}^*$ and $S_{21} = S_{12}^*$, all S -matrix elements grow equally fast and we have⁸

$$\gamma(\omega) = \lim_{L \rightarrow \infty} \frac{1}{L} \ln |S_{22}(L, 0)| . \quad (141)$$

Comparing this equation with Eq. (111), we see that the inverse localization length $\ell^{-1}(\omega) \equiv \gamma(\omega)$ is in fact equal to $\text{Re} \Gamma(\omega)$. The equation

$$\boxed{\ell^{-1}(\omega) = \text{Re} \Gamma(\omega)} \quad (142)$$

is known as the *Thouless formula* [63] and was first shown to be valid for the FGM by Hayn and John [67] in a different and more complicated way. But note that these authors have only derived Eq. (142) up to an integration constant which they had to determine by different means.

3.5.2 Localization length at $\omega = 0$ for real $\Delta(x)$

Although we are going to postpone detailed calculations of the DOS and the localization length to the next sections, let us now consider the localization length at frequency $\omega = 0$ for a real disorder potential $\Delta(x)$ and $V(x) = 0$. In this case, $M(x) = -i\sigma_2\Delta(x)$, so that the S -matrix may be expressed without the path-ordering operator as

$$S(x, x') = \cosh \left[\int_{x'}^x \Delta(y) dy \right] \sigma_0 - \sinh \left[\int_{x'}^x \Delta(y) dy \right] \sigma_2 . \quad (143)$$

It follows from Eq. (141) that the inverse localization length at $\omega = 0$ is given by

$$\ell^{-1}(0) = \lim_{L \rightarrow \infty} \frac{1}{L} \ln \left(\cosh \left[\int_0^L \Delta(x) dx \right] \right) = |\langle \Delta(x) \rangle_x| = |\Delta_{\text{av}}| , \quad (144)$$

where we have used the fact that the average $\langle \Delta(x) \rangle_x \equiv \lim_{L \rightarrow \infty} \frac{1}{L} \int_0^L \Delta(x) dx$ is equal to the expectation value Δ_{av} . The inverse localization length at frequency $\omega = 0$ is equal to the absolute value of the expectation value of the backscattering potential $\langle \Delta(x) \rangle$ and does not depend on the random fluctuations around this average value. Note that this result is valid for arbitrary higher correlation functions of $\Delta(x)$. In the case $\langle \Delta(x) \rangle = 0$, the localization length diverges for $\omega = 0$ which clearly distinguishes the point $\omega = 0$. The $\omega = 0$ eigenstate is delocalized!

4 Exact results

In this section, we review exact results for the density of states (DOS) and the inverse localization length of the fluctuating gap model in the white noise limit and the limit of infinite correlation lengths ξ .

⁸It should be noted that the above reasoning is not true in the improbable case where $\tilde{\psi}_0$ is very close to the eigenvector to the smallest eigenvalue of S . However, since the definition of the Lyapunov exponent involves the limit $L \rightarrow \infty$, this only happens with zero probability.

4.1 The white noise limit

For small correlation lengths ξ , the disorder of the fluctuating gap model (FGM) may be approximated by Gaussian white noise. This $\xi \rightarrow 0$ limit is of special interest because in this case the disorder at different space points is uncorrelated which basically admits for an exact analytic solution of the model. Various methods may now be applied to find analytic results for the density of states (DOS). Ovchinnikov and Erikhman [16] were the first to solve the commensurate case for which the random backscattering potential $\Delta(x)$ is real. They showed that in the symmetric phase for which $\langle \Delta(x) \rangle = 0$, the DOS has a Dyson singularity previously found by Dyson [17]. In the case of $\langle \Delta(x) \rangle \neq 0$ which models a phase below a phase transition, the DOS either exhibits a singularity or a pseudogap near the Fermi energy depending on the ratio of the disorder and the static gap. Using the technique of S -matrix summation, Golub and Chumakov [64] confirmed the results by Ovchinnikov and Erikhman and were also able to solve the incommensurate case. In the incommensurate case which is described by a complex backscattering potential, there is no singularity and the disorder can only lead to a filling up of the pseudogap. The incommensurate case was also considered by Abrikosov and Dorotheev [65].

In recent years, the method of supersymmetry developed by Efetov [66] has been established as a powerful tool to describe disordered systems in the white noise limit. First, Hayn and John [67] re-derived the Ovchinnikov and Erikhman result for the DOS and were also able to give an analytic expression for the localization length. Later, Hayn and Fischbeck [68, 69] used the method of supersymmetry to generalize the known results for the integrated DOS to the case of three independent disorder parameters which describe forward, backward, and umklapp scattering. These solutions include both the commensurate and the incommensurate case as special cases. Finally, both the integrated DOS and the localization length were calculated by Hayn and Mertsching [26] in the most general case with a complex static gap parameter and three disorder parameters.

In this section, we use the formalism developed in the previous section and follow the ideas of Lifshits, Gredeskul and Pastur [20] to show that the probability density for the distribution of the reduced phase φ satisfies a continuity equation. The stationary probability flux of the continuity equation turns out to be equal to the integrated DOS. We then derive an equation closely related to a Fokker-Planck equation which allows to rederive the integrated DOS for the most general case exactly. Before considering the most general case we discuss the commensurate case, i.e. the Ovchinnikov and Erikhman limit which we can solve in analogy to Halperin's calculation of the integrated DOS of a particle with an effective mass in a white noise disorder potential [70]. The treatment of the general case is similar but more awkward than the Ovchinnikov and Erikhman limit because instead of a linear differential equation of second order one has to face a linear differential equation of fourth order. The equations to determine the integrated DOS and the localization length are, however, the same as those derived by Hayn and Mertsching using the method of supersymmetry [26] so that we recover their general results which also include the incommensurate case which we will discuss afterwards.

4.1.1 Equality of the integrated density of states and the stationary probability flux

As shown in the previous section, the averaged integrated DOS can be written in the thermodynamic limit as [see Eq. (128)]

$$\mathcal{N}(\omega) = \langle F_\omega(V, \Delta, \varphi) \rangle / 2\pi . \quad (145)$$

$F_\omega(V, \Delta, \varphi)$ is linear in the disorder V , $\text{Re } \Delta$, $\text{Im } \Delta$ and given by

$$F_\omega(V, \Delta, \varphi) = 2(\omega - V) + 2 \text{Re } \Delta \cos \varphi + 2 \text{Im } \Delta \sin \varphi . \quad (146)$$

The unreduced phase $\varphi(x, \omega)$ satisfies the equation of motion (121) which can also be written as

$$\partial_x \varphi(x, \omega) = F_\omega(V(x), \Delta(x), \varphi(x, \omega)) . \quad (147)$$

Continuity equation

The space-dependent probability distribution can be defined as

$$P_\omega(x, \varphi) = \langle \delta_{2\pi}(\varphi - \varphi(x, \omega)) \rangle , \quad (148)$$

where $\delta_{2\pi}(x) \equiv \sum_{m=-\infty}^{\infty} \delta(x - 2\pi m)$ is the 2π -periodic delta function. A continuity equation may be derived by partially differentiating $P_\omega(x, \varphi)$ with respect to x which results in $\partial_x P_\omega(x, \varphi) = -\partial_\varphi \langle \delta_{2\pi}(\varphi - \varphi(x, \omega)) \partial_x \varphi(x, \omega) \rangle$. Replacing $\partial_x \varphi(x, \omega)$ by the right-hand side of Eq. (147), the *continuity equation* reads

$$\boxed{\partial_x P_\omega(x, \varphi) + \partial_\varphi J_\omega(x, \varphi) = 0 ,} \quad (149)$$

where the *probability flux* $J_\omega(x, \varphi)$ is given by

$$J_\omega(x, \varphi) = \langle \delta_{2\pi}(\varphi - \varphi(x, \omega)) F_\omega(V(x), \Delta(x), \varphi(x, \omega)) \rangle . \quad (150)$$

Letting x go to infinity, the probability distribution and the probability flux become stationary, i.e. independent of x . Due to the continuity equation (149), J_ω becomes also independent of φ . Integrating the stationary form of Eq. (150) with respect to φ from 0 to 2π therefore leads to $2\pi J_\omega = \langle F_\omega(V, \Delta, \varphi) \rangle$, so that together with Eq. (145) we find the remarkable relationship [20]

$$\boxed{\mathcal{N}(\omega) = J_\omega .} \quad (151)$$

The integrated DOS, i.e. the number of states in the energy interval $(0, \omega]$ per unit length, is equal to the stationary probability flux. Note that this result is valid for any disorder potential and is not restricted to the white noise limit which we will consider in the following.

4.1.2 White noise and the Fokker-Planck equation

While for arbitrary finite correlation lengths ξ and Gaussian statistics, it does not seem to be possible to find an exact analytic expression for the (integrated) DOS, the white noise limit $\xi \rightarrow 0$, $V_\sigma^2 \xi \rightarrow D_V$, $(\text{Re } \Delta_\sigma)^2 \xi \rightarrow D_R$, and $(\text{Im } \Delta_\sigma)^2 \xi \rightarrow D_I$ admits for an exact solution. This is due to the fact that in this case the disorder at different space points is uncorrelated. In the white noise limit, the disorder is characterized by the correlation functions

$$\langle V(x) \rangle = 0, \quad \langle V(x)V(x') \rangle = 2D_V \delta(x - x'), \quad (152)$$

$$\langle \text{Re } \Delta(x) \rangle = \text{Re } \Delta_0, \quad \langle \text{Re } \tilde{\Delta}(x) \text{Re } \tilde{\Delta}(x') \rangle = 2D_R \delta(x - x'), \quad (153)$$

$$\langle \text{Im } \Delta(x) \rangle = \text{Im } \Delta_0, \quad \langle \text{Im } \tilde{\Delta}(x) \text{Im } \tilde{\Delta}(x') \rangle = 2D_I \delta(x - x'), \quad (154)$$

where $\tilde{\Delta}(x) \equiv \Delta(x) - \Delta_0$. It is no loss of generality to assume that the first moment of the forward scattering potential $V(x)$ vanishes because a finite value would only lead to a renormalization of ω . Since the probability distribution of the disorder is assumed to be Gaussian, higher correlation functions are simply given by Wick's theorem.

To cast the continuity equation into a Fokker-Planck equation, we make use of the Gaussian nature of the disorder, so that for a functional $f\{V(y)\}$ of the disorder $V(y)$ we have $\langle V(x)f\{V(y)\} \rangle = \int dx' \langle V(x)V(x') \rangle \left\langle \frac{\delta f\{V(y)\}}{\delta V(x')} \right\rangle$, where in the last term we take the functional derivative of $f\{V(y)\}$ with respect to $V(x')$. Using Eq. (152), this simplifies to

$$\langle V(x)f\{V(y)\} \rangle = 2D_V \left\langle \frac{\delta f\{V(y)\}}{\delta V(x)} \right\rangle. \quad (155)$$

If we want to apply this relation to Eq. (150), $f\{V(y)\}$ has to be replaced by the 2π -periodic delta-function $\delta_{2\pi}(\varphi - \varphi(x, \omega))$ whose phase $\varphi(x, \omega)$ is a functional of the disorder involving the disorder at all space points $y \leq x$. Using the chain rule for the functional derivative, we get

$$\langle \delta_{2\pi}(\varphi(x, \omega) - \varphi) V(x) \rangle = -2D_V \partial_\varphi \left\langle \delta_{2\pi}(\varphi(x, \omega) - \varphi) \frac{\delta \varphi(x, \omega)}{\delta V(x)} \right\rangle. \quad (156)$$

Writing $\varphi(x, \omega)$ as $\varphi(x, \omega) - \varphi(0, \omega) = \int_0^x dx' F_\omega(V(x'), \Delta(x'), \varphi(x', \omega))$, we find $\frac{\delta \varphi(x, \omega)}{\delta V(x')} = -2\theta(x - x')$. Since in our case $x = x'$, $\theta(0)$ needs to be defined carefully (see also Itzykson and Drouffe [71]). Recalling that we have introduced the delta function $\delta(x)$ as the limit $\xi \rightarrow 0$ of a symmetric function of x , we see that to maintain this symmetry, we have to define $\theta(0) = 1/2$. It therefore follows with $P_\omega(x, \varphi) = \langle \delta_{2\pi}(\varphi - \varphi(x, \omega)) \rangle$ that

$$\langle \delta_{2\pi}(\varphi - \varphi(x, \omega)) V(x) \rangle = 2D_V \partial_\varphi P_\omega(x, \varphi). \quad (157)$$

Similarly, we can show that

$$\langle \delta_{2\pi}(\varphi - \varphi(x, \omega)) \text{Re } \tilde{\Delta}(x) \rangle = -2D_R \partial_\varphi (\cos \varphi P_\omega(x, \varphi)), \quad (158)$$

$$\langle \delta_{2\pi}(\varphi - \varphi(x, \omega)) \text{Im } \tilde{\Delta}(x) \rangle = -2D_I \partial_\varphi (\sin \varphi P_\omega(x, \varphi)). \quad (159)$$

Making use of these relations, the probability flux $J_\omega(x, \varphi)$ is given by

$$\begin{aligned} J_\omega(x, \varphi) = & 2[\omega + \operatorname{Re} \Delta_0 \cos \varphi + \operatorname{Im} \Delta_0 \sin \varphi] P_\omega(x, \varphi) \\ & - 4 [D_V \partial_\varphi P_\omega(x, \varphi) + D_R \cos \varphi \partial_\varphi (\cos \varphi P_\omega(x, \varphi)) \\ & + D_I \sin \varphi \partial_\varphi (\sin \varphi P_\omega(x, \varphi))] . \end{aligned} \quad (160)$$

The probability flux can also be written as

$$J_\omega(x, \varphi) = A_\omega(\varphi) P_\omega(x, \varphi) - \frac{1}{2} \partial_\varphi [B(\varphi) P_\omega(x, \varphi)] , \quad (161)$$

where

$$A_\omega(\varphi) = 2[\omega + \operatorname{Re} \Delta_0 \cos \varphi + \operatorname{Im} \Delta_0 \sin \varphi] - 4(D_R - D_I) \cos \varphi \sin \varphi , \quad (162)$$

$$B(\varphi) = 8 [D_V + D_R \cos^2 \varphi + D_I \sin^2 \varphi] . \quad (163)$$

Note that the forward scattering disorder D_V only leads to a renormalization of D_R and D_I . We therefore define $\tilde{D}_R \equiv D_R + D_V$ and $\tilde{D}_I \equiv D_I + D_V$.

Eq. (161) together with the continuity equation explicitly shows that the probability distribution satisfies the following one-dimensional *Fokker-Planck equation* [59, 60]:

$$\partial_x P_\omega(x, \varphi) = -\partial_\varphi [A_\omega(\varphi) P_\omega(x, \varphi)] + \frac{1}{2} \partial_\varphi^2 [B(\varphi) P_\omega(x, \varphi)] . \quad (164)$$

To find an analytic expression for the integrated DOS, we use the fact that, as shown above, $\mathcal{N}(\omega)$ is equal to the stationary probability flux. A good starting point to calculate the integrated DOS is therefore the stationary form of Eq. (161), which is nothing but the integrated stationary Fokker-Planck equation with the constant of integration being the stationary probability flux that is equal to the integrated DOS

$$\mathcal{N}(\omega) = A_\omega(\varphi) P_\omega(\varphi) - \frac{1}{2} \partial_\varphi [B(\varphi) P_\omega(\varphi)] . \quad (165)$$

In principle, one could first find a solution for $[B(\varphi) P_\omega(\varphi)]$ to this first-order differential equation subject to the boundary condition $[B(2\pi) P_\omega(2\pi)] = [B(0) P_\omega(0)]$ with $\mathcal{N}(\omega)$ as a parameter and could then use the normalization condition $\int_0^{2\pi} d\varphi P_\omega(\varphi) = 1$ to determine $\mathcal{N}(\omega)$. While this procedure works quite well in the incommensurate case with $D_R = D_I$ and after a variable transformation also in the commensurate case (without forward scattering) for which $D_I = D_V = 0$, the most general case considered here seems to defy such a treatment. Here, we therefore present an alternative method which allows to recover all known results in the white noise limit.

4.1.3 The density of states in the white noise limit

To find the (integrated) DOS for arbitrary parameters D_R, D_I, D_V and complex Δ_0 , we first use the variable transformation

$$z = \tan \left(\frac{\varphi}{2} - \frac{\pi}{4} \right) . \quad (166)$$

The trigonometric functions $\sin \varphi$ and $\cos \varphi$ can now be expressed in terms of z as $\sin \varphi = \frac{1-z^2}{1+z^2}$, and $\cos \varphi = -\frac{2z}{1+z^2}$. Since $\frac{dz}{d\varphi} = \frac{1}{2}(1+z^2)$, we find $\partial_\varphi = \frac{1}{2}(1+z^2)\partial_z$,

and the probability distribution $P(\varphi)$ has to be replaced by $\frac{1}{2}(1+z^2)P(z)$. Using these relations, Eq. (165) turns into

$$\begin{aligned} \mathcal{N}(\omega) = & \left[(\omega + \text{Im } \Delta_0) - 2(\text{Re } \Delta_0 - (2\tilde{D}_R - \tilde{D}_I))z + (\omega - \text{Im } \Delta_0)z^2 \right. \\ & \left. + 2\tilde{D}_I z^3 \right] P(z) - \tilde{D}_I \partial_z \left(\left[1 + 2\tilde{D}_I^{-1}(2\tilde{D}_R - \tilde{D}_I)z^2 + z^4 \right] P(z) \right). \end{aligned} \quad (167)$$

Taking the Fourier transform of this equation leads to

$$\begin{aligned} 2\pi\mathcal{N}(\omega)\delta(k) = & (\omega + \text{Im } \Delta_0)\tilde{P}(k) - 2i(\text{Re } \Delta_0 - (2\tilde{D}_R - \tilde{D}_I))\tilde{P}'(k) \\ & - (\omega - \text{Im } \Delta_0)\tilde{P}''(k) - 2i\tilde{D}_I\tilde{P}'''(k) \\ & - i\tilde{D}_I k \left[\tilde{P}(k) - 2\tilde{D}_I^{-1}(2\tilde{D}_R - \tilde{D}_I)\tilde{P}''(k) + \tilde{P}''''(k) \right], \end{aligned} \quad (168)$$

where

$$\tilde{P}(k) = \int_{-\infty}^{\infty} e^{-ikz} P(z) dz \quad (169)$$

is the Fourier transform of $P(z)$ which is also known as the *characteristic function* [72]. Normalization of the probability distribution $P(z)$ implies $\tilde{P}(k=0) = 1$. Assuming higher derivatives of $P(z)$ to be integrable, the other boundary conditions are given by demanding that $\tilde{P}(k) \rightarrow 0$ sufficiently rapidly as $|k| \rightarrow \infty$.

4.1.4 The commensurate case without forward scattering

Before we proceed with the most general case, let us first consider the Ovchinnikov and Erikhman limit, i.e. the commensurate case without forward scattering. In this case, Δ_0 is real and may be assumed to be positive, $D_I = D_V = 0$ and we set $D \equiv D_R$. Eq. (168) reduces to a second order differential equation with the boundary conditions $\tilde{P}(0) = 1$ and $\tilde{P}(k) \rightarrow 0$ as $|k| \rightarrow \infty$:

$$2\pi\mathcal{N}(\omega)\delta(k) = \omega\tilde{P}(k) + 4iD \left(1 - \frac{\Delta_0}{2D} \right) \tilde{P}'(k) + 4iD \left(k + \frac{i\omega}{4D} \right) \tilde{P}''(k). \quad (170)$$

Integrating this equation from $-\epsilon$ to $+\epsilon$ with $\epsilon \rightarrow 0^+$ leads to

$$2\pi\mathcal{N}(\omega) = -\omega \left[\tilde{P}'(0^+) - \tilde{P}'(0^-) \right]. \quad (171)$$

Since $P(z)$ is real, $\tilde{P}(-k) = \tilde{P}^*(k)$, and $\tilde{P}'(-k) = -\tilde{P}'^*(k)$, which implies

$$\mathcal{N}(\omega) = -\frac{\omega}{\pi} \text{Re } \tilde{P}'(0^+). \quad (172)$$

$\tilde{P}'(0^+)$ can be determined by first finding a solution to the differential equation (170) for $k > 0$ which vanishes as k approaches infinity and then normalizing this solution such that $\tilde{P}(0) = 1$. Because Eq. (170) is homogeneous for $k > 0$, it therefore follows that if $g(k)$ is any solution to the homogeneous differential equation which obeys $g(k) \rightarrow 0$ as $k \rightarrow \infty$, then $\mathcal{N}(\omega) = -\frac{\omega}{\pi} \text{Re } [g'(0)/g(0)]$. We introduce $y(t) \equiv g(k)$ with $t = -i(k + i\omega/4D)$. The integrated DOS is now given by

$$\mathcal{N}(\omega) = \frac{\omega}{\pi} \text{Im} \left(\frac{y' \left(\frac{\omega}{4D} \right)}{y \left(\frac{\omega}{4D} \right)} \right), \quad (173)$$

where $y(t)$ has to satisfy the differential equation

$$t y''(t) + \left(1 - \frac{\Delta_0}{2D}\right) y'(t) + \frac{\omega}{4D} y(t) = 0, \quad (174)$$

with the only restriction that $y(t)$ should approach zero as t goes to $i\infty$. The general solution of this differential equation can be expressed in terms of a linear combination of Bessel functions of the first and second kind, $J_\nu(x)$ and $N_\nu(x)$ (Abramowitz and Segun (A&S) [73]). The only solution which satisfies the boundary condition involves the Hankel function of the first kind, $H_\nu^{(1)}(x) = J_\nu(x) + iN_\nu(x)$. Introducing

$$\nu = \frac{\Delta_0}{2D}, \quad (175)$$

we find $y(t) = (\nu/2)^t H_\nu^{(1)}((\omega t/D)^{1/2})$. Because the prefactor is real and we only need the imaginary part of the quotient $y'(\omega/4D)/y(\omega/4D)$, Eq. (173) turns into

$$\mathcal{N}(\omega) = \frac{\omega}{\pi} \operatorname{Im} \left(\frac{[H_\nu^{(1)}(\frac{\omega}{2D})]'}{H_\nu^{(1)}(\frac{\omega}{2D})} \right). \quad (176)$$

Note that this equation is valid for arbitrary ω and is even analytic in the upper half plane. In the following discussion of the Ovchinnikov and Erikhman limit, we will again restrict ourselves to $\omega > 0$. It follows

$$\mathcal{N}(\omega) = \frac{\omega}{\pi} \frac{J_\nu(\frac{\omega}{2D}) N'_\nu(\frac{\omega}{2D}) - J'_\nu(\frac{\omega}{2D}) N_\nu(\frac{\omega}{2D})}{J_\nu^2(\frac{\omega}{2D}) + N_\nu^2(\frac{\omega}{2D})}. \quad (177)$$

The numerator can be simplified by using the Wronski relation [A&S, Eq. (9.1.16)] $J_\nu(x) N'_\nu(x) - J'_\nu(x) N_\nu(x) = \frac{2}{\pi x}$, so that as our final expression for the integrated DOS we are left with

$$\boxed{\mathcal{N}(\omega) = \frac{4D}{\pi^2 [J_\nu^2(\frac{\omega}{2D}) + N_\nu^2(\frac{\omega}{2D})]}}. \quad (178)$$

This result was first obtained by Ovchinnikov and Erikhman [16] in a more complicated manner. Differentiating Eq. (178) with respect to ω , we find

$$\rho(\omega) = -\frac{4 [J_\nu(\frac{\omega}{2D}) J'_\nu(\frac{\omega}{2D}) + N_\nu(\frac{\omega}{2D}) N'_\nu(\frac{\omega}{2D})]}{\pi^2 [J_\nu^2(\frac{\omega}{2D}) + N_\nu^2(\frac{\omega}{2D})]^2}, \quad (179)$$

where the derivatives of Bessel functions could in principle also be written in terms of Bessel functions. For $\Delta_0 = 0$ which implies $\nu = 0$, D is the only characteristic energy scale, and it is useful to measure all energies in terms of D . The insert at the top of Fig. 7 shows the DOS $\rho(\omega)$ plotted versus ω/D . The DOS clearly exhibits a singularity near $\omega = 0$ whose asymptotic behavior can be found by noting that $J_0(0)$ is finite while

$N_0(x)$ diverges logarithmically for small x . It follows⁹ with $N_0(x) \sim (2/\pi) \ln x$ [A&S, Eq. 9.1.8]

$$\mathcal{N}(\omega) \sim \frac{D}{\ln^2(\omega/2D)}, \quad (180)$$

such that the asymptotics of the DOS for $\Delta_0 = 0$ is given by

$$\rho(\omega) \sim -\frac{1}{(\omega/2D) \ln^3(\omega/2D)}. \quad (181)$$

Recall that to generalize this result towards arbitrary frequencies ω , we have to replace ω by $|\omega|$. The singularity described by Eq. (181) is called a *Dyson singularity* and was first found by Dyson in a different model [17] involving also off-diagonal disorder. Outside this singularity, the DOS is almost equal to the DOS of the disorder-free model, taking its minima $\rho(\omega^*) = 0.9636 \rho_0$ at $\omega^* = \pm 1.2514 D$.

If $\Delta_0 \neq 0$, Δ_0 is another characteristic energy scale. $\nu \equiv \Delta_0/2D$ then basically gives the ratio of the two relevant energy scales Δ_0 and D . The DOS plotted against ω/Δ_0 for different values of the parameter ν is shown at the top of Fig. 7. While the singularity only survives for $\nu < 1/2$, the DOS is constant for $\nu = 1/2$ and for $\nu > 1/2$ the effects of the constant gap Δ_0 dominate those due to the disorder and a pseudogap emerges.

The algebraic dependence of the DOS at small ω on the parameter ν can be found by using again an asymptotic expansion of the Bessel functions. If $\nu > 0$ is fixed and $x \rightarrow 0$, the Bessel function $J_\nu(x)$ is finite and $N_\nu(x) \sim -(1/\pi)\Gamma(\nu)(x/2)^{-\nu}$ [A&S, Eq. (9.1.9)]. It follows

$$\mathcal{N}(\omega) \sim \frac{4D}{\Gamma^2(\nu)} \left(\frac{\omega}{4D}\right)^{2\nu}, \quad (182)$$

so that

$$\rho(\omega) \sim \frac{2\nu}{\Gamma^2(\nu)} \left(\frac{\omega}{4D}\right)^{2\nu-1}. \quad (183)$$

This implies that for $\nu < 1/2$ the DOS in fact diverges algebraically as ω approaches zero because in this case the exponent is negative. Although the algebraic divergence differs from the divergence found in Dyson's model, we will nevertheless refer to this singularity as a Dyson singularity. For $\nu > 1/2$, however, the exponent is positive and the DOS vanishes algebraically.

For large ν the disorder becomes irrelevant and the DOS reduces to the mean-field result $\rho(\omega) = \rho_0 \theta(\omega^2 - \Delta_0^2)\omega/(\omega^2 - \Delta_0^2)^{1/2}$.

⁹Note that the argument of the logarithm in the asymptotic form given by Ovchinnikov and Erikhman deviates by a factor 1/2 from our result. Nevertheless both expressions lead to the same asymptotic behavior. To take into account next to leading terms one has to use $N_0(x) = 2/\pi \ln(ax) + \mathcal{O}(x)$, where $a = e^\gamma/2$ which follows from A&S, Eq. (9.1.89). Here, $\gamma \approx 0.5772$ is Euler's constant which leads to $a \approx 0.8905$. This value is closer to our choice $a = 1$ than to Ovchinnikov's and Erikhman's choice $a = 1/2$.

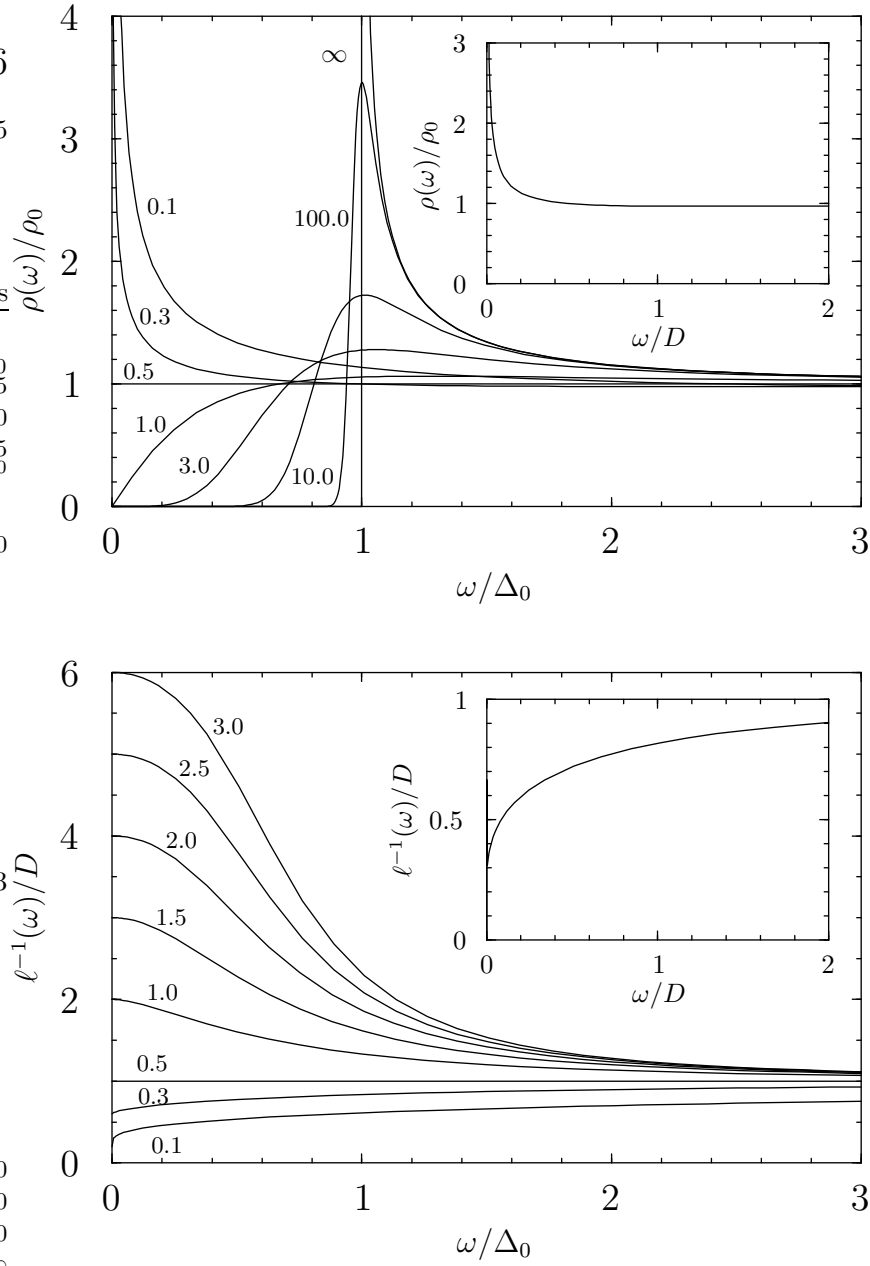


Fig. 7 The DOS $\rho(\omega)$ and the inverse localization length $\ell^{-1}(\omega)$ in the white noise limit for the commensurate case plotted versus ω/Δ_0 for $\nu = \Delta_0/2D = 0.1, 0.3, 0.5, 1.0, 3.0, 10.0, 100.0, \infty$ or $\nu = \Delta_0/2D = 0.1, 0.3, 0.5, 1.0, 1.5, 2.0, 2.5, 3.0$, respectively. The inserts show the respecting graphs for the case $\Delta_0 = 0$, i.e. $\nu = 0$.

Localization length

Since $\Gamma(\omega) \equiv \ell^{-1}(\omega) - i\pi\mathcal{N}(\omega)$ is an analytic function in the upper half plane, we can also easily find an analytic expression for the localization length $\ell^{-1}(\omega)$. It follows from Eq. (176) that up to a constant

$$\Gamma(\omega) = -\omega \frac{\left[H_\nu^{(1)}\left(\frac{\omega}{2D}\right) \right]'}{H_\nu^{(1)}\left(\frac{\omega}{2D}\right)}. \quad (184)$$

The inverse localization length is now given by

$$\ell^{-1}(\omega) = \text{Re} \Gamma(\omega) = -\omega \frac{J_\nu\left(\frac{\omega}{2D}\right) J_\nu'\left(\frac{\omega}{2D}\right) + N_\nu\left(\frac{\omega}{2D}\right) N_\nu'\left(\frac{\omega}{2D}\right)}{J_\nu^2\left(\frac{\omega}{2D}\right) + N_\nu^2\left(\frac{\omega}{2D}\right)}. \quad (185)$$

Comparing the right-hand side of this equation with Eqs. (178) and (179), we find

$$\ell^{-1}(\omega) = D \frac{\omega \rho(\omega)}{\mathcal{N}(\omega)}. \quad (186)$$

This equation is exact and can already be found Ref. [20].

If $\Delta_0 = 0$, it follows from Eqs. (180) and (181) that $\ell^{-1}(\omega)$ vanishes logarithmically as ω approaches zero,

$$\ell^{-1}(\omega) \sim -\frac{2D}{\ln(\omega/2D)}. \quad (187)$$

Using Eqs. (182) and (183), we get for arbitrary Δ_0

$$\ell^{-1}(0) = \Delta_0, \quad (188)$$

which, as can be seen from Eq. (187) is also true for $\Delta_0 = 0$. Eq. (188) agrees with Eq. (144), so that $\Gamma(\omega)$ involves no extra constant. For large frequencies, $\rho(\omega) \rightarrow \rho_0$ and $\mathcal{N}(\omega) \rightarrow \rho_0 \omega$, such that

$$\ell^{-1}(\omega) \rightarrow D. \quad (189)$$

A plot of the inverse localization length $\ell^{-1}(\omega)$ for various values of $\nu = \Delta_0/2D$ is given at the bottom of Fig. 7.

4.1.5 Solving the general case with arbitrary parameters D_R , D_I , D_V and Δ_0

While in the commensurate case we only had to solve a differential equation of second order, for $D_I \neq 0$, Eq. (168) is a differential equation of fourth order and more difficult to solve. Without loss of generality we may assume that $\tilde{D}_R > \tilde{D}_I$ (later we can also take the limit $\tilde{D}_R \rightarrow \tilde{D}_I$). Integrating Eq. (168) from $-\epsilon$ to $+\epsilon$ with $\epsilon \rightarrow 0^+$, we can proceed as before and express the integrated DOS in terms of $\tilde{P}(k)$ and derivatives thereof evaluated at $\pm 0^+$. Integrating the terms linear in k by parts and using again the fact that $\tilde{P}^{(n)}(-k) = (-1)^n \tilde{P}^{(n)*}(k)$, we find

$$\mathcal{N}(\omega) = \frac{1}{\pi} \text{Im} \left[-i(\omega - \text{Im} \Delta_0) \tilde{P}'(0^+) + D_I \tilde{P}''(0^+) \right]. \quad (190)$$

So, if $y(k)$ is any solution to the homogeneous differential equation

$$(\omega + \text{Im } \Delta_0)y(k) - 2i(\text{Re } \Delta_0 - (2\tilde{D}_R - \tilde{D}_I))y'(k) - (\omega - \text{Im } \Delta_0)y''(k) - 2i\tilde{D}_I y'''(k) - i\tilde{D}_I k \left[y(k) - 2\tilde{D}_I^{-1}(2\tilde{D}_R - \tilde{D}_I)y''(k) + y''''(k) \right] = 0, \quad (191)$$

which vanishes for $k \rightarrow \infty$ sufficiently rapidly, then the integrated DOS is given by

$$\mathcal{N}(\omega) = \frac{1}{\pi} \text{Im} \left[-i(\omega - \text{Im } \Delta_0) \frac{y'(0)}{y(0)} + D_I \frac{y''(0)}{y(0)} \right]. \quad (192)$$

Again, since $\Gamma(\omega) \equiv \ell^{-1}(\omega) - i\pi\mathcal{N}(\omega)$ is an analytic function in the upper half plane, up to a constant we have

$$\Gamma(\omega) = i(\omega - \text{Im } \Delta_0) \frac{y'(0)}{y(0)} - \tilde{D}_I \frac{y''(0)}{y(0)}. \quad (193)$$

Using the method of supersymmetry invented by Efetov [66], Hayn and Mertsching [26] derived the set of equations (191) and (193) by different means¹⁰. Applying the method of Laplace transforms they found an exact expression with the constant of integration chosen such that one obtains the correct asymptotic behavior for large frequencies determined in the Born approximation, $\Gamma(\omega) = D - i\omega = D_R + D_I - i\omega$. Here, instead of presenting a lengthy derivation, we will only cite the exact result found in [26]:

$$\Gamma(\omega) = 2D_I + 4\tilde{D}_R \left[z(1-z) \frac{F'(z)}{F(z)} + z\delta_R - i(1-z)\epsilon \right]. \quad (194)$$

In this equation, $F(z)$ is the hypergeometric function

$$F(z) = F\left(\frac{1}{2} - i\epsilon + i\delta_I - \delta_R, \frac{1}{2} - i\epsilon - i\delta_I - \delta_R, 1 - 2i\epsilon; z\right), \quad (195)$$

with the parameters δ_R , δ_I , ϵ , and z (in our notation) given by

$$\delta_R = \frac{\text{Re } \Delta_0}{4 \left(\tilde{D}_R (\tilde{D}_R - \tilde{D}_I) \right)^{1/2}}, \quad \delta_I = \frac{\text{Im } \Delta_0}{4 \left(\tilde{D}_I (\tilde{D}_R - \tilde{D}_I) \right)^{1/2}}, \quad (196)$$

$$\epsilon = \frac{\omega}{4 \left(\tilde{D}_R \tilde{D}_I \right)^{1/2}}, \quad z = \frac{\tilde{D}_R - \tilde{D}_I}{\tilde{D}_R}. \quad (197)$$

Recall that we incorporated the parameter of the forward scattering disorder, D_V , into D_R and D_I by defining $\tilde{D}_R \equiv D_R + D_V$ and $\tilde{D}_I \equiv D_I + D_V$. Only the additive constant $2D_I$ in Eq. (194) does not get renormalized by D_V . This is due to the fact that for large frequencies $\Gamma(\omega) \sim D_R + D_I - i\omega$ is independent of D_V . The imaginary part of Eq. (194) determines the integrated DOS,

$$\mathcal{N}(\omega) = \rho_0 \left(\frac{\tilde{D}_R}{\tilde{D}_I} \right)^{1/2 - 2\delta_R} \frac{\omega}{|F|^2}. \quad (198)$$

¹⁰Hayn and Mertsching use a slightly different notation but apart from this and some irrelevant different signs their expressions are equal to ours.

Taking the confluent limit $D_I \rightarrow 0$ of Eq. (194), one can recover Eq. (184) which describes the commensurate case without forward scattering. Turning on the forward scattering disorder D_V in the general expression gradually removes the singularity in the DOS for $\nu < 1/2$. Below, we are only going to discuss the incommensurate case. Other special cases can be found in [26, 67–69, 74].

4.1.6 The incommensurate case

In the incommensurate case, $D_R = D_I \equiv D/2$, and the forward scattering potential D_V only leads to a renormalization of D . If we introduce $\tilde{D} \equiv D + D_V = \tilde{D}_R/2 + \tilde{D}_I/2$ and take the confluent limit $D_I \rightarrow D_R$ in Eq. (194), we obtain

$$\Gamma(\omega) = D - i\omega + \Delta_0 \frac{I_{1-i\omega/\tilde{D}}\left(\frac{\Delta_0}{D}\right)}{I_{-i\omega/\tilde{D}}\left(\frac{\Delta_0}{D}\right)}, \quad (199)$$

which is equivalent to

$$\Gamma(\omega) = D + \Delta_0 \frac{I'_{-i\omega/\tilde{D}}\left(\frac{\Delta_0}{D}\right)}{I_{-i\omega/\tilde{D}}\left(\frac{\Delta_0}{D}\right)}. \quad (200)$$

The imaginary part of Eq. (199) determines the integrated DOS,

$$\mathcal{N}(\omega) = \frac{\tilde{D}}{\pi} \sinh\left(\frac{\pi\omega}{\tilde{D}}\right) \frac{\rho_0}{\left|I_{i\omega/\tilde{D}}\left(\frac{\Delta_0}{D}\right)\right|^2}. \quad (201)$$

This expression agrees with Ref. [64]. A plot of the DOS for different values of the parameter $\nu = \Delta_0/2D$ is shown at the left-hand side of Fig. 8. There is no Dyson singularity, and in the absence of a static gap Δ_0 , the disorder has no effect on the DOS so that $\rho(\omega) = \rho_0$ for $\nu = 0$. At zero frequency, $\rho(0)$ is always finite and the DOS vanishes with increasing ν as $\rho(0) = \rho_0/[I_0(2\nu)]^2$. For a given Δ_0 , the disorder leads to a filling of the gap. As in the commensurate case, in the limit $D \rightarrow 0$, i.e. $\nu \rightarrow \infty$, the DOS reduces to the mean-field result $\rho(\omega) = \rho_0 \theta(\omega^2 - \Delta_0^2) |\omega|/(\omega^2 - \Delta_0^2)^{1/2}$.

Taking the real part of Eq. (199), we get for the inverse localization length

$$\ell^{-1}(\omega) = D + \Delta_0 \frac{I_{i\omega/\tilde{D}}\left(\frac{\Delta_0}{D}\right) I_{1-i\omega/\tilde{D}}\left(\frac{\Delta_0}{D}\right) + I_{-i\omega/\tilde{D}}\left(\frac{\Delta_0}{D}\right) I_{1+i\omega/\tilde{D}}\left(\frac{\Delta_0}{D}\right)}{2 \left|I_{i\omega/\tilde{D}}\left(\frac{\Delta_0}{D}\right)\right|^2}. \quad (202)$$

In contrast to the commensurate case, the localization length at $\omega = 0$ is finite for any Δ_0 and given by

$$\ell^{-1}(0) = D + \Delta_0 \frac{I_1\left(\frac{\Delta_0}{D}\right)}{I_0\left(\frac{\Delta_0}{D}\right)}. \quad (203)$$

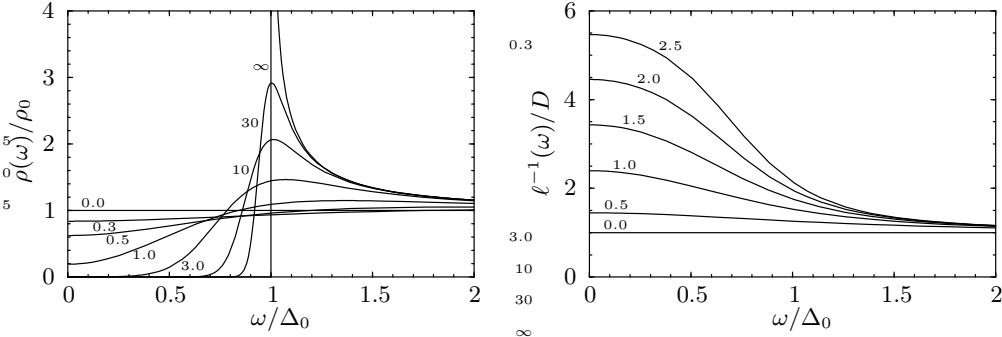


Fig. 8 The DOS $\rho(\omega)$ and the inverse localization length $\ell^{-1}(\omega)$ in the white noise limit for the incommensurate case plotted versus ω/Δ_0 for $\nu = \Delta_0/2D = 0.0, 0.3, 0.5, 1.0, 3.0, 10.0, 30.0, \infty$ or $\nu = \Delta_0/2D = 0.0, 0.5, 1.0, 1.5, 2.0, 2.5$, respectively.

While for $\Delta_0/\tilde{D} \rightarrow 0$ one has $\ell^{-1}(0) \rightarrow D$ (and also $\ell^{-1}(\omega) \rightarrow D$ for every ω), for $\Delta_0/\tilde{D} \gg 1$ one finds $\ell^{-1}(0) \sim \Delta_0 + D/2 - D_V/2$. For weak disorder, the disorder creates a few localized states with energies $|\omega| < \Delta_0$ whose inverse localization length is given by $\ell^{-1}(\omega) \sim \sqrt{\Delta_0^2 - \omega^2}$. A plot of the inverse localization length for different values of the parameter ν and $D_V = 0$ is given at the right-hand side of Fig. 8.

4.2 Infinite correlation lengths

In the limit of infinite correlation lengths, $\Delta(x)$ becomes independent of x and exact results for the averaged DOS of the FGM may be obtained. The limit of large correlation lengths ξ is of special importance for Peierls systems because the correlation length of the order parameter diverges at the Peierls transition. Sadovskii was the first to consider the fluctuating gap model (FGM) with infinite correlation lengths [75] and calculated the one-electron Green function for the incommensurate case by summing up all diagrams in the perturbation expansion. This Green function leads to a DOS which exhibits a pseudogap at the Fermi energy. The commensurate case was later solved by Wonneberger and Lautenschlager [76].

Taking the ensemble average

The limit of infinite correlation lengths can be solved by averaging the desired quantity calculated with a static gap Δ over an appropriate probability distribution of Δ . This amounts to taking an ensemble average.

4.2.1 The commensurate case

For real Δ and Gaussian statistics we have

$$\langle \dots \rangle = \int_{-\infty}^{\infty} \frac{d\Delta}{\sqrt{2\pi\Delta_s^2}} e^{-\Delta^2/2\Delta_s^2} \dots \quad (204)$$

Calculating the DOS by averaging $\theta(\omega^2 - \Delta^2) \omega / \sqrt{\omega^2 - \Delta^2}$ with respect to the above probability distribution, one obtains

$$\rho_\infty(\omega) = \rho_0 \sqrt{\frac{\pi}{2}} \frac{\omega}{\Delta_s} e^{-\omega^2/4\Delta_s^2} I_0\left(\frac{\omega^2}{4\Delta_s^2}\right). \quad (205)$$

Here, $I_0(u)$ is the modified Bessel function with index 0.

If we define the inverse localization length $\ell_\infty^{-1}(\omega)$ for $\xi = \infty$ by the Thouless formula, we have $\ell_\infty^{-1}(\omega) = \langle \sqrt{\Delta^2 - \omega^2} \theta(\Delta^2 - \omega^2) \rangle$, such that

$$\ell_\infty^{-1}(\omega) \sqrt{\frac{2}{\pi}} \frac{\omega^2}{\Delta_s} \int_1^\infty du e^{-(\omega^2/2\Delta_s^2)u^2} \sqrt{u^2 - 1}. \quad (206)$$

4.2.2 The incommensurate case

For complex $\Delta(x)$ and Gaussian statistics, the process of averaging can be written as

$$\langle \dots \rangle = \int \frac{d\text{Re}\Delta d\text{Im}\Delta}{\pi\Delta_s^2} e^{-|\Delta|^2/\Delta_s^2} \dots \quad (207)$$

A similar calculation as above leads to

$$\rho_\infty(\omega) = 2\rho_0 \frac{\omega}{\Delta_s} e^{-(\omega^2/\Delta_s^2)} \text{Erfi}\left(\frac{\omega}{\Delta_s}\right), \quad (208)$$

$$\ell_\infty^{-1}(\omega) = \Delta_s \frac{\sqrt{\pi}}{2} e^{-\omega^2/\Delta_s^2}. \quad (209)$$

Here, $\text{Erfi}(u) \equiv \int_0^u e^{x^2} dx$ is the error function with an imaginary argument.

Plots of $\rho_\infty(\omega)$ and $\ell_\infty^{-1}(\omega)$ can be found in the next section. While in the commensurate case the DOS vanishes linearly in ω , it only vanishes quadratically in the incommensurate case. This is due to the fact that the probability distribution for complex Δ has less weight for small $|\Delta|$ than the one for real Δ . The inverse localization length assumes for both the commensurate and the incommensurate case a finite value at $\omega = 0$ and drops to zero as ω increases. That $\ell_\infty^{-1}(0)$ is finite in the commensurate case seems to contradict the general result $\ell_\infty^{-1}(0) = \Delta_{\text{av}} = 0$ derived in Section 3. One should keep in mind, however, that for $\xi = \infty$ we have only defined $\partial_\omega \ell_\infty^{-1}(\omega)$ by $\text{Re} \langle \mathcal{G}(x, x; \omega) \rangle$. While for finite ξ a single chain is representative for an ensemble of chains, for $\xi = \infty$, there is no self-averaging effect. On the other hand, it seems plausible to assume that the above results for $\xi = \infty$ give a good approximation to the case of finite ξ if ξ is much larger than any microscopic length scale involved. In particular, we have to demand $\Delta_s \xi \gg 1$ and $\omega \xi \gg 1$. The above results for the DOS and the inverse localization length at $\omega = 0$ can therefore not be expected to hold for finite correlation lengths. In fact, we will see in the next section that for any finite ξ we find in the commensurate case $\rho(0) = \infty$ and $\ell^{-1}(0) = 0$. For $\Delta_s \xi \gg 1$ and $\omega \xi \gg 1$, however, we will find a remarkable agreement between the two solutions as predicted above.

5 Finite correlation lengths

While in the limit of very small and infinite correlation lengths ξ of the random disorder, the fluctuating gap model (FGM) admits for an exact analytic calculation of the density of states (DOS) and the inverse localization length, in the intermediate regime of finite ξ there are only approximate solutions available. It especially turns up the question: “How accurate are Sadovskii’s solutions [10], which for a long time were thought to be exact?” An answer to this question is of particular interest because Sadovskii’s solutions have become quite popular since the experimental discovery of a pseudogap in the underdoped cuprates above the critical temperature T_c [11–13]. In this section, we will calculate the DOS and the inverse localization length for Gaussian statistics, as approximately done by Sadovskii with very high accuracy numerically. Finally, we will consider the case of only phase fluctuations for which we recently found an exact solution by applying a gauge transformation to the Green function and mapping the original problem onto a problem involving only white noise [25].

5.1 Singularities in the density of states

The exact results of the FGM derived in the white noise limit in the previous section imply under certain circumstances a Dyson singularity in the DOS. This singularity arises only in the commensurate case [i.e. for real $\Delta(x)$] and only if the forward scattering potential and $\Delta_{\text{av}} = \langle \Delta(x) \rangle$ are sufficiently small [see Eqs. (181) and (183)]. Since the white noise limit describes the low-energy physics of physical systems characterized by small correlation lengths ξ , this statement should also be true for small but finite ξ . As far as I know, it was first shown by myself in collaboration with Peter Kopietz that the DOS $\rho(\omega)$ of the FGM exhibits a singularity at the Fermi energy for any finite value of the correlation length ξ if the fluctuating order parameter field $\Delta(x)$ is real and its average $\langle \Delta(x) \rangle$ is sufficiently small [22]. To detect the singularity, we applied the boundary condition $\Delta_{\text{BC}} = V_{\text{BC}} = 0$, such that the complete spectrum turned out to be continuous [see Eq. (94) and its following remark]. In the Comment [77], Millis and Monien showed that the local DOS $\rho(\omega = 0, x)$ calculated in our Letter [22] is equal to the absolute square of the wave function $\psi(x)$, which led them to claim that we have not calculated the DOS at all. However, as pointed out in the Reply [78], for the boundary conditions used in Ref. [22], one finds $\rho(\omega, x) = |\psi_\omega|^2$, i.e. the local DOS is equal to the absolute square of the wave function. This clearly invalidates the argument given by Millis and Monien. Today, I would not use the artificial boundary conditions which lead to a continuous spectrum any more: The existence of the Dyson singularity put forward in the Letter [22] can also be seen in the discrete case by considering the equation of motion (121) for $V(x) = 0$ and real $\Delta(x)$ which after the shift $\varphi \rightarrow \varphi - \pi/2$ reads

$$\partial_x \varphi(x) = 2\omega + 2\Delta(x) \sin \varphi(x) . \quad (210)$$

The Dyson singularity in the DOS is due to phase resonance: If ω is small (compared to Δ_s , $\Delta_s^2 \xi$ and ξ^{-1}) but positive, the change of $\varphi(x)$ is dominated by the fluctuating term $2\Delta(x) \sin \varphi(x)$. Only near $\varphi(x) = n\pi$ (with n an integer) we have $\partial_x \varphi(x) = 2\omega > 0$, such that $\varphi(x)$ can only grow on average. As $(\varphi(x) - n\pi) \approx \omega/\Delta_s$, fluctuation effects

of $\Delta(x)$ become important, driving $\varphi(x)$ from $n\pi + \omega/\Delta_s$ to $(n+1)\pi - \omega/\Delta_s$. Near $\varphi(x) = (n+1)\pi$, the constant force 2ω dominates again and the above picture repeats itself.

As we decrease ω , the “time” (which corresponds to the space coordinate x) to move $\varphi(x)$ from $n\pi - \omega/\Delta_s$ to $n\pi + \omega/\Delta_s$ will not change, but fluctuations of $\Delta(x)$ will need slightly longer to drive $\varphi(x)$ from $n\pi + \omega/\Delta_s$ to $(n+1)\pi - \omega/\Delta_s$, implying that $\varphi(x)$ decreases more slowly than ω as ω decreases. Now, the average DOS for frequencies between 0 and ω is given by

$$\rho(\zeta\omega) = \frac{\mathcal{N}(\omega)}{\omega} = \lim_{x \rightarrow \infty} \frac{\varphi_\omega(x)}{2\pi\omega x}, \quad (211)$$

where ζ is a number between 0 and 1. Letting ω approach zero, it follows $\rho(0) = \infty$. This divergence describes the Dyson singularity in the DOS. The above reasoning is independent of the probability distribution of $\Delta(x)$. However, it should be noted that $\Delta(x)$ must not be dominated by one sign. If $\varphi(x) \approx n\pi$ and $(-1)^n \Delta(x)$ is negative, $\varphi(x)$ will fluctuate around the stable position near $n\pi + \omega/\Delta_s$. $\varphi(x) = (n+1)\pi$ can only be reached if $(-1)^n \Delta(x)$ is positive on average over a finite interval. We therefore conclude that we expect a Dyson singularity if $\Delta(x)$ is real and fluctuates around $\Delta_{\text{av}} \equiv \langle \Delta(x) \rangle$ with Δ_{av} sufficiently small.

For complex $\Delta(x)$, fluctuations of the phase of $\Delta(x)$ can be mapped via the gauge transformation (130) onto a forward scattering potential. Since the amplitude $|\Delta(x)|$ is always positive and the phase fluctuations lead to an effective local shift of the frequency ω , there should be no Dyson singularity. Instead, we expect a suppression of the DOS, i.e. a pseudogap.

5.2 Numerical algorithm

In the following, we present an exact algorithm which for stepwise constant potentials allows for simultaneous numerical calculations of the integrated DOS and the inverse localization length. By choosing the step size sufficiently small, the integrated DOS and the inverse localization length may be calculated for arbitrary given potentials. Let us partition the interval $(0, L)$ into N intervals (x_n, x_{n+1}) of length $\delta_n = x_{n+1} - x_n$ with $x_0 = 0 < x_1 < \dots < x_N = L$, such that $\Delta_n \equiv \Delta(x)$ and $V_n \equiv V(x)$ for $x_n < x < x_{n+1}$. Let us also define $\tilde{\omega}_n$ as $\tilde{\omega}_n \equiv \omega - V_n$.

To find an exact analytic solution for the given stepwise constant potentials of the equations of motion (121) and (122), let us consider again the related S -matrix $S(L, 0; \omega)$, which can be written as the finite product

$$S(L, 0; \omega) = \prod_{n=0}^{N-1} S_n \equiv \prod_{n=0}^{N-1} S(x_{n+1}, x_n; \omega), \quad (212)$$

where S_n is given for $\omega_n^2 < |\Delta_n|^2$ by Eq. (91) and for $\omega_n^2 > |\Delta_n|^2$ by Eq. (92). Eq. (212) implies the recurrence relation $S(x_{n+1}, 0; \omega) = S_n S(x_n, 0; \omega)$, which can be cast into the following recurrence relations for $\varphi_n \equiv \varphi(x_n)$ and $\zeta_n \equiv \zeta(x_n)$:

$$\varphi_{n+1} = \varphi_n - 2 \operatorname{Im}(\ln z_n), \quad (213)$$

$$\zeta_{n+1} = \zeta_n + 2 \operatorname{Re}(\ln z_n), \quad (214)$$

where $z_n = (S_n)_{22} + (S_n)_{21} \exp(i\varphi_n)$. Note that Eqs. (213) and (214) are integrated forms of the equations of motion (121) and (122). The real and imaginary part of $\ln z_n$ can be determined by writing $\ln z_n$ as $\ln z_n \equiv \ln |z_n| + i \arg(z_n)$. The argument of z_n , $\arg(z_n)$ can be obtained up to a multiple of 2π from

$$\arg(z_n) = 2\pi m_n + \operatorname{sgn}[\operatorname{Im} z_n] \arccos\left(\frac{\operatorname{Re} z_n}{|z_n|}\right). \quad (215)$$

To find the integer

$$m_n = \left[\frac{\arg(z_n)}{2\pi} + \frac{1}{2} \right]_{\text{int}}, \quad (216)$$

we define $z_n(x)$ by z_n with δ_n replaced by $x - x_n$. $z_n(x)$ is an analytic function of x and at $x = x_{n+1}$ agrees with z_n . For $\tilde{\omega}_n^2 < |\Delta_n|^2$, it follows from Eq. (91) that $\operatorname{Im}[z_n(x)] \propto \sinh[\sqrt{|\Delta_n|^2 - \tilde{\omega}_n^2}(x - x_n)]$ does not change its sign for any $x > x_n$, such that $|\arg[z_n(x)]| < \pi$ and m_n has to be zero. For $\tilde{\omega}_n^2 > |\Delta_n|^2$, however, $\operatorname{Im}[z_n(x)] \propto \sin[\sqrt{\tilde{\omega}_n^2 - |\Delta_n|^2}(x - x_n)]$, such that $|\arg(z_n(x))/\pi|_{\text{int}} = \left[\sqrt{\tilde{\omega}_n^2 - |\Delta_n|^2}(x - x_n)/\pi \right]_{\text{int}}$. Since the constant of proportionality is negative for $\tilde{\omega}_n > |\Delta_n|$ and positive for $\tilde{\omega}_n < -|\Delta_n|$, it follows

$$m_n = \left[\frac{1}{2} - \frac{\operatorname{sgn}(\tilde{\omega}_n) \sqrt{\tilde{\omega}_n^2 - |\Delta_n|^2} \delta_n}{2\pi} \right]_{\text{int}}. \quad (217)$$

To summarize, we can simultaneously calculate the integrated DOS and the inverse localization length for arbitrary stepwise constant potentials using the following iterative algorithm with the initial values $\varphi_0 = \zeta_0 = 0$,

$$\varphi_{n+1} = \varphi_n - 2 \left[2\pi m_n + \operatorname{sgn}[\operatorname{Im} z_n] \arccos\left(\frac{\operatorname{Re} z_n}{|z_n|}\right) \right], \quad (218)$$

$$\zeta_{n+1} = \zeta_n + 2 \ln |z_n|, \quad (219)$$

where z_n and m_n are given by

$$z_n = (S_n)_{22} + (S_n)_{21} \exp(i\varphi_n), \quad (220)$$

$$m_n = \begin{cases} \left[\frac{1}{2} - \frac{\operatorname{sgn}(\tilde{\omega}_n) \sqrt{\tilde{\omega}_n^2 - |\Delta_n|^2} \delta_n}{2\pi} \right]_{\text{int}}, & \tilde{\omega}_n^2 - |\Delta_n|^2 > 0 \\ 0, & \tilde{\omega}_n^2 - |\Delta_n|^2 \leq 0 \end{cases}, \quad (221)$$

and the matrix elements of S_n are determined by Eqs. (91) and (92).

5.2.1 Generation of disorder

In the case of finite correlation lengths, specific extensive physical quantities (which are obtained by relating extensive quantities to the length of the system) show a self-averaging effect as the length of the chain increases [20], i.e. they become independent

of the concrete realization of the disorder. This self-averaging effect can be understood by partitioning a very long macroscopic chain into a large number of chains, each one still being much longer than the correlation length and any other microscopic length scale. In this case, boundary effects between adjacent parts of the original chain may be neglected and we are practically left with an ensemble of a large number of independent chains. Physical quantities can now be calculated for each chain individually, assuming independently all possible values with their respective statistical weight. Specific extensive quantities are now given by the ensemble-average, giving a non-random value in the thermodynamic limit. The DOS and the inverse localization length can therefore be calculated by generating one typical very long chain.

Gaussian disorder

To generate Gaussian disorder at the sample points x_n with the first two moments satisfying

$$\langle \Delta(x) \rangle = \Delta_{\text{av}} \quad , \quad \langle \tilde{\Delta}(x) \tilde{\Delta}(x') \rangle = \Delta_s^2 e^{-|x-x'|/\xi} \quad , \quad (222)$$

where $\tilde{\Delta}(x) \equiv \Delta(x) - \Delta_{\text{av}}$, we use a realization of an Ornstein-Uhlenbeck process described in more general form in Ref. [23] Using the Box-Muller algorithm [79], we generate independent Gaussian random numbers g_n with $\langle g_n \rangle = 0$ and $\langle g_n^2 \rangle = 1$. For real $\Delta(x)$, we generate $\tilde{\Delta}_n = \Delta_n - \Delta_{\text{av}}$ recursively by

$$\tilde{\Delta}_0 = \Delta_s g_0 \quad , \quad \tilde{\Delta}_{n+1} = a_n \tilde{\Delta}_n + \sqrt{1 - a_n^2} \Delta_s g_{n+1} \quad , \quad (223)$$

where $a_n = e^{-|\delta_n|/\xi}$. This Markov process leads to a Gaussian random process with the desired correlation functions. The Markov property of the algorithm allows us to generate the disorder simultaneously with the iteration of the recurrence relations (218) and (219), so that the algorithm presented above practically needs no memory space and, in principle, arbitrary long chains can be considered. If we choose $|\delta_n|/\xi \ll 1$ (in practical calculations we choose $|\delta_n|/\xi \approx 0.0001$ to 0.05 depending on $\Delta_s \xi$ and make sure that lessening of $|\delta_n|/\xi$ does not change the results), the (integrated) DOS and the inverse localization length may be calculated with arbitrary accuracy numerically.

Of course, the above algorithm can also be used to generate V_n and in the complex case, $\text{Re } \Delta_n$ and $\text{Im } \Delta_n$ can be generated by replacing Δ_s by $\Delta_s/\sqrt{2}$ (see Ref. [23]).

5.2.2 *Results*

First numerical calculations of the DOS of the FGM in the regime of finite correlation lengths were done by myself in collaboration with Peter Kopietz using an algorithm similar to the one presented here [24]. Simultaneously, Millis and Monien presented their data obtained by an exact diagonalization of a lattice regularization of the FGM [80]. However, these authors did not make any attempts to relate their results to the continuous FGM which would have allowed for a more direct comparison with the solutions given by Sadovskii [10].

In contrast to the algorithm described in Ref. [24], the algorithm presented here does not only allow for a numerical calculation of the (integrated) DOS, it is also capable of a simultaneous evaluation of the localization length which for finite ξ has never been published before.

Commensurate case

In Fig. 9, we show our numerical results for the DOS $\rho(\omega)$ and inverse localization length $\ell^{-1}(\omega)$ for real $\Delta(x)$ (with $\Delta_{\text{av}} = 0$ and $V(x) = 0$), which refers to the symmetric phase of a commensurate system with no forward scattering. Except for $\Delta_s \xi = 1000, 0.2$ we have chosen the same values of the dimensionless parameter $\Delta_s \xi$ as in Fig. 7 of Ref. [10]. One clearly sees the Dyson singularity in the DOS which exists for any finite value of ξ and overshadows the pseudogap at sufficiently small energies. One can also see that this Dyson singularity is accompanied by a singularity in the inverse localization length. The inverse localization length drops to zero at $\omega = 0$, in accordance with the exact result $\ell^{-1}(0) = \langle \Delta_{\text{av}} \rangle$ [see Eq. (144)].

The Dyson singularity in the DOS is missed by Sadovskii's algorithm [10]. For a more quantitative description of the Dyson singularity we have plotted the logarithm of the integrated DOS \mathcal{N}/Δ_s versus the logarithm of $-\ln(\omega/\Delta_s)$. For frequencies between $\omega = 10^{-11}\Delta_s$ and $\omega = 10^{-6}\Delta_s$, we find that the data can be very well fitted by a straight line, such that

$$\mathcal{N}(\omega) = \rho_0 \frac{\Delta_s B(\xi)}{|\ln(\omega/\Delta_s)|^{\alpha(\xi)}}, \quad (224)$$

which implies for the DOS

$$\rho(\omega) = \rho_0 \frac{A(\xi)}{(\omega/\Delta_s) |\ln(\omega/\Delta_s)|^{1+\alpha(\xi)}}, \quad (225)$$

with $A(\xi) = \alpha(\xi) B(\xi)$. Plots of the exponent $\alpha(\xi)$ and the weight factors of the Dyson singularity $A(\xi)$ and $B(\xi)$ are shown in Figs. 10 and 11. For $\Delta_s \xi \ll 1$ our data is consistent with the white noise result $\alpha = 2$. As $\Delta_s \xi$ increases, the exponent $\alpha(\xi)$ decreases, assuming for large correlation lengths ξ the finite value

$$\alpha(\xi) \approx 0.41, \quad \Delta_s \xi \gtrsim 500. \quad (226)$$

Fitting the data for $A(\xi)$ in the regime between $\Delta_s \xi = 500$ and $\Delta_s \xi = 10000$ to a power law shows that the weight of the singularity of the DOS vanishes as

$$A(\xi) = 0.175 (\Delta_s \xi)^{-0.65}. \quad (227)$$

The plot of the DOS given in Fig. 9 shows that for large correlation lengths ξ the Dyson singularity only overshadows a pseudogap, such that $\rho(\omega)$ takes a minimal value at a certain frequency $\omega^*(\xi)$. A double-logarithmic plot of $\rho(\omega^*)$ versus $(\Delta_s \xi)^{-1}$ is given by the triangles in Fig. 12. The straight line gives a fit to a power-law:

$$\rho(\omega^*)/\rho_0 = C (\Delta_s \xi)^{-\mu} \quad (228)$$

We find

$$C = 0.482 \pm 0.010, \quad \mu = 0.3526 \pm 0.0043 \quad (229)$$

The circles in Fig. 12 show ω^* where $\rho(\omega)$ is minimal. The long solid line is a fit to a power-law

$$\omega^*/\Delta_s = D (\Delta_s \xi)^{-\gamma}. \quad (230)$$

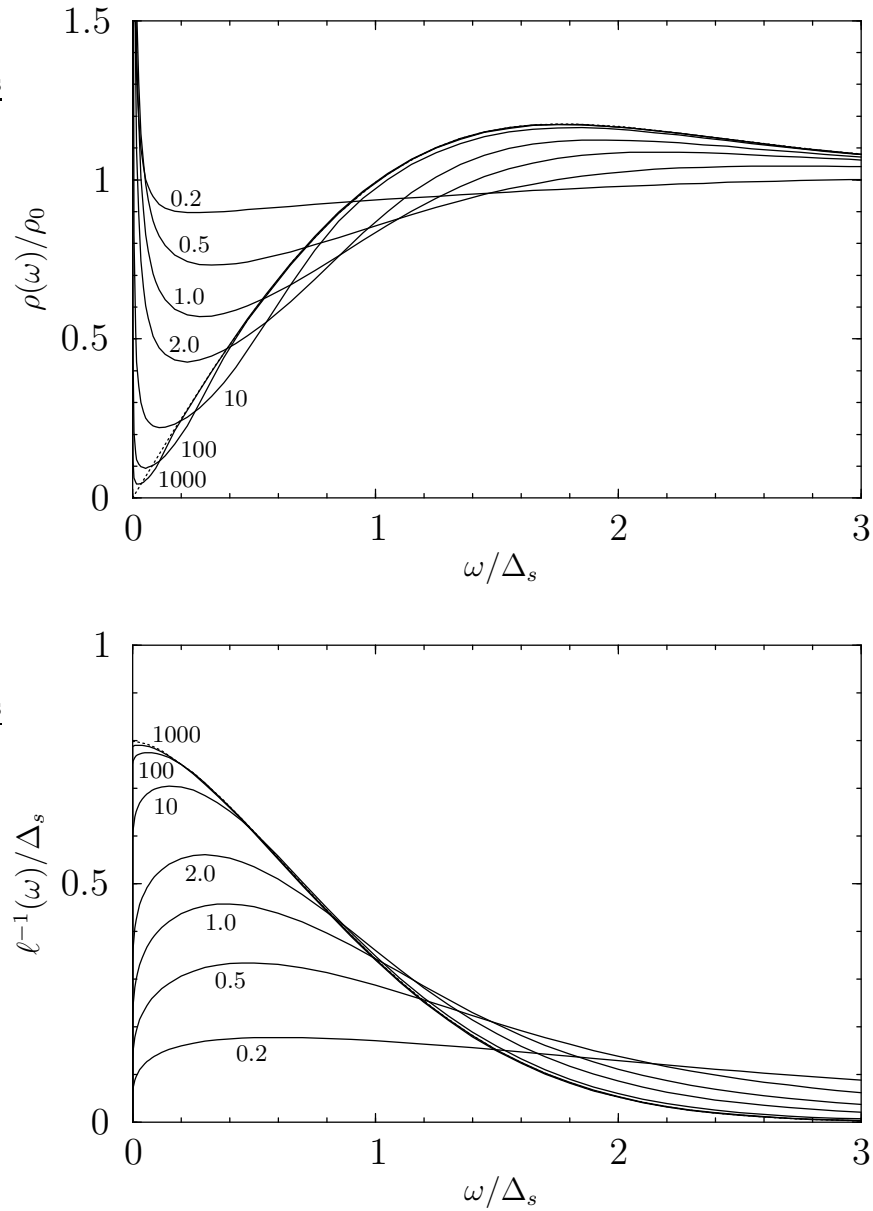


Fig. 9 Plot of the DOS $\rho(\omega)$ and the inverse localization length $\ell^{-1}(\omega)$ for real $\Delta(x)$ with Gaussian statistics, $\Delta_s L = 10^8$, and finite correlation lengths $\Delta_s \xi = 1000, 100, 10, 2.0, 1.0, 0.5$, and 0.2 . For any finite ξ , we find $\rho(0) = \infty$ and $\ell^{-1}(\omega) = 0$. The dashed line represents the exact result derived in Section 4 and for $\omega \gtrsim 0.2\Delta_s$ is almost indistinguishable from the result for $\Delta_s \xi = 1000$.

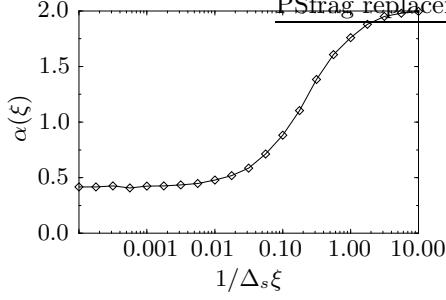


Fig. 10 Plot of the exponent $\alpha(\xi)$ defined by Eq. (224) for frequencies between $\omega = 10^{-6}\Delta_s$ and $\omega = 10^{-11}\Delta_s$. While our results for small $\Delta_s\xi$ are consistent with the white noise result $\alpha = 2$, in the opposite limit $\Delta_s\xi \gg 1$ we find $\alpha \approx 0.41$.

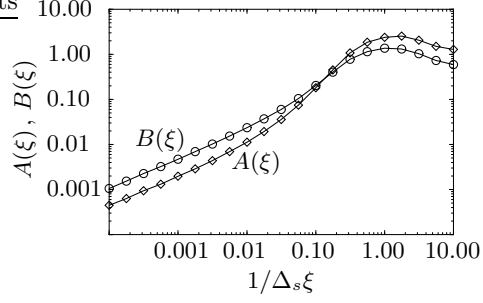


Fig. 11 Plot of the weight factors $A(\xi)$ and $B(\xi)$ of the Dyson singularity defined by Eqs. (224) and (225) for frequencies between $\omega = 10^{-6}\Delta_s$ and $\omega = 10^{-11}\Delta_s$. As the correlation length increases, both weight factors scale to zero.

Here, we find

$$D = 0.2931 \pm 0.0074, \quad \gamma = 0.3513 \pm 0.0051. \quad (231)$$

such that within numerical accuracy $\mu = \gamma$. The proportionality of $\rho(\omega^*)$ to the energy scale ω^* , which can be interpreted as the width of the Dyson singularity, can also directly be seen in Fig. 9. Finally we note that for $\Delta_s\xi \lesssim 0.2$ our algorithm produces results consistent with the white noise limit $\Delta_s\xi \ll 1$. From the exact solution of Ovchinnikov and Erikhman [16] we obtain $\rho(\omega^*)/\rho_0 \rightarrow 0.9636$ and $\omega^* \rightarrow 1.2514 \Delta_s^2\xi$ which determines the short solid line in Fig. 12, describing $\omega^*(\xi)$ in the white-noise limit.

Incommensurate case

The DOS $\rho(\omega)$ and inverse localization length $\ell^{-1}(\omega)$ for complex $\Delta(x)$ (and $\Delta_{\text{av}} = V(x) = 0$), which refers to the symmetric phase of the commensurate case with no forward scattering are presented in Fig. 13. Neither the DOS nor the inverse localization length involve a singularity. In fact, a direct comparison of our results for the DOS with those obtained from Sadovskii's algorithm shows a good agreement.

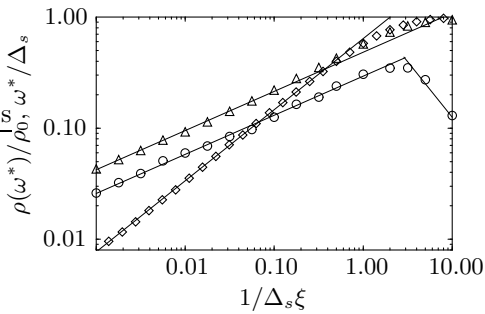


Fig. 12 Double-logarithmic plot of $\rho(\omega^*)/\rho_0$ as a function of $1/\Delta_s\xi$ for real $\Delta(x)$ (triangles) and complex $\Delta(x)$ (diamonds), where ω^* is the energy for which the DOS assumes its minimum. While $\omega^* = 0$ for complex $\Delta(x)$, the circles give the double-logarithmic plot of ω^*/Δ_s for real $\Delta(x)$ as a function of $1/\Delta_s\xi$.

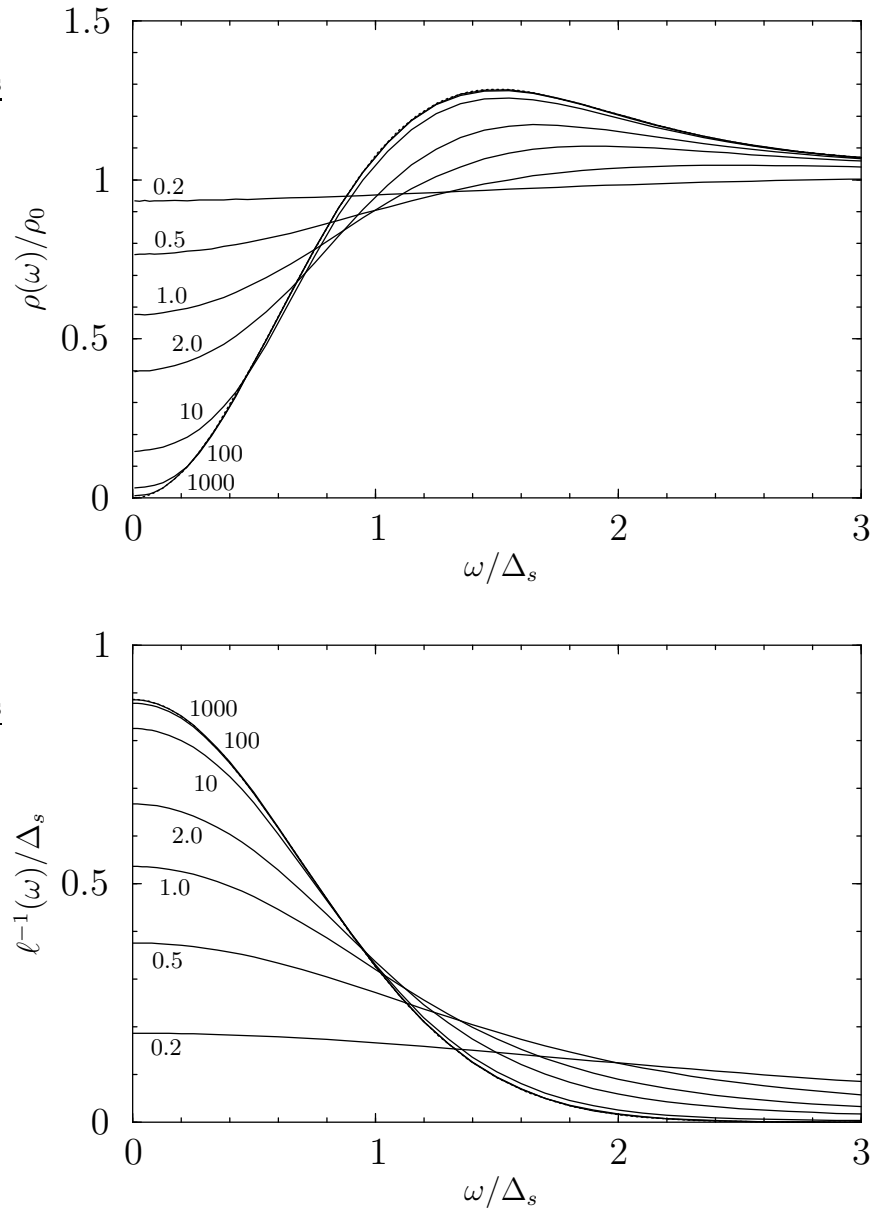


Fig. 13 Plot of the DOS $\rho(\omega)$ and the inverse localization length $\ell^{-1}(\omega)$ for complex $\Delta(x)$ with Gaussian statistics, $\Delta_s L = 10^8$, and finite correlation lengths $\Delta_s \xi = 1000, 100, 10, 2.0, 1.0, 0.5$, and 0.2 . The dashed line represents the exact result derived in Section 4. This line is hardly recognizable because it is almost indistinguishable from the line for $\Delta_s \xi = 1000$.

For a more quantitative comparison, the diamonds in Fig. 12 show the DOS $\rho(0)$ at the Fermi energy. A fit to a power-law gives

$$\rho(0)/\rho_0 = C (\Delta_s \xi)^{-\mu}, \quad (232)$$

with

$$C = 0.6397 \pm 0.0066, \quad \mu = 0.6397 \pm 0.0024. \quad (233)$$

Note that within numerical accuracy we find $C = \mu$. This result should be compared with Sadovskii's approximate result $C = 0.541 \pm 0.013$ and $\mu = 1/2$.

5.3 Phase fluctuations only

As already discussed at the end of Section 2, far below the mean-field critical temperature T_c^{MF} , amplitude fluctuations of the complex order parameter $\Delta(x) \equiv |\Delta(x)|e^{i\vartheta(x)}$ are frozen out and only phase fluctuations survive. In terms of the ‘‘superfluid velocity’’ $V(x) = \partial_x \vartheta(x)/2$, the process of averaging can be written as

$$\langle \dots \rangle = \frac{\int \mathcal{D}\{V\} \dots e^{-\beta F\{V\}}}{\int \mathcal{D}\{V\} e^{-\beta F\{V\}}}, \quad (234)$$

where $F\{V\}$ is the free energy functional given in Eq. (35). Since $F\{V\}$ is Gaussian and local, the process of averaging is described by Gaussian white noise. The first two moments of $V(x)$ are given by $\langle V(x) \rangle = 0$ and

$$\langle V(x)V(x') \rangle = 2 \frac{1}{4\xi(T)} \delta(x - x'), \quad (235)$$

with [see Eq.39] $\xi(T) = s\rho_s(T)/2T$. Well below the mean-field temperature T_c^{MF} , we can use the BCS gap equation $\Delta_s = 1.764 T_c^{\text{MF}}$ and $\rho_s(T) \approx \rho_0 = \pi^{-1}$ to get for the dimensionless parameter¹¹ $\Delta_s \xi(T)$

$$\Delta_s \xi(T) = 0.281 s T_c^{\text{MF}}/T. \quad (236)$$

As already shown in Section 2, Eq. (235) implies the exponentially decaying correlation function $\langle \Delta(x)\Delta^*(x') \rangle = \Delta_s^2 \exp(-|x - x'|/\xi(T))$.

To calculate physical quantities like the DOS or the inverse localization length, we use the gauge invariance of these quantities under the gauge transformation (130) and map the phase fluctuations of the order parameter $\Delta(x) = \Delta_s e^{i\vartheta(x)}$ onto the effective forward scattering potential $V(x) = \partial_x \vartheta(x)/2$.

5.3.1 Density of states and inverse localization length

The DOS and the inverse localization length for the remaining problem involving only a constant gap parameter and forward scattering described by Gaussian white noise were already calculated in the previous section. With the exception of the constant shift in the inverse localization length, the results are identical with those for the incommensurate case without forward scattering and $\langle \Delta(x) \rangle = \Delta_0 \neq 0$. Substituting

¹¹The prefactor can be expressed in terms of the Euler constant γ , such that $\Delta_s \xi(T) = s T_c^{\text{MF}}/2e^{\gamma} T$.

in Eqs. (199) and (200) Δ_0 by Δ_s , \tilde{D} by $1/4\xi(T)$ and setting $D = 0$ (since there is only forward scattering) which implies a completely different interpretation of the resulting equations, we get $\Gamma(\omega) = -i\omega + \Delta_s I_{1-i4\omega\xi}(4\Delta_s\xi)/I_{-i4\omega\xi}(4\Delta_s\xi)$, or, equivalently,

$$\Gamma(\omega) = \Delta_s \frac{I'_{-i4\omega\xi}(4\Delta_s\xi)}{I_{-i4\omega\xi}(4\Delta_s\xi)}. \quad (237)$$

It follows from Eq. (201) that the integrated DOS is given by

$$\mathcal{N}(\omega) = \rho_0 \frac{\sinh(4\pi\omega\xi)}{4\pi\xi} \frac{1}{|I_{i4\omega\xi}(4\Delta_s\xi)|^2}. \quad (238)$$

Plots of the DOS and the inverse localization length for characteristic values of $\Delta_s\xi$ are shown in Fig. 14. At the Fermi energy, the DOS simplifies to

$$\rho(0) = \frac{\rho_0}{[I_0(4\Delta_s\xi)]^2}, \quad (239)$$

such that, as the temperature is lowered and the correlation length grows, the DOS at the Fermi energy vanishes exponentially,

$$\rho(0) \sim 8\pi\rho_0\Delta_s\xi \exp(-8\Delta_s\xi), \quad 4\Delta_s\xi \gg 1. \quad (240)$$

This result is in contrast to the power-law behavior of the DOS as predicted by Gaussian statistics. A plot of the DOS at the Fermi energy is shown in Fig. 15 as a function of $1/\Delta_s\xi$. For a comparison, we have also plotted $\rho(0)$ for Gaussian statistics and the result found in the Born approximation, which at low temperatures can only poorly describe the quantitative behavior of the pseudogap. For $T = T_c^{\text{MF}}/4$ which corresponds to $\Delta_s\xi \approx 2.0$, we find that the DOS $\rho(0)$ for phase fluctuations only is less than $10^{-5}\rho_0$ while the Born approximation and the numerical exact result for Gaussian statistics suggest a value of order $\rho_0/4$.

As can also be seen in Fig. 15, there is no pseudogap for $\Delta_s\xi \lesssim 0.1$. Note, however, that these correlation lengths correspond to temperatures of order T_c^{MF} , where amplitude fluctuations are important. Nevertheless, using only phase fluctuations gives a good qualitative description of the DOS for all temperatures T .

For temperatures well below the mean-field temperature T_c^{MF} where our theory becomes quite accurate, we have, according to Eq. (236), $\Delta_s\xi \gg 1$, such that the Bessel function $I_{i\nu}(\nu z) = e^{-\pi\nu/2} J_{i\nu}(i\nu z)$ may be approximated by an Airy function. For large correlation lengths we expand the resulting equation for ω around Δ_s and obtain to leading order in $1/4\Delta_s\xi$ a maximum of the DOS $\rho(\omega)$ at Δ_s , described by the inverted parabola

$$\rho(\omega) \sim \rho_0 \left[a(4\Delta_s\xi)^{1/3} - b(4\Delta_s\xi)^{5/3} \left(\frac{\omega}{\Delta_s} - 1 \right)^2 \right], \quad (241)$$

with $a = \frac{1}{2^{4/3}\pi} \frac{c_2}{c_1^3} \approx 0.731$ and $b = \frac{1}{2^{2/3}\pi} \frac{1}{c_1^2} \left[3 \left(\frac{c_2}{c_1} \right)^3 - 1 \right] \approx 0.258$, where $c_1 = \text{Ai}(0) = 3^{-2/3}/\Gamma(2/3) \approx 0.355$ and $c_2 = -\text{Ai}'(0) = 3^{-1/3}/\Gamma(1/3) \approx 0.259$. Note that Eq. (241) implies that the maximum of the DOS diverges as $(4\Delta_s\xi)^{1/3} \propto T^{-1/3}$.

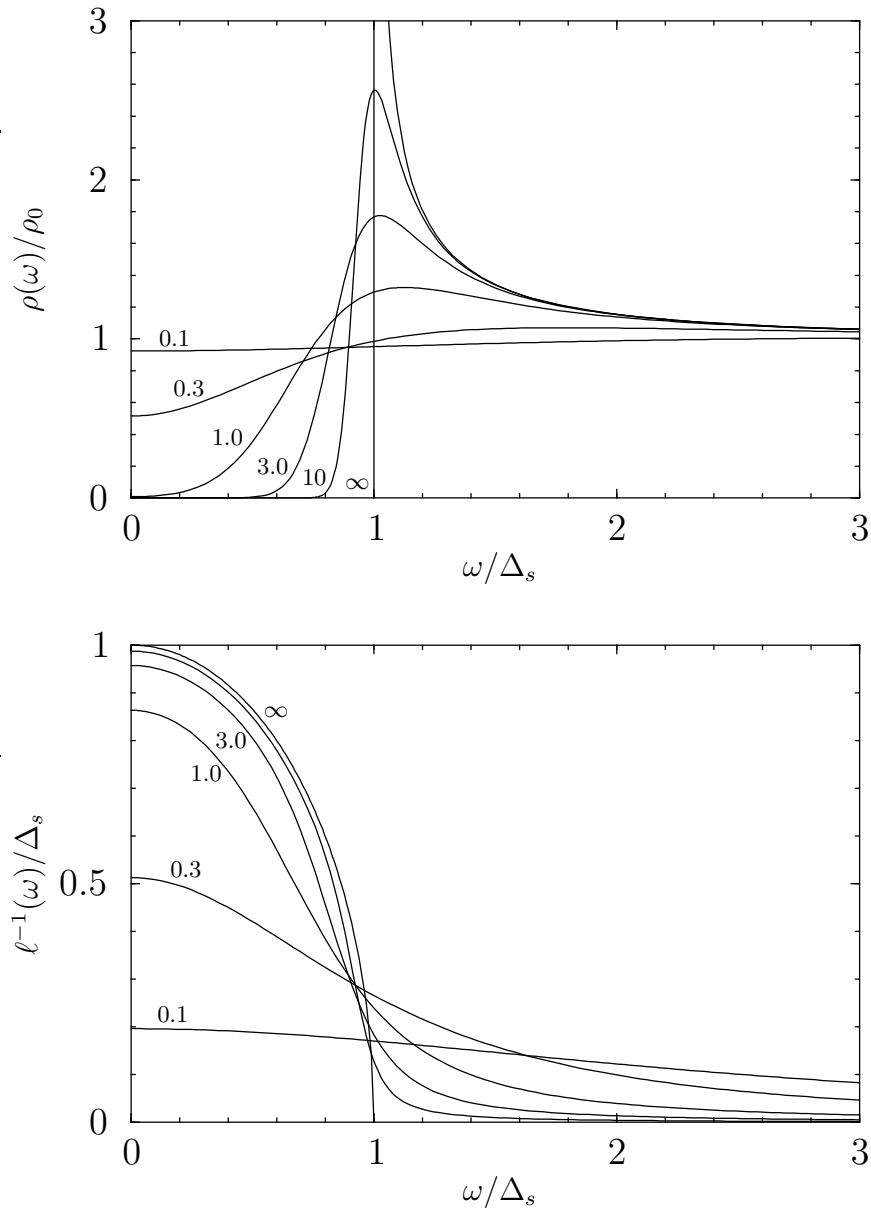


Fig. 14 Plot of the DOS $\rho(\omega)$ and the inverse localization length $\ell^{-1}(\omega)$ for phase fluctuations only and $\Delta_s \xi = 0.1, 0.3, 1.0, 3.0, 10.0$ and ∞ .

Away from $\omega = \Delta_s$, we find for $\omega > \Delta_s$

$$\rho(\omega) \sim \rho_0 \left(1 + \frac{\Delta_s^2}{4\omega^2} \right), \quad 4\Delta_s \xi \left(\frac{\omega}{\Delta_s} - 1 \right)^{3/2} \gg 1, \quad (242)$$

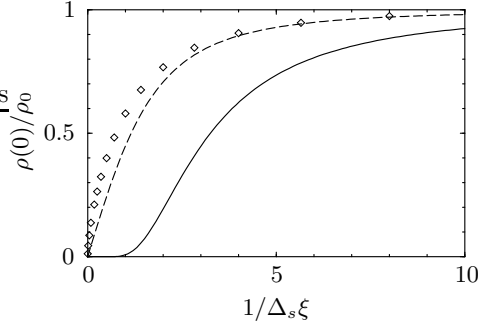


Fig. 15 Plot of the DOS $\rho(0)/\rho_0$ as a function of $1/\Delta_s\xi$. The solid line gives the DOS for phase fluctuations only while the dashed line is the result found in the leading order Born approximation [see Eq. 66] and the diamonds give the DOS evaluated for Gaussian statistics [see Subsection 5.2]

which is independent of $\Delta_s\xi$ and agrees with the mean-field result. And for $\omega < \Delta_s$ we find

$$\begin{aligned} \rho(\omega) \sim 8\rho_0 \sqrt{\Delta_s^2 - \omega^2} \xi \arccos(\omega/\Delta_s) [1 + \exp(-8\pi\omega\xi)] \\ \times \exp\left(-8[\sqrt{\Delta_s^2 - \omega^2} \xi - \omega\xi \arccos(\omega/\Delta_s)]\right), \\ 4\Delta_s\xi \left(1 - \frac{\omega}{\Delta_s}\right)^{3/2} \gg 1. \end{aligned} \quad (243)$$

If $\omega \ll \Delta_s$ and $4\omega^2\xi/\Delta_s \ll 1$, this result simplifies to

$$\rho(0) \sim 8\pi\rho_0\Delta_s\xi \cosh(4\pi\omega\xi) \exp(-8\Delta_s\xi). \quad (244)$$

5.3.2 Pauli paramagnetic susceptibility

The Pauli paramagnetic susceptibility is defined as the contribution of the conduction electrons to the susceptibility and can be written in terms of the DOS. A magnetic field H shifts the energy levels of the electrons by an amount $\pm\mu_B H$, where μ_B is the Bohr magneton and the sign depends on the spin orientation of the electron with respect to the field. The resulting different occupation of spin-up and spin-down states leads to a magnetization density $M(T)$ which for small magnetic fields is linear in H . If $\rho(\omega) = \rho(-\omega)$ as in the FGM, the susceptibility $\chi(T) \equiv dM(T)/dH$ can be written as

$$\chi(T) = \frac{\mu_B^2}{T} \int_0^\infty d\omega \rho(\omega) \frac{1}{\cosh^2(\omega/2T)}. \quad (245)$$

Placing the asymptotic expression (243) with $\xi(T) = \rho_s/T$ into this equation, we find

$$\begin{aligned} \chi(T)/\chi_0 \sim \frac{16\rho_s}{T^2} \int_0^\infty d\omega \sqrt{\Delta_s^2 - \omega^2} \arccos\left(\frac{\omega}{\Delta_s}\right) \frac{1 + \exp[-8\pi\rho_s\omega/T]}{(1 + \exp[-2\omega/T])^2} \\ \times \exp\left(-\frac{\Delta_s}{T} \left[\frac{\omega}{\Delta_s} \left(1 - 8\rho_s \arccos\left(\frac{\omega}{\Delta_s}\right)\right) + 8\rho_s \sqrt{1 - (\omega/\Delta_s)^2} \right]\right), \end{aligned} \quad (246)$$

where $\chi_0 = 2\mu_B^2\rho_0$. For $\rho_s > \rho_0/4$ (and $T \lll T_c^{\text{MF}}$), the integrand is sharply peaked at $\omega = \cos(1/8\rho_s)\Delta_s$, such that the integral may be evaluated by a saddle point

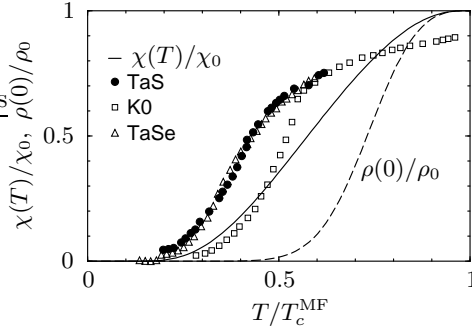


Fig. 16 Plot of the susceptibility $\chi(T)$ calculated for $\xi(T) = \rho_s(T)/T$ [with $\rho_s(T)$ given by Eq. (37)] and $\Delta_s(T)$ determined by the minimum of the Ginzburg-Landau functional. For a comparison, we also show as the dashed line the DOS at the Fermi energy, $\rho(0)$.

integration, resulting in

$$\frac{\chi(T)}{\chi_0} \sim \sqrt{\frac{\pi}{\rho_s}} \left(\frac{\sin(1/8\rho_s) \Delta_s}{T} \right)^{3/2} \exp\left(-\frac{8\rho_s \sin(1/8\rho_s) \Delta_s}{T}\right), \quad (247)$$

$$T \ll 4\rho_s \Delta_s (1 - \cos(1/8\rho_s))^{3/2}.$$

Note, that the temperature restriction is necessary for the asymptotic expansion of the DOS to be valid. Although the susceptibility $\chi(T)$ vanishes exponentially, the exponent $8\rho_s \sin(1/8\rho_s) \Delta_s/T$ is smaller than the exponent $8\rho_s \Delta_s/T$, which governs the DOS at the Fermi energy. However, as ρ_s approaches $\rho_0/4$, the two exponents become identical, such that for $\rho_s \leq \rho_0/4$ the DOS and the susceptibility have the same exponential dependence on T .

A numerical evaluation of the susceptibility $\chi(T)/\chi_0$ for $\xi(T) = \rho_s(T)/T$ given by Eq. (37) and $\Delta_s(T)$ determined by the BCS gap equation (38) is shown in Fig. 16. For a comparison, we have also plotted the DOS $\rho(0)/\rho_0$ as a function of temperature. The two are not identical because for small temperatures (and $\rho_s = \rho_0$), the major contribution to the integral in Eq. (245) comes from the frequency region just below Δ_s . In Fig. 16, we also show susceptibility data taken from Ref. [82] for incommensurate quasi one-dimensional conductors which undergo a Peierls transition.

It is quite surprising that our plot of the susceptibility is very similar to the plot obtained by Lee, Rice and Anderson [9] which perfectly fits experimental data [8, 81, 82]. However, to explain experimental data, Lee, Rice and Anderson [9] had to base their calculations on a *real* order parameter with a correlation length which for low temperatures increases exponentially as the temperature is lowered. Only the exponentially increasing correlation length of a real order parameter could lead to an exponentially decreasing susceptibility and the prediction of $T_c^{3D} \approx T_c^{MF}/4$. Here, we have shown that these predictions should also hold for a complex order parameter with a correlation length which increases as $1/T$. Since most Peierls chains are incommensurate and the susceptibility of many incommensurate Peierls chains has been compared with the theory by Lee, Rice and Anderson [9], our results are of major experimental relevance. For a comparison between theory and experiment, it should be recalled that we have only used a strictly one-dimensional model with phase fluctuations only. At higher temperatures, one should also include amplitude

fluctuations.

5.3.3 Thermodynamic quantities

The DOS encapsulates the whole thermodynamics. Let us first consider the electronic free energy $F_{\text{el}}(T)$ with respect to the gapped state for which we have $\rho_{\infty}(\omega) = \rho_0 \theta(\omega^2 - \Delta_s^2) |\omega| / (\omega^2 - \Delta_s^2)$:

$$F_{\text{el}}(T) - F_{\text{el}}^{\xi=\infty}(T) = -\frac{sL}{\beta} \int_{-\infty}^{\infty} d\omega [\rho(\omega) - \rho_{\infty}(\omega)] \ln(1 + e^{-\beta\omega}) . \quad (248)$$

Partial integration leads to

$$\begin{aligned} F_{\text{el}}(T) - F_{\text{el}}^{\xi=\infty}(T) &= -sL \int d\omega [\mathcal{N}(\omega) - \mathcal{N}_{\infty}(\omega)] \frac{1}{e^{\beta\omega} + 1} \\ &= s\rho_0 L \text{Im} \int d\omega [\Gamma(\omega) - \Gamma_{\infty}(\omega)] \frac{1}{e^{\beta\omega} + 1} , \end{aligned} \quad (249)$$

where $\Gamma(\omega) = \ell^{-1}(\omega) - i\pi\mathcal{N}(\omega)$ and $\Gamma_{\infty}(\omega) = \sqrt{\Delta_s^2 - (\omega + i0)^2}$. The square root has to be taken such that $\Gamma_{\infty}(\omega) \rightarrow -i\omega$ for $\omega \rightarrow \infty$. Since $\Gamma(\omega)$ is analytic in the upper half plane, the integral may be done by closing the integral in the upper half plane and using the residue theorem. We find

$$F_{\text{el}}(T) - F_{\text{el}}^{\xi=\infty}(T) = -s\rho_0 L \frac{2\pi}{\beta} \sum_{\tilde{\omega}_n > 0} [\text{Re} \Gamma(i\tilde{\omega}_n) - \tilde{\omega}_n] . \quad (250)$$

For the FGM with phase fluctuations only, we obtain by placing Eq. (237) into this equation

$$F_{\text{el}}(T) - F_{\text{el}}^{\xi=\infty}(T) = s\rho_0 L \Delta_s \frac{2\pi}{\beta} \sum_{\tilde{\omega}_n > 0} \left[\sqrt{1 + \left(\frac{\tilde{\omega}_n}{\Delta_s}\right)^2} - \frac{I'_{4\tilde{\omega}_n \xi}(4\Delta_s \xi)}{I_{4\tilde{\omega}_n \xi}(4\Delta_s \xi)} \right] . \quad (251)$$

Up to an irrelevant additive constant, $F_{\text{el}}^{\xi=\infty}(T)$ is given by

$$F_{\text{el}}^{\xi=\infty}(T) = -s\rho_0 L 2\Delta_s^2 \int_1^{\infty} du \sqrt{u^2 - 1} \frac{1}{e^{\Delta_s u/T} + 1} , \quad (252)$$

which for small temperatures is exponentially small:

$$F_{\text{el}}^{\xi=\infty}(T) \sim -s\rho_0 L \sqrt{2\pi} \Delta_s^2 e^{-\Delta_s/T} , \quad T \ll \Delta_s . \quad (253)$$

While in the general case we have to add Eqs. (251) and (252) to get the free energy $F_{\text{el}}(T)$, for low temperatures we can neglect the exponentially small contribution given by Eq. (253), such that $F_{\text{el}}(T)$ is determined by the right-hand side of Eq. (251).

For $T \ll T_c^{\text{MF}}$, the dimensionless correlation length $\Delta_s \xi$ is large, and a uniform asymptotic expansion of $I_{\nu}(\nu z)$ and $I'_{\nu}(\nu z)$ [see A&S, Eqs. (9.7.7) and (9.7.9)] can be used to find for the leading terms of the free energy

$$\boxed{F_{\text{el}}(T) \sim s\rho_0 L \Delta_s^2 \left[\frac{\pi}{4} \frac{1}{4\Delta_s \xi} - \frac{1}{12} \frac{1}{(4\Delta_s \xi)^2} \right]} . \quad (254)$$

Electronic specific heat

An experimentally accessible thermodynamic quantity is the electronic specific heat which can be expressed in terms of the free energy as

$$C_{\text{el}}(T) = -T \frac{d^2 F_{\text{el}}(T)}{dT^2} . \quad (255)$$

The low-temperature behavior of $C_{\text{el}}(T)$ can be obtained from Eq. (254): Using $\xi(T) = s\rho_s(0)/2T$, it directly follows

$$\boxed{C_{\text{el}}(T) \sim \frac{1}{8} \left(\frac{\rho_0}{s\rho_s(0)} \right)^2 C_{\text{el}}^0(T) ,} \quad (256)$$

where the specific heat of free electrons is given by

$$C_{\text{el}}^0(T) = s \frac{\pi^2}{3} \rho_0 L T . \quad (257)$$

Although the DOS exhibits a pseudogap and vanishes exponentially near the Fermi energy as the temperature is lowered, the electronic specific heat $C_{\text{el}}(T)$ vanishes only linearly in T , as for free electrons.

We conclude this section with a summary of the central results of the FGM valid at low temperatures where phase fluctuations dominate in Table 1.

Table 1 Asymptotic low temperature results for the FGM describing electrons with spin. Note that we have reintroduced the Fermi velocity v_F and note also that the mean-field critical temperature T_c^{MF} serves as the only energy scale. For generalizations of the formulas see the text.

superfluid density	$\rho_s(T) \sim \rho_0 = \frac{1}{\pi v_F}$
correlation length	$\xi(T) \sim \frac{v_F}{\pi T}$
density of states	$\frac{\rho(0)}{\rho_0} \sim \frac{14.1 T_c^{\text{MF}}}{T} \exp\left(-\frac{4.49 T_c^{\text{MF}}}{T}\right)$
inverse localization length	$\ell^{-1}(0) \sim \frac{1.76 T_c^{\text{MF}}}{v_F}$
susceptibility	$\frac{\chi(T)}{\chi_0} \sim 1.74 \left(\frac{T_c^{\text{MF}}}{T}\right)^{3/2} \exp\left(-\frac{1.72 T_c^{\text{MF}}}{T}\right)$
electronic specific heat	$\frac{C_{\text{el}}(T)}{C_{\text{el}}^0(T)} \sim \frac{1}{32}$

6 Conclusion

In this work, we have discussed the density of states (DOS) of the fluctuating gap model (FGM) and related quantities like the inverse localization length, the Pauli paramagnetic susceptibility and the low-temperature specific heat. We introduced the FGM as an effective low-energy model describing the electronic properties of Peierls chains and emphasized the fact that the FGM also finds its applications in other physical contexts: Spin chains can be mapped by a Jordan-Wigner transformation onto the FGM and in order to explain the pseudogap-phenomenon in underdoped cuprates above a phase transition, higher-dimensional generalizations of the FGM have been used.

With the rediscovery of the FGM in the context of high-temperature superconductivity, a previously unnoticed subtle error in Sadovskii's widely used Green function of the FGM was brought to light. This error called for a reinvestigation of the FGM.

After setting up a non-perturbative theory which, in principle, allows to express the one-particle Green function as a functional of an arbitrary given realization of the disorder, we derived a simple equation of motion whose solution determines the DOS and the inverse localization length. Starting from this equation, we could rederive all known results for the FGM in the white noise limit.

Considering the equation of motion governed by the phase which determines the DOS, we argued that the Dyson singularity found in the white noise limit for commensurate Peierls chains should not be an artifact of the white noise limit, but should be present for any finite correlation length in contradiction to Sadovskii's solution. Our following numerical calculation of the DOS and inverse localization length confirmed this prediction and showed also that for large correlation lengths, the Dyson singularity only overshadows a pseudogap. Although Sadovskii's algorithm misses this singularity, his solutions for the incommensurate case where there are no singularities in the DOS give a fairly good approximation to the exact result.

In the pseudogap-regime below the mean-field critical temperature, fluctuations of the order parameter cannot be described by Gaussian statistics. Instead, as the temperature is lowered, amplitude fluctuations get gradually frozen out, and the amplitude takes on a value given by the minimum of the Ginzburg-Landau functional and only long-wavelength gapless phase fluctuations survive. Using a gauge transformation to map the phase fluctuations of the order parameter onto an effective forward scattering potential, we could even find an exact solution for the FGM involving only phase fluctuations which should be valid in the low temperature regime. We found that the low-temperature specific heat is linear in T and that both the DOS at the Fermi energy and the Pauli paramagnetic susceptibility vanish exponentially as the temperature T is lowered, the ratio of the former to the latter also vanishing exponentially. The Pauli paramagnetic susceptibility has been measured in various experiments and is in good agreement with our results.

Having discussed quantities related to the DOS, one would also like to calculate quantities like the spectral function. This has been done for a special non-Gaussian probability distribution involving amplitude and phase fluctuations in Ref. [52], but accurate results for realistic probability distributions (e.g. for phase fluctuations only) are not known yet.

I would like to thank K. Schönhammer, R. Hayn and especially P. Kopietz for helpful discussions. This work was financially supported by the DFG (Grant No. Ko 1442/4-2).

References

- [1] J. Fröhlich, Proc. Royal Soc. London Ser. **A223** (1954) 296
- [2] R. E. Peierls, *Quantum Theory of Solids*, Oxford University Press, New York 1955
- [3] C. G. Kuper, Proc. Royal Soc. London **A227** (1955) 214
- [4] M. J. Rice and S. Strässler, Solid State Commun. **13** (1973) 125
- [5] M. J. Rice and S. Strässler, Solid State Commun. **13** (1973) 1389
- [6] G. Grüner and A. Zettl, Phys. Rep. **119** (1985) 117
- [7] G. Grüner, Rev. of Mod. Phys. **60** (1988) 1129
- [8] G. Grüner, *Density Waves in Solids*, Addison-Wesley, Reading 1994
- [9] P. A. Lee, T. M. Rice and P. W. Anderson, Phys. Rev. Lett. **31** (1973) 462
- [10] M. V. Sadovskii, Zh. Eksp. Teor. Fiz. **77** (1979) 2070 [Sov. Phys. JETP **50** (1979) 989]
- [11] J. Schmalian, D. Pines and B. Stojković, Phys. Rev. Lett. **80** (1998) 3839
- [12] J. Schmalian, D. Pines and B. Stojković, Phys. Rev. B **60** (1999) 667
- [13] M. V. Sadovskii, cond-mat/0102111, to appear in Physics Uspekhi
- [14] O. Tchernyshyov, Phys. Rev. B **59** (1999) 1358
- [15] E. Z. Kuchinskii and M. V. Sadovskii, Zh. Eksp. Teor. Fiz. **115** (1999) 1765 [JETP **88** (1999) 968]
- [16] A. A. Ovchinnikov and N. S. Erikhman, Zh. Eksp. Teor. Fiz. **73** (1977) 650 [Sov. Phys. JETP **46** (1977) 340]
- [17] F. J. Dyson, Phys. Rev. **92** (1953) 1331
- [18] R. H. McKenzie, Phys. Rev. Lett. **77** (1996) 4804
- [19] M. Fabrizio and R. Mélin, Phys. Rev. Lett. **78** (1997) 3382
- [20] I. M. Lifshits, S. A. Gredeskul, and L. A. Pastur, *Introduction to the Theory of Disordered Systems*, Wiley, New York 1988
- [21] M. Mostovoy and J. Knoester, Int. J. Mod. Phys. B **13** (1999) 1601
- [22] L. Bartosch and P. Kopietz, Phys. Rev. Lett. **82** (1999) 988
- [23] L. Bartosch, PhD thesis, Georg-August-Universität, Göttingen, 2000 (<http://webdoc.sub.gwdg.de/diss/2000/bartosch/thesis.pdf>)
- [24] L. Bartosch and P. Kopietz, Phys. Rev. B **60** (1999) 15488
- [25] L. Bartosch and P. Kopietz, Phys. Rev. B **62** (2000) R16223
- [26] R. Hayn and J. Mertsching, Phys. Rev. B **54** (1996) R5199
- [27] W. Kohn, Phys. Rev. Lett. **2** (1959) 393
- [28] N. W. Ashcroft und N. D. Mermin, *Solid State Physics*, Saunders College Publishing, Philadelphia 1988
- [29] P. Monceau, *Electronic Properties of Inorganic Quasi One-Dimensional Compounds*, D. Reidel Publ. Co., Dordrecht, Boston 1985
- [30] U. Eckern and A. Geier, Z. Phys. B **65** (1996) 15
- [31] J. W. Negele and H. Orland, *Quantum Many-Particle Physics*, Addison-Wesley, Redwood City 1988
- [32] L. Tewordt, Phys. Rev. **132** (1963) 595
- [33] L. Tewordt, Z. Phys. **180** (1964) 385
- [34] N. R. Werthamer, Phys. Rev. **132** (1963) 663
- [35] N. R. Werthamer, in *The Ginzburg-Landau Equations and Their Extensions in Superconductivity*, edited by R. D. Parks, Marcel Dekker, New York 1969
- [36] I. Kosztin, S. Kos, M. Stone, and A. J. Leggett, Phys. Rev. B **58** (1998) 9365
- [37] S. Kos and M. Stone, Phys. Rev. B **59** (1999) 9545
- [38] L. Bartosch and P. Kopietz, Phys. Rev. B **60** (1999) 7452
- [39] N. D. Mermin and H. Wagner, Phys. Rev. Lett. **17** (1966) 1133
- [40] R. H. McKenzie, Phys. Rev. B **52** (1995) 16428
- [41] D. J. Scalapino, M. Sears and R. A. Ferrell, Phys. Rev. B **9** (1972) 3409

- [42] V. J. Emery and S. A. Kivelson, *Nature* **374** (1995) 434
- [43] V. J. Emery and S. A. Kivelson, *Phys. Rev. Lett.* **74** (1995) 3253
- [44] A. A. Abrikosov, L. P. Gorkov, and I. E. Dzyaloshinskii, *Methods of Quantum Field Theory in Statistical Physics*, Dover, New York 1963
- [45] J. R. Schrieffer, *Theory of Superconductivity*, Benjamin, New York 1964
- [46] M. Tinkham, *Introduction to Superconductivity*, 2nd ed., Mc Graw-Hill, New York 1996
- [47] J. E. Bunder and R. H. McKenzie, *Phys. Rev. B* **60** (1999) 344
- [48] G. Grüner, *Rev. of Mod. Phys.* **66** (1994) 1
- [49] M. Steiner, M. Fabrizio and A. O. Gogolin, *Phys. Rev. B* **57** (1998) 8290
- [50] M. Steiner, Yang-Chen, M. Fabrizio and A. O. Gogolin, *Phys. Rev. B* **59** (1999) 14848
- [51] D. Waxman, *Ann. Phys. (N.Y.)* **223** (1993) 129
- [52] L. Bartosch and P. Kopietz, *Eur. Phys. J. B* **17** (2000) 555
- [53] R. H. McKenzie and D. Scarratt, *Phys. Rev. B* **54** (1996) R12709
- [54] J. Schwinger, *Phys. Rev.* **128** (1962) 2425
- [55] M. E. Peskin and D. V. Schroeder, *An Introduction to Quantum Field Theory*, Addison-Wesley, Reading 1995
- [56] P. Kopietz, *Bosonization of Interacting Fermions in Arbitrary Dimensions*, Springer, Berlin 1997
- [57] A. A. Abrikosov and I. A. Ryzhkin, *Zh. Eksp. Teor. Fiz.* **71** (1976) 1204 [*Sov. Phys. JETP* **44** (1976) 630]
- [58] N. Schopohl, in "Quasiclassical Methods in the Theory of Superconductivity and Superfluidity" edited by D. Rainer and J. A. Sauls, Bayreuth, Germany 1998 (cond-mat/9804064)
- [59] C. W. Gardiner, *Handbook of Stochastic Methods for physics, chemistry, and the natural sciences*, Springer-Verlag, Berlin, Heidelberg 1983
- [60] N. G. van Kampen, *Stochastic Processes in Physics and Chemistry*, North-Holland, Amsterdam 1981
- [61] S. A. Brazovskii and I. E. Dzyaloshinskii, *Zh. Eksp. Teor. Fiz.* **71** (1976) 2338 [*Sov. Phys. JETP* **44** (1976) 1233]
- [62] N. F. Mott and W. D. Twose, *Adv. Phys.* **10** (1961) 107
- [63] D. J. Thouless, *J. Phys. C* **5** (1972) 77
- [64] A. A. Golub and Y. M. Chumakov, *Fiz. Nizk. Temp.* **5** (1979) 900 [*Sov. J. Low Temp. Phys.* **5** (1980) 427]
- [65] A. A. Abrikosov and E. A. Dorotheyev, *J. Low Temp. Phys.* **46** (1982) 53
- [66] K. B. Efetov, *Supersymmetry in disorder and chaos*, Cambridge University Press, Cambridge 1997
- [67] R. Hayn and W. John, *Z. Phys. B* **67** (1987) 169
- [68] H. J. Fischbeck and R. Hayn, *Phys. Status Solidi B* **158** (1990) 565
- [69] R. Hayn and H. J. Fischbeck, *Z. Phys. B* **76** (1989) 33
- [70] B. I. Halperin, *Phys. Rev.* **139** (1965) A104
- [71] C. Itzykson and J. C. Drouffe, *Statistical Field Theory*, Vol. II, Cambridge University Press, Cambridge 1989
- [72] W. Feller, *An Introduction to Probability Theory and its Applications*, Vol. II, 2nd ed., Wiley, New York 1971
- [73] M. Abramowitz and I. A. Stegun, *Handbook of mathematical functions*, Dover Publications, New York 1965
- [74] J. Mertsching, *Phys. Status Solidi B* **174** (1992) 129
- [75] M. V. Sadovskii, *Zh. Eksp. Teor. Fiz.* **66** (1974) 1720 [*Sov. Phys. JETP* **39** (1974) 845]
- [76] W. Wonneberger and R. Lautenschlager, *J. Phys. C* **9** (1976) 2865
- [77] A. Millis and H. Monien, *Phys. Rev. Lett.* **84**(2000) 2546
- [78] L. Bartosch and P. Kopietz, *Phys. Rev. Lett.* **84** (2000) 2547
- [79] W. H. Press, B. P. Flannery, S. A. Teukolsky, and W. T. Vetterling, *Numerical Recipes in C*, 2nd ed., Cambridge University Press, Cambridge 1992
- [80] A. Millis and H. Monien, *Phys. Rev. B* **61** (2000) 12496
- [81] D. C. Johnston, *Phys. Rev. Lett.* **52** (1984) 2049
- [82] D. C. Johnston, M. Maki and G. Grüner, *Solid State Commun.* **53** (1985) 5

